Bioremediation Modeling and Traveling Wave Analysis

Dissertation
zur Erlangung des Doktorgrades
der Fakultät für Mathematik, Informatik
und Naturwissenschaften
der Universität Hamburg

vorgelegt
im Department Mathematik
von

Caroline v. Dresky

aus Lübeck

Hamburg
2010

Als Dissertation angenommen vom Department
Mathematik der Universität Hamburg

auf Grund der Gutachten von Prof. Dr. Ingenuin Gasser
und Prof. Athanasios Tzavaras

Hamburg, den 3. Juni 2010

Prof. Dr. Vicente Cortés
Leiter des Departments Mathematik

Contents

Chapter 1

Introduction

The contamination of groundwater and soil is a problem of great importance. Consequently, appropriate techniques for restoring contaminated sites are required. The most commonly used method is the *pump-and-treat remediation technique*, which involves the delivery of contaminated groundwater to the surface and its above ground treatment. This method is characterized by its simplicity and flexibility, but experiences in recent years prove its low efficiency. For this reason, alternative remediation techniques have become the object of research.

A promising technology in this context is *bioremediation*, which involves the degradation of a pollutant by microorganisms. The main aspects of this technique are the following: Microorganisms require certain substrates for living and reproducing. The idea is to let microorganisms consume the contaminant in their metabolic processes, and convert it to a neutral and non-toxic product. While the pollutant is available in excess, usually other substrates that are essential for the metabolism are limited. A typical bioremediation procedure therefore involves the injection of substrates of low availability in order to provide an environment in which microorganisms can grow significantly and utilize the contaminant.

One example of the successful restoration of a contaminated site by bioremediation is the Hamburg Airport in Germany. In an area of the airport the groundwater is contaminated by chlorinated hydrocarbon, in particular by tetrachloroethylene. Besides this contaminant, the microorganisms involved require an appropriate substrate that provides electrons for chemical reactions in their metabolism. Due to the shortage of such substrates only a partial natural degradation of tetrachloroethylene was observed. In order to create better conditions for the growth of the microorganisms, ethanol has been injected as an electron donor. Under these conditions a complete degradation of tetrachloroethylene to non-toxic carbon dioxide is measured. Since this degradation is of significant magnitude, bioremediation turns out to be an effective technique for restoring the contaminated site at the Hamburg Airport (for more details we refer to [Gru08]).

In addition to the effectiveness described above, the cost-efficiency and environmental friendliness of bioremediation makes it a promising technology for reducing groundwater and soil contamination.

In order to estimate the impact of a pollutant, as well as the efficiency of bioremediation methods, mathematical models are of particular interest. Beginning with the one presented by Borden and Bedient in [Bor86], various bioremediation models have been proposed and studied over the last few decades. For a list of articles concerning bioremediation models consult the references in [Xin98]. More recent models can be found in [Cir99, Klö02, Che06].

Of special note is the model presented by Odencrantz et al. in [Ode93]. Due to its relative simplicity, while capturing the main aspects of bioremediation, this particular model has been well studied; see for example [Mur98, Xin98, Xin00].

In the present work we will derive and analyze a particular bioremediation model which on the one hand has similarities to the models mentioned above, but which on the other hand shows some substantial differences that require an independent analysis.

In *chapter 2* we will derive a model that describes the biodegradation of an arbitrary number of contaminants. This one-dimensional model consists of advection-reaction equations for the pollutants, and a rate equation for the microorganisms involved. It turns out that great importance is attached to the growth rate of the microorganisms, which in turn is closely linked to enzymatic reactions inside their cells. Since these correlations can be of various types, mathematical models must be built on a case-by-case basis. With respect to this fact we derive a bioremediation model under specific conditions. The awareness of these underlying assumptions enables us to explain or criticize similar models that are discussed in various articles without a detailed declaration of model assumptions.

In *chapters 3 and 4* we examine the bioremediation model outlined in the previous chapter for one and two substrates. These two models will be analyzed with respect to an important class of specific solutions, namely traveling waves. These solutions are characterized by propagation with constant speed and unmodified shape, and they become important due to their occurrence in various problems in the natural sciences. Some of the bioremediation models mentioned above have already been tested for traveling waves; see for example [Mur98, Log01, Che06]. But due to substantial differences between these models and the models derived in this thesis, an independent analysis is required.

Chapter 3 is concerned with the existence of traveling wave solutions. Phase plane arguments yield results with respect to the existence, the shape and propagation speed of traveling waves in both models of interest.

In *chapter 4* we will study the stability of the traveling wave solutions. In this investigation, linear stability results are deduced from spectral analysis of certain differential operators that are related to the bioremediation models under consideration. These theoretical results have been supplemented with numerical simulations.

Closing this work, *chapter 5* contains a summary of the previous results, while more detailed conclusions are presented at the end of each chapter.

Acknowledgements

This thesis would not have been possible without the support of several people and organizations who I would like to express my gratitude to.

First of all I wish to thank both my advisors for their outstanding support. I am much obliged to *Prof. Dr. Ingenuin Gasser* who was always there to listen and give precious advice. Additionally, I am very thankful for his encouragement and help in building collaborations and getting financial support. Likewise, I am deeply indebted to *Prof. Athanasios Tzavaras* for his constant interest in my research and many valuable discussions. His advice and guidance motivated me over and over again and helped me progress with my thesis. Moreover, I am very grateful to all members of the *DEASE* project who enabled me to gain many wonderful and priceless experiences by working and living abroad. In this context I also thankfully appreciate the financial support by the *Rudolf und Erika Koch-Stiftung*. And last but not least I owe my deepest gratitude to my partner *Andreas Heese*. I am very grateful for his constant support and for his love and care that helped me overcome several difficult phases.

Chapter 2

Mathematical Modeling

The purpose of this chapter is to develop a bioremediation model, i.e. a mathematical model that describes the degradation of one or more contaminants in a certain environment by microorganisms.

To this end we will first provide some biological and chemical background information about microorganisms that is needed for the modeling process.

Having this knowledge we derive a mathematical model consisting of ordinary differential equations that describes the microbial growth and the related degradation of the main food sources. We will first consider microorganisms whose growth depends on one main source of energy and generalize this model afterwards to the case of the dependency on $m \in \mathbb{N}$ sources.

Finally, we will extend the microbial growth model to a bioremediation model by taking into account spatial dynamics and making some further adjustments.

The notations that are used in this chapter are listed in table 2.1 on page 32.

2.1 Background information

2.1.1 Microorganisms

Microorganisms are microscopically small organisms. They include for example bacteria, many fungi and microscopic algae. In the following we will concentrate on bacteria, a large group of unicellular microorganisms.

Bacteria reproduce by cell division, i.e. after growing to a fixed size the cell is divided into two identical daughter cells. For this reproduction process and for maintaining their vital functions they need energy, as well as carbon as the most important substance for synthesizing cell mass. Various energy and carbon metabolisms exist, but most bacteria, including *Escherichia coli*, one of the best known bacteria, are *chemoorganoheterotrophic*. This technical term describes the

following characteristics [Got86]:

- Energy for living and growing is obtained from a chemical reaction (*chemotrophic*) in which usually electrons are transferred from one compound (electron donor) to another (electron acceptor). Hence, compounds from the environment are consumed in this reaction.

- The electron donor in this energy yielding reaction is an organic compound (*organotrophic*), very often fatty acids, amino acids and carbohydrate.

  The electron acceptor for most of the bacteria is oxygen, but there also exist bacteria that can use other molecules such as nitrate or sulfate.

- The carbon source is an organic compound (*heterotrophic*).

To sum up, if an organic electron donor, an electron acceptor and an organic carbon source are available (as well as some additional essential bioelements), the large group of chemoorganoheterotrophic bacteria is able to live and reproduce. More precisely, for vital functions and reproducing, various chemical reactions take place in the bacterial cells that involve, among others, the above mentioned essential compounds such as electron donor, electron acceptor and carbon source. Since most of these chemical reactions are enzymatic, we will also provide some information about enzymes.

2.1.2 Enzymes

Enzymes are proteins that catalyze chemical reactions, i.e. they increase the rates of those reactions. Almost all processes in biological cells require enzymes to proceed at significant rates. The variety of specific enzymes that a cell is equipped with is genetically determined.

In an enzymatic reaction one or more *substrates* are converted by the enzyme into one or more *products*. In this process the substrates bind to the *active site* of the enzyme, and a substrate-enzyme complex is built. In a second stage the enzyme enables the conversion of the substrates into products, which are released from the complex. While the substrates are degraded and the products are synthesized in this process, the enzyme itself is not consumed in this reaction.

The simplest case of enzymatic reactions is a *single-substrate reaction*, i.e. the transformation of one single substrate S to one single product P by a specific enzyme E. This mechanism is schematically described in figure 2.1.

However, the majority of enzymatic reactions is represented by *multi-substrate reactions*, which are catalyzed by enzymes that convert more than one substrate into one or more products. We distinguish two main types of multi-substrate reactions [Bis08, Coo07]:

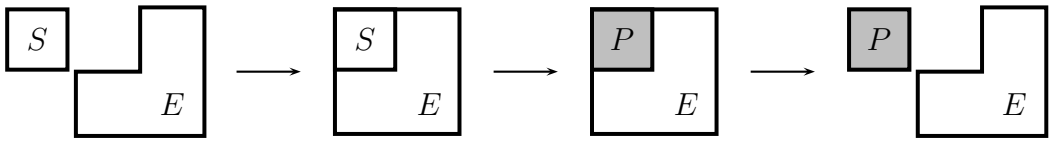

Figure 2.1: Schematic illustration of an enzymatic reaction in which one single substrate is transformed to a single product

1. *Sequential mechanism*: All substrates have to bind to the enzyme before the first product can be released. This mechanism can either be *ordered*, when the substrates and products are bound and released in an obligatory order, or *random*, when there is no fixed binding sequence.

2. *Ping-pong mechanism*: At least one product is released before the last substrate has bound to the enzyme.

Finally, we can combine the knowledge about the metabolism of bacteria and enzymatic reactions in biological cells:

For vital processes and reproduction bacteria need certain compounds. These substrates, mainly an electron donor, an electron acceptor and a carbon source, are transformed by enzymatic chemical reactions inside the bacterial cells. In these reactions the substrates are degraded, and products, which are either essential in vital processes and for synthesizing new cell material or by-products of energy yielding chemical reactions, are produced, while the catalyzing enzyme is not consumed in these reactions. This mechanism is visualized in figure 2.2, where we concentrate on one single enzymatic reaction, and where S_i $(i = 1, \ldots, m)$, E and P_j $(j = 1, \ldots, k)$ denote the substrates, enzyme and products involved in this enzymatic reaction.

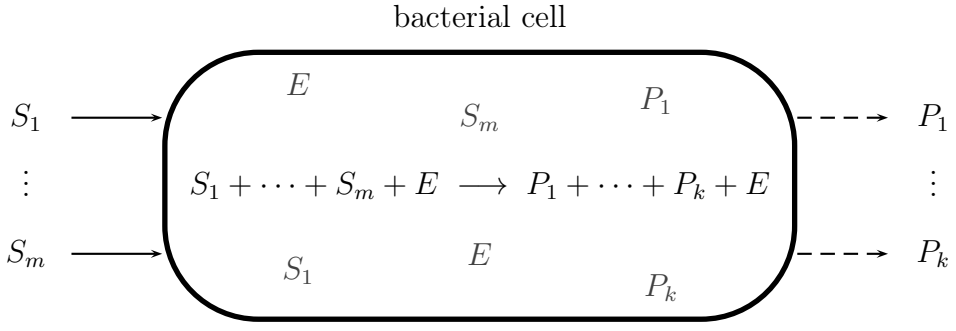

Figure 2.2: Schematic illustration of an enzymatic reaction in a bacterial cell that involves m substrates and k products

2.2 Bacterial growth depending on one substrate

Below we will first introduce an empirically found mathematical model for bacterial growth that depends on one single substrate. This model will be explained afterwards by presenting a modeling process that yields the same equations.

2.2.1 Proposed model

In 1942 the biochemist Jacques Monod proposed a mathematical model for bacterial growth depending on one single substrate [Mon42]. Although bacteria always require more than just one compound to keep vital functions alive (compare subsection 2.1.1), he could describe bacterial growth depending on only one main substrate by keeping all other potential limiting factors in large excess compared to this one [Mon49].

Monod supposed that the cell concentration of bacteria (n) grows exponentially. Furthermore, he assumed that the concentration of substrate (s_1) decreases proportionally to the bacterial growth, i.e.

$$\frac{ds_1}{dt} = -\frac{1}{Y_{n/s_1}}\frac{dn}{dt} \tag{2.1}$$

with a factor whose reciprocal Y_{n/s_1}, the so-called *yield constant*, describes how many units of bacteria can be built out of one unit of substrate. Based on these assumptions Monod proposed the bacterial growth model

$$\frac{ds_1}{dt} = -\frac{1}{Y_{n/s_1}}\mu n \tag{2.2}$$

$$\frac{dn}{dt} = \mu n. \tag{2.3}$$

The growth rate μ represents the overall velocity of several reactions in which cell substance is synthesized. Most of these reactions are enzymatic, and every single rate depends on the concentration of the involved substrate and the amount of enzyme [Mon49]. The specific growth rate μ is therefore not constant but also depends on the involved substrates and enzymes. The relation between μ and s_1 is a very important one in growth dynamics. Monod suggested in his dissertation 1942 the formula

$$\mu(s_1) = \mu_{max}\frac{s_1}{s_1 + K_1}, \tag{2.4}$$

which he found empirically by studies on batch cultures of *E. coli* and *M. tubercolosis* in glucose dilutions (see figure 2.3). The constant μ_{max} is the maximum specific growth rate, which is asymptotically approached by increasing the substrate concentration. The constant K_1 represents the half saturation concentration of the substrate, which occurs if the rate is half the maximum [Mon42]. This so-called *Monod constant* is also a measure for the affinity between bacteria

and substrate: The smaller K_1 is, the higher is the affinity. Bacteria related to a small constant K_1 are therefore able to grow strongly even if the environment only provides a low substrate concentration [Sch04].

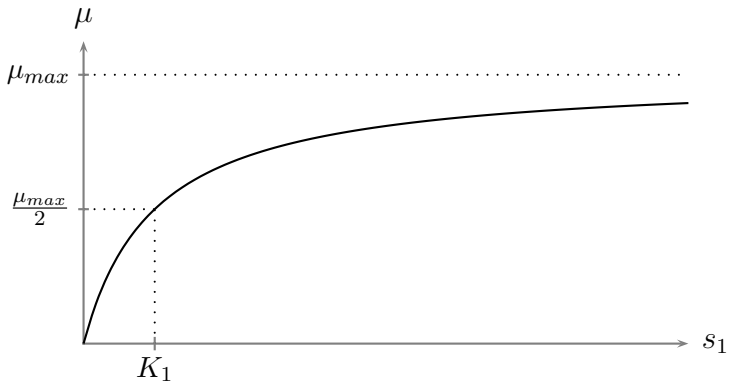

Figure 2.3: Specific bacterial growth rate suggested by Monod

2.2.2 Modeling

Since Monod suggested the growth rate (2.4), different approaches have been made to explain this empirically found formula. The obvious analogy to the Michaelis-Menten equation[1] in enzyme kinetics (see [Mic13]), which was not mentioned by Monod before [Mon49], indicates a connection to a single-substrate enzyme reaction. This led the microbiologist S. John Pirt to the assumption that the bacterial growth depends, besides on the substrate, on one special enzyme, namely the *substrate uptake enzyme*, which controls the growth rate and is therefore the *bottleneck* in the whole process [Pir90].

Although it has often been assumed that a complicated process consisting of a certain number of reactions is controlled by a "master reaction" (see [Bla05]), there exists also criticism against this hypothesis; see [Mon49, Pan95]. Nevertheless, we will explain the approach of Pirt in the following. For this purpose we will first present some information about basic enzymatic reactions, which build the basis of this ansatz (the used notation is defined in table 2.1).

Enzyme kinetics (single-substrate reactions)

According to Pirt we assume that one specific enzymatic reaction limits the bacterial growth. Therefore, the reaction rate of this enzymatic process must play an important role for the growth of bacteria that depend on this reaction. For this reason we will describe a certain enzymatic reaction mathematically and derive its reaction rate.

[1] This equation, which represents the reaction rate of a single-substrate enzyme reaction, will be derived and explained later in this section.

In this section we concentrate on single-substrate reactions. More precisely, we consider the case of a single enzyme E that combines reversibly with one molecule of substrate S_1 to form a complex S_1E, which turns in a second stage non-reversibly to a product P. This mechanism was proposed by Michaelis and Menten in 1913 for the reaction of saccharose with the enzyme *invertase* to glucose and fructose[2]; see [Mic13]. This reaction is represented by

$$S_1 + E \underset{k_{-1}}{\overset{k_1}{\rightleftharpoons}} S_1E \overset{k_f}{\to} P + E, \tag{2.5}$$

where the parameters k_i, $i \in \{-1, 1, f\}$, denote the rate constants of the particular reaction steps. The related differential equations that describe this two stage chemical reaction are

$$\frac{ds_1}{dt} = -k_1 s_1 e + k_{-1} c_1 \tag{2.6}$$

$$\frac{dc_1}{dt} = \quad k_1 s_1 e - k_{-1} c_1 - k_f c_1 \tag{2.7}$$

$$\frac{de}{dt} = -k_1 s_1 e + k_{-1} c_1 + k_f c_1 \tag{2.8}$$

$$\frac{dp}{dt} = \quad k_f c_1 \tag{2.9}$$

with the natural initial conditions

$$s_1(0) = s_0, \quad c_1(0) = 0, \quad e(0) = e_0, \quad p(0) = 0.$$

Here, the small letters stand for the concentrations of the compounds that are denoted by capital letters, whereas the concentration of the complex S_1E is denoted by c_1. The numerical solution of this model for a characteristic set of parameters is shown in figure 2.4.

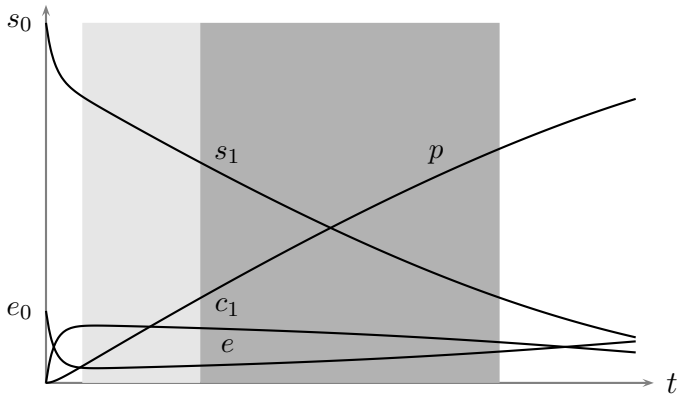

Figure 2.4: Dynamics of an enzymatic reaction that follows mechanism (2.5)(see also [Voe02]). For an explanation of the gray areas see the text in assumption A2.

[2]In this context glucose and fructose together are considered to be one product.

Taking into account the induced conservation laws

$$\begin{aligned}\frac{d}{dt}(e+c_1) &= 0 \quad \Leftrightarrow \quad e(t) = e_0 - c_1(t)\\ \frac{d}{dt}(s_1+c_1+p) &= 0 \quad \Leftrightarrow \quad p(t) = s_0 - s_1(t) - c_1(t)\end{aligned}$$

we can reduce model (2.6)-(2.9) to

$$\frac{ds_1}{dt} = -k_1 s_1(e_0 - c_1) + k_{-1}c_1 \tag{2.10}$$

$$\frac{dc_1}{dt} = k_1 s_1(e_0 - c_1) - k_{-1}c_1 - k_f c_1 \tag{2.11}$$

with

$$s_1(0) = s_0, \quad c_1(0) = 0. \tag{2.12}$$

This nonlinear problem is not integrable in closed form. The reaction rate of the enzymatic reaction, which is defined as the rate of product formation, i.e. dp/dt, is therefore not computable explicitly.

However, there exist different assumptions that yield approximations for the solution and build the basis for the derivation of the rate equation:

A1. **Equilibrium assumption:** In 1913 the medical scientists and biochemists Leonor Michaelis and Maud Leonora Menten assumed that the concentrations satisfy $c_1, e_0 << s_1 \approx s_0$. Moreover, they assumed that the rate constants meet $k_f << k_{-1}$ so that k_f is negligible in comparison with k_{-1}, and the substrate and enzyme are in *equilibrium* with their complex [Mic13]. The law of mass action then yields the equation

$$k_1 s_1(e_0 - c_1) = k_{-1}c_1. \tag{2.13}$$

This equation was the basis for Michaelis and Menten for computing the rate equation of the enzymatic reaction (see below), but they did not present an analysis of the overall dynamics.

If we do so, we realize that this equilibrium assumption cannot hold for large time intervals: Plugging equation (2.13) into (2.10)-(2.12) yields that no substrate is consumed and that the complex concentration does not change at any time, which does not satisfactorily approximate the overall dynamics. Nevertheless, a precise meaning to equation (2.13) can be given by using asymptotic expansion methods and perturbation theory: Roughly speaking, we first scale the variables by appropriate reference parameters and detect small parameters by taking into account $k_f << k_{-1}$ and $e_0 << s_0$.

Furthermore, we derive an asymptotic expansion of the solution with respect to one of the small parameters. Substituting this expansion into the scaled problem and comparing coefficients yields that the main term of the asymptotic expansion satisfies

$$\begin{aligned} \frac{ds_1}{dt} &= -k_f c_1 \\ 0 &= -k_1 s_1 (e_0 - c_1) + k_{-1} c_1, \end{aligned}$$

and hence

$$\frac{ds_1}{dt} = -k_f e_0 \frac{s_1}{s_1 + K} \tag{2.14}$$

$$c_1 = e_0 \frac{s_1}{s_1 + K} \tag{2.15}$$

with $K = \frac{k_{-1}}{k_1}$. Singular perturbation methods show that the solution of (2.14)/(2.15) approximates the solution of (2.10)/(2.11) after a certain transient in which c_1 grows and s_1 almost stays constant. In this time interval the Michaelis-Menten assumption (2.13) holds, but neither s_1 nor c_1 are constant. For more details we refer to appendix A.

Although the assumption $k_f << k_{-1}$ is not always applicable, Michaelis and Menten did important pioneering work in enzyme kinetics by deriving equation (2.15) and the resulting rate equation (2.19), which will be explained later in this section.

A2. **Quasi-steady-state assumption:** In 1925 the botanist George Edward Briggs and the theoretical biologist John Burdon Sanderson Haldane generalized the assumptions of Michaelis and Menten. Instead of an assumption concerning the rate constants, they only proposed that the concentrations of the complex and enzyme are always negligibly small, compared with the concentrations of the substrate and product. In particular, they expected the initial conditions to satisfy $e_0 << s_0$. From this assumption they inferred that the rate of change of c_1 has to be small as well, compared with the rate of change of s_1 and p after a short transient [Bri25]. This results in a *quasi-steady-state assumption*[3] for c_1:

$$k_1 s_1 (e_0 - c_1) - (k_{-1} + k_f) c_1 = 0. \tag{2.16}$$

Just as Michaelis and Menten, Briggs and Haldane concentrated on presenting the rate equation of the enzymatic reaction by using the equation above, but they did not analyze the overall dynamics.

[3]The name of this assumption refers to the fact that due to (2.16) we can consider the concentration of the complex to stay *almost* constant, whereas it stays constant in a true steady state [Seg89].

Plugging equation (2.16) into (2.11) yields a steady-state situation for c_1, i.e. the concentration of the complex never changes, which does not describe satisfactorily the dynamics of the enzymatic reaction at all times. This apparent inconsistency can be solved by using asymptotic and perturbation theory. Following the procedure explained in A1 yields that the solution of (2.10)/(2.11) after a short period, in which c_1 grows and s_1 almost stays constant, can be approximated by the solution of

$$\begin{aligned} \frac{ds_1}{dt} &= -k_1 s_1(e_0 - c_1) + k_{-1}c_1 \\ 0 &= \quad k_1 s_1(e_0 - c_1) - (k_{-1} + k_f)c_1, \end{aligned}$$

and therefore by

$$\frac{ds_1}{dt} = -k_f c_1 = -k_f e_0 \frac{s_1}{s_1 + K} \tag{2.17}$$

$$c_1 = e_0 \frac{s_1}{s_1 + K} \tag{2.18}$$

with $K = \frac{k_{-1}+k_f}{k_1}$. Hence, the assumption (2.16) of Briggs and Haldane holds without c_1 being in a true steady state (a more detailed explanation is presented in appendix A).

As shown in figure 2.4 for a representative enzymatic reaction, the assumption of c_1 being much smaller than s_1 and the derivative of c_1 being almost zero holds in the entire gray interval. The additional assumption that c_1 is negligible compared with p is satisfied in the dark gray interval.[4]

The assumption of Briggs and Haldane is of more general applicability than assumption A1 by Michaelis and Menten, which involves an additional statement concerning the product yielding rate constant k_f. After all, besides the different orders of magnitude of k_f, the results only differ in the constants K. However, these apparent small differences have a large impact on the solutions (for more details see appendix A).

Summing up, by assuming A1 or A2 we are able to approximate the dynamics of model (2.10)/(2.11) after a fast transient. For a detailed analysis of the dynamics we refer to appendix A, and concentrate in the following on deriving the *rate equation* of the enzymatic reaction. The reaction rate, which is defined as the rate of product formation and hence a function of the substrate concentration, is an important measure in enzyme kinetics. In this field of research, a special meaning belongs to the initial reaction rate, i.e. the substrate concentration is given by

[4]The additional assumption concerning the product concentration p is used by Briggs and Haldane to derive (2.16), but it is not involved in the asymptotic derivation of (2.17)/(2.18), for which reason this approximation holds well in the entire gray interval.

the initial concentration. Measuring the initial reaction rate minimizes the influence of complicating factors occurring during the reaction. Therefore, it yields a more meaningful parameter than the value measured at any other time t [Voe02]. Nevertheless, in this mathematical analysis we will consider the more general reaction rate at time t, and hence the rate depending on the substrate concentration at time t.

Substituting (2.13) and (2.16), respectively, in (2.9) yields the rate equation

$$v(s_1) := \frac{dp}{dt} = k_f c_1 = k_f e_0 \frac{s_1}{s_1 + K}.$$

By increasing the substrate concentration such that all enzymes are saturated with substrate, the rate asymptotically approaches the maximum value

$$v_{max} := k_f e_0.$$

The rate of the enzymatic reaction is thus given by

$$v(s_1) = v_{max} \frac{s_1}{s_1 + K} \tag{2.19}$$

(see figure 2.5). This function, with respect to the initial concentration $s_1(t) = s_0$, is referred to as the *Michaelis-Menten equation*, which is the basic equation in enzyme kinetics.

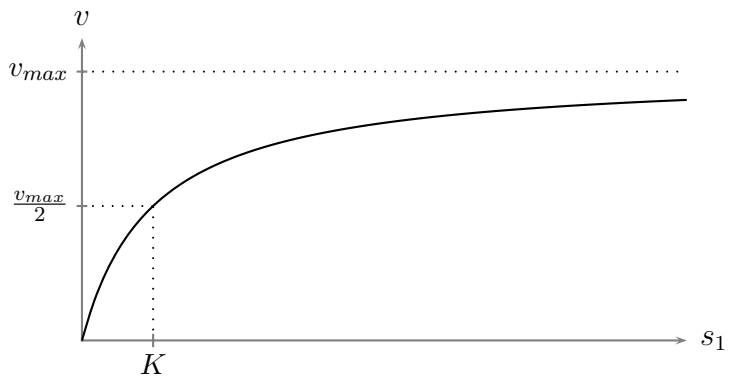

Figure 2.5: Reaction rate of the single-substrate reaction (2.5)

The so-called *Michaelis constant* K, which occurs in the Michaelis-Menten equation (2.19), depends on the particular assumption that was made during the derivation: Following assumption A1 by Michaelis and Menten, the constant is given by $K = \frac{k_{-1}}{k_1}$, while it denotes $K = \frac{k_{-1}+k_f}{k_1}$ if the derivation is based on assumption A2 by Briggs and Haldane[5].

[5]The more general constant that results from the derivation of Briggs and Haldane is also often referred to as *Michaelis constant*.

This kinetic constant represents the substrate concentration that occurs if the rate is half the maximum. Hence, the smaller K is, the less substrate is needed to be available to reach a certain reaction rate. In the case of the Michaelis-Menten derivation, the Michaelis constant equals the dissociation constant of the complex, which is a measure for the preference of the substrate to occur either as substrate itself or bound in the complex. Therefore, the constant K also represents the affinity, i.e. the binding strength, between the substrate and the enzyme: The smaller K, the higher is the affinity, and hence the greater is the reaction rate $v(s_1)$ for a fixed concentration s_1 (see [Mic13]).

With this knowledge about enzymatic reactions we can concentrate on modeling bacterial growth that depends on one particular single-substrate reaction.

Bacterial growth

We assume that the substrate uptake enzyme, which controls the bacterial growth, can be characterized by mechanism (2.5). The growth limiting enzymatic reaction is therefore modeled by the differential equations (2.6)-(2.9). Taking the quasi-steady-state assumption A2 by Briggs and Haldane into account (because of its more general applicability than A1), and using the proportionality between the substrate degradation and the bacterial growth, proposed by Monod in (2.1), we get the mathematical model

$$\frac{ds_1}{dt} = - \quad v(s_1) \tag{2.20}$$

$$\frac{dn}{dt} = Y_{n/s_1} v(s_1). \tag{2.21}$$

Here, $v(s_1)$ represents the rate equation (2.19) of the limiting enzymatic reaction. The second differential equation will be written in the form

$$\frac{dn}{dt} = Y_{n/s_1} v(s_1) =: \mu(s_1) n \tag{2.22}$$

so that

$$\mu(s_1) = \frac{Y_{n/s_1}}{n} v(s_1) = \frac{Y_{n/s_1}}{n} v_{max} \frac{s_1}{s_1 + K}$$

represents the specific growth rate of the bacteria.

Now, we assume that the total concentration of enzyme depends linearly on the concentration of bacteria, i.e.

$$e_0 = \alpha n, \tag{2.23}$$

where α is the fixed fraction of enzyme of a bacterium. The maximum growth

rate, which is asymptotically approached by increasing the substrate concentration, is then given by

$$\mu_{max} := \frac{Y_{n/s_1}}{n} v_{max} = Y_{n/s_1} k_f \alpha.$$

The specific growth rate of the bacteria thus reads

$$\mu(s_1) = \mu_{max} \frac{v(s_1)}{v_{max}} = \mu_{max} \frac{s_1}{s_1 + K} \tag{2.24}$$

with $K = \frac{k_{-1}+k_f}{k_1}$. Hence, the equations (2.20)/(2.22)/(2.24) form the bacterial growth model that results from the assumptions stated above. In particular, the bacterial growth rate depends on the rate equation of the limiting enzymatic reaction, and the Monod constant equals the Michaelis constant.

The bacterial growth model derived in the current section equals in form the equations (2.2)-(2.4). Therefore, the following assumptions seem to be reasonable to explain the bacterial growth model proposed by Monod on the basis of empirical studies:

1. The substrate decreases proportionally to the bacterial growth (see (2.1)).
2. The bacterial growth is controlled by a certain *substrate uptake enzyme* that follows the kinetic mechanism (2.5).
3. The quasi-steady-state assumption A2 by Briggs and Haldane is applicable.
4. The total concentration of enzyme is proportional to the bacteria concentration (see (2.23)).

2.3 Bacterial growth depending on multiple substrates

In section 2.2 we studied bacteria whose growth depends on one substrate. We assumed that all other essential compounds are available in excess and that the growth limiting process is an enzymatic reaction that involves just one substrate and one product. Enzymes of that kind are very rare. Typically, more than one substrate and more than one product are involved in an enzymatic reaction.

In this section we will generalize the results of section 2.2 and study bacteria whose growth is associated to an enzymatic reaction that involves more than one substrate. Analogous to the last section we will first introduce a mathematical model which is found in various articles without a detailed declaration of model assumptions. By generalizing the assumptions stated in the previous section we will then derive a bacterial growth model, which will be compared with the first-mentioned one.

2.3.1 Proposed model

If we take over Monod's initial assumptions concerning the growth rates of substrate and bacteria (see subsection 2.2.1), the general bacterial growth model reads

$$\frac{ds_i}{dt} = -\frac{1}{Y_{n/s_i}}\mu(s_1,\dots,s_m)n, \qquad i = 1,\dots,m \tag{2.25}$$

$$\frac{dn}{dt} = \qquad \mu(s_1,\dots,s_m)n \tag{2.26}$$

with a growth rate $\mu : \mathbb{R}^m \to \mathbb{R}$ that depends on the enzymatic reactions inside the bacterial cells.

The simplest choice for μ is the multiplication of m single-substrate growth rates

$$\mu(s_1,\dots,s_m) = \mu_{max}\prod_{i=1}^{m}\frac{s_i}{s_i + K_i}, \tag{2.27}$$

which is used in various bacterial growth and bioremediation models, for example in [Meg72, Bor86, Ode93] for $m = 2$, in [Wid88] for $m = 3$, in [Ben84] for $m = 4$ and in [Sch98, May01, Hem07] for a general number $m \in \mathbb{N}$ of substrates.

2.3.2 Modeling

As said before, the growth rate μ depends on the enzymatic reactions in the bacterial cells. Similar to the assumption of Pirt concerning the single-substrate case, we assume that there exists one particular growth limiting enzyme that converts m substrates into one or more products. Analogous to the previous section we will first provide some required information about enzymatic *multi-substrate reactions* and concentrate afterwards on the derivation of a bacterial growth model, which will be compared to model (2.25)-(2.27).

Enzyme kinetics (multi-substrate reactions)

According to subsection 2.1.2, two main mechanisms exist to convert m substrates into products: sequential mechanisms, in which all substrates bind to the enzyme before the first product is released, and ping-pong mechanisms, in which at least one product is released before the last substrate has bound to the enzyme.

In this context we concentrate on ordered sequential mechanisms[6]. Therefore, we only present the mathematical modeling and derivation of the rate equation for these particular reactions in which m substrates are converted into one product[7].

[6] For random sequential and ping-pong mechanisms see remark 1 on page 26.

[7] Analogous to the invertase reaction, which was studied by Michaelis and Menten, we can consider several products to be a single one.

If we assume that b_i molecules of substrate S_i combine with the enzyme, i.e. that $S_i^* = b_i S_i$, where b_i represent stoichiometric constants ($i = 1, \ldots, m$), we can write the kinetic mechanism in the form

$$S_1^* + E \underset{k_{-1}}{\overset{k_1}{\rightleftharpoons}} S_1^*E + S_2^* \underset{k_{-2}}{\overset{k_2}{\rightleftharpoons}} \ldots \underset{k_{-(m-1)}}{\overset{k_{m-1}}{\rightleftharpoons}} S_1^* \ldots S_{m-1}^* E + S_m^* \underset{k_{-m}}{\overset{k_m}{\rightleftharpoons}} S_1^* \ldots S_m^* E \overset{k_f}{\to} P + E. \tag{2.28}$$

With the notation $c_0 := e$ the associated differential equations are

$$\begin{aligned}
\frac{ds_i^*}{dt} &= -k_i c_{i-1} s_i^* + k_{-i} c_i, && i = 1, \ldots, m \\
\frac{dc_i}{dt} &= k_i c_{i-1} s_i^* - k_{-i} c_i - k_{i+1} c_i s_{i+1}^* + k_{-(i+1)} c_{i+1}, && i = 1, \ldots, m-1 \\
\frac{dc_m}{dt} &= k_m c_{m-1} s_m^* - k_{-m} c_m - k_f c_m \\
\frac{de}{dt} &= -k_1 s_1^* e + k_{-1} c_1 + k_f c_m \\
\frac{dp}{dt} &= k_f c_m
\end{aligned}$$

with initial conditions

$$s_i^*(0) = s_{i0}^*, \quad c_i(0) = 0, \quad e(0) = e_0, \quad p(0) = 0.$$

Using the induced conservation laws

$$\begin{aligned}
\frac{d}{dt}(e + \sum_{i=1}^{m} c_i) &= 0 \quad \Leftrightarrow \quad e(t) = e_0 - \sum_{i=1}^{m} c_i(t) \\
\frac{d}{dt}(s_1^* + \sum_{i=1}^{m} c_i + p) &= 0 \quad \Leftrightarrow \quad p(t) = s_{10}^* - s_1^*(t) - \sum_{i=1}^{m} c_i(t)
\end{aligned}$$

we can reduce the above model to the differential equations for the substrates and complexes.

As a generalization of Briggs' and Haldane's assumption in the single-substrate case, we assume that all substrates on the one hand and all complexes on the other hand are of the same order of magnitude, and that the concentrations of the complexes and the enzyme are much smaller than of the substrates, which yields particularly $e_0 << s_{i0}^*$. Following again the procedure that was proposed on page 11 in section 2.2, i.e. scaling, asymptotic expansion methods and perturbation theory, and taking into account $s_i^* = \frac{1}{b_i} s_i$ yields that the dynamics after a certain transient can be approximated by

$$\frac{ds_i}{dt} = -b_i k_f c_m, \qquad i = 1, \ldots, m \tag{2.29}$$

$$0 = k_i c_{i-1} \frac{s_i}{b_i} - k_{-i} c_i - k_{i+1} c_i \frac{s_{i+1}}{b_{i+1}} + k_{-(i+1)} c_{i+1}, \quad i = 1, \ldots, m-1 \tag{2.30}$$

$$0 = k_m c_{m-1} \frac{s_m}{b_m} - k_{-m} c_m - k_f c_m \tag{2.31}$$

(for more details see appendix A). With respect to the common nomenclature for the single-substrate case (compare A2 on page 12), we refer to the equations (2.30)/(2.31) as *quasi-steady-state assumptions* for all complexes.

In order to solve the equations (2.29)-(2.31), we have to compute the complex concentrations c_i depending on the substrates s_j and the total enzyme e_0, and to solve the differential equations for s_j $(i, j = 1, \ldots, m)$.

However, with respect to the following investigations, which require besides equation (2.29) only the rate equation

$$v(s_1, \ldots, s_m) := \frac{dp}{dt} = k_f c_m,$$

we restrict our concentration on the computation of c_m.

Various approaches have been made to simplify the computation of rate equations for complex kinetic mechanisms that involve a fixed number of substrates and products; see [Bis08]. These approaches attempt to avoid solving the quasi-steady-state equations directly, which can, depending on the complexity of the mechanism, be confusing and error-prone. Nevertheless, in this context we present a direct solving of the quasi-steady-state equations. This procedure results in a formula for the rate equation of mechanism (2.28), which is applicable to any number of substrates. In order to describe this method, we write the components that a complex or enzyme depends on in brackets behind the variable.

(i) *Backward computation of the complexes:* Solving of the equations (2.30) and (2.31) for $i = m, \ldots, 1$, where in every computation the last one is taken into account, yields

$$c_i = c_i(s_i, \ldots, s_m, b_i, \ldots, b_m, c_{i-1}), \quad i = m, \ldots, 1$$

(ii) *Forward computation of the complexes:* Substitution of c_{i-1} from (i) into c_i:

$$c_i = c_i(s_i, \ldots, s_m, b_i, \ldots, b_m, e), \quad i = 1, \ldots, m$$

(iii) *Computation of the enzyme:* Insertion of c_i from (ii) in $e = e_0 - \sum_{j=1}^{m} c_j$:

$$e = e(s_1, \ldots, s_m, b_1, \ldots, b_m, e_0)$$

(iv) *Computation of c_m:* Substitution of e from (iii) into c_m from (ii):

$$c_m = c_m(s_1, \ldots, s_m, b_1, \ldots, b_m, e_0).$$

The calculation of c_m according to the above procedure yields

$$c_m = \frac{\prod_{j=1}^{m} s_j}{\sum_{i=1}^{m} \left(A_i \prod_{j=1}^{i-1} s_j \right) + \sum_{i=1}^{m-1} \sum_{l=2}^{m-i+1} \left(B_{il} \prod_{\substack{j=1 \\ j \notin \{i, \ldots, m-l+1\}}}^{m} s_j \right) + \prod_{j=1}^{m} s_j} e_0 \tag{2.32}$$

with

$$A_i = \frac{k_{-m} + k_f}{k_m} b_m \prod_{j=i}^{m-1} \frac{k_{-j}}{k_j} b_j$$

$$B_{il} = \frac{k_f}{k_{m-l+1}} b_{m-l+1} \prod_{j=i}^{m-l} \frac{k_{-j}}{k_j} b_j.$$

Since the maximum reaction rate, which is asymptotically approached when all substrates are available in excess, is

$$v_{max} := k_f e_0,$$

the rate equation of the enzymatic reaction is given by

$$v(s_1, \ldots, s_m) = v_{max} \frac{c_m}{e_0}. \tag{2.33}$$

For a better understanding of this rate equation we will explain the meaning of the kinetic constants A_i and B_{il}. Analogous to the Michaelis constant that has been defined for single-substrate reactions as the particular substrate concentration that occurs if the reaction rate is half the maximum, we can define Michaelis constants for multi-substrate reactions: With K_i we denote the concentration of substrate S_i that corresponds to the half maximum rate if all other substrates are available in excess. This results in the following Michaelis constants for the ordered sequential mechanism (2.28):

$$K_i = \begin{cases} B_{i\,m-i+1} & = \frac{k_f}{k_i} b_i, & i = 1, \ldots, m-1 \\ A_m & = \frac{k_{-m}+k_f}{k_m} b_m, & i = m. \end{cases} \tag{2.34}$$

Hence, the kinetic constants A_i and B_{il} are products of Michaelis constants K_i of the substrates and dissociation constants K_i^d of the various complexes.

Below we will state explicitly the rate equations for reactions that involve two and three substrates, respectively, and exemplify them with specific enzymatic reactions.

Example 1 $(m = 2)$**.** The rate equation of an ordered sequential mechanism in which two substrates are converted irreversibly into one product is given by

$$v(s_1, s_2) = v_{max} \frac{s_1 s_2}{A_1 + A_2 s_1 + B_{12} s_2 + s_1 s_2}$$

with

$$A_1 = \frac{k_{-2} + k_f}{k_2} \frac{k_{-1}}{k_1} b_1 b_2 = K_2 K_1^d \qquad B_{12} = \frac{k_f}{k_1} b_1 = K_1$$

$$A_2 = \frac{k_{-2} + k_f}{k_2} b_2 = K_2$$

(see [Coo07] for $b_1 = b_2 = 1$). In order to exemplify this reaction, we consider the aromatic metabolism of anaerobic bacteria. A key enzyme in the degradation of aromatic compounds is *4-hydroxybenzoyl-CoA reductase*. In the bacterium *Thauera aromatica* this enzyme catalyzes a reaction in which an external electron donor and 4-hydroxybenzoyl-CoA react to form benzoyl-CoA. This reaction can be simplified described by the reaction mentioned above. For more details we refer to [Bol01, Bol05b, Bol05c].

Example 2 ($m=3$)**.** The rate equation of an ordered sequential mechanism that involves three substrates is given by

$$v(s_1, s_2, s_3) = v_{max} \frac{s_1 s_2 s_3}{A_1 + A_2 s_1 + A_3 s_1 s_2 + B_{12} s_3 + B_{13} s_2 s_3 + B_{22} s_1 s_3 + s_1 s_2 s_3}$$

with

$$A_1 = \frac{k_{-3} + k_f}{k_3} \frac{k_{-1}}{k_1} \frac{k_{-2}}{k_2} b_1 b_2 b_3 = K_3 K_1^d K_2^d \qquad B_{12} = \frac{k_f}{k_2} \frac{k_{-1}}{k_1} b_1 b_2 = K_2 K_1^d$$

$$A_2 = \frac{k_{-3} + k_f}{k_3} \frac{k_{-2}}{k_2} b_2 b_3 = K_3 K_2^d \qquad B_{13} = \frac{k_f}{k_1} b_1 = K_1$$

$$A_3 = \frac{k_{-3} + k_f}{k_3} b_3 = K_3 \qquad B_{22} = \frac{k_f}{k_2} b_2 = K_2$$

(see [Bis08] for $b_1 = b_2 = b_3 = 1$). As an example we consult again the aromatic metabolism of anaerobic bacteria, in particular of the bacterium *Thauera aromatica*. The reaction mentioned in example 1 is followed by a reaction, which is supposed to be the bottleneck in the metabolism of anaerobic bacteria that utilize aromatic compounds as their source of energy or carbon. In this reaction, which is catalyzed by the enzyme *benzoyl-CoA reductase*, an external electron donor, ATP and benzoyl-CoA, which is the product of the reaction stated in example 1, react to form a dienoyl-CoA compound. This reaction can be simplified represented by the above mechanism. For more details see [Möb04, Bol05a, Bol05b, Bol05c].

With this knowledge about enzymatic reactions we can move on to modeling bacterial growth that depends on an ordered sequential multi-substrate reaction.

Bacterial growth

We assume that the substrate uptake enzyme, which limits the bacterial growth, follows the kinetic mechanism (2.28). Hence, we study bacteria whose growth depends on $m \in \mathbb{N}$ substrates that bind in the growth limiting kinetic mechanism in an obligatory order to an enzyme, and produce a single product, which might be required for vital functions or reproduction.

Assuming furthermore that the quasi-steady-state assumptions (2.30)/(2.31) hold, and taking the proportionality (2.1) between the substrate uptake and the bacterial growth into account, we get the model

$$\frac{ds_i}{dt} = \quad -b_i v(s_1, \ldots, s_m), \quad i = 1, \ldots, m \tag{2.35}$$

$$\frac{dn}{dt} = b_1 Y_{n/s_1} v(s_1, \ldots, s_m). \tag{2.36}$$

The function v represents the rate equation (2.33) of the enzymatic reaction. With the assumption (2.23) concerning the linearity between the total enzyme and the bacteria concentration, we write (2.36) in the form

$$\frac{dn}{dt} = b_1 Y_{n/s_1} v(s_1, \ldots, s_m) =: \mu(s_1, \ldots, s_m) n$$

with the specific bacterial growth rate

$$\mu(s_1, \ldots, s_m) = \frac{b_1 Y_{n/s_1}}{n} v(s_1, \ldots, s_m) = \frac{b_1 Y_{n/s_1}}{n} v_{max} \frac{c_m}{\alpha n}.$$

If we denote the maximum growth rate, which is asymptotically approached when all substrates are available in excess, by

$$\mu_{max} := \frac{b_1 Y_{n/s_1}}{n} v_{max} = b_1 Y_{n/s_1} k_f \alpha,$$

the specific growth rate of the bacteria is given by

$$\mu(s_1, \ldots, s_m) = \mu_{max} \frac{v(s_1, \ldots, s_m)}{v_{max}} = \mu_{max} \frac{c_m}{\alpha n}. \tag{2.37}$$

The notation

$$\frac{1}{Y_{n/s_i}} := \frac{b_i}{b_1} \frac{1}{Y_{n/s_1}}, \qquad i = 2, \ldots, m$$

then yields model (2.25)/(2.26) with growth rate (2.37).

To sum up, the model derived above is based on a generalization of the assumptions in the single-substrate case, i.e. the assumptions 1-4 on page 15 are generalized for m substrates.

2.3.3 Comparison and Examples

It is of interest to know whether the bacterial growth rate (2.27), which can be found in various articles for different numbers of involved substrates, and the growth rate (2.37), which has been derived above, are equal for all $m \in \mathbb{N}$.

For a better comparison we first write the growth rate (2.37) in the form

$$\mu(s_1,\dots,s_m)=\mu_{max}\frac{\prod_{j=1}^{m}s_j}{\prod_{j=1}^{m}(s_j+K_j)+L(s_1,\dots,s_m)}. \tag{2.38}$$

We are aware of the fact that the constants K_j can be chosen arbitrarily from the mathematical point of view since the differences to the biologically reasonable choice as half-saturation or Monod constants are included in L. In the following we assume that the Monod constants K_j can be chosen by equalizing those products of both denominators of (2.37) and (2.38) that include only one single constant K_j multiplied by one or more substrates[8]. This assumption yields the constants

$$K_j=\begin{cases} B_{j\,m-j+1} & =\frac{k_f}{k_j}b_j, & j=1,\dots,m-1\\ A_m & =\frac{k_{-m}+k_f}{k_m}b_m, & j=m, \end{cases}$$

i.e. just as in the single-substrate case the Monod constants equal the Michaelis constants (2.34), which are related to the growth limiting enzymatic reaction.

With the above definition of the Monod constants the function L is given by

$$L(s_1,\dots,s_m)=\sum_{i=1}^{m-1}\Big(\tilde{A}_i\prod_{j=1}^{i-1}s_j\Big)+\sum_{i=1}^{m-1}\sum_{l=2}^{m-i}\Big(\tilde{B}_{il}\prod_{\substack{j=1\\ j\notin\{i,\dots,m-l+1\}}}^{m}s_j\Big)-Q(s_1,\dots,s_m)$$

with

$$\tilde{A}_i=K_m\left(\prod_{j=i}^{m-1}K_j^d-\prod_{j=i}^{m-1}K_j\right)=\frac{k_{-m}+k_f}{k_m}b_m\left(\prod_{j=i}^{m-1}\frac{k_{-j}}{k_j}b_j-\prod_{j=i}^{m-1}\frac{k_f}{k_j}b_j\right)$$

$$\tilde{B}_{il}=K_{m-l+1}\left(\prod_{j=i}^{m-l}K_j^d-\prod_{j=i}^{m-l}K_j\right)=\frac{k_f}{k_{m-l+1}}b_{m-l+1}\left(\prod_{j=i}^{m-l}\frac{k_{-j}}{k_j}b_j-\prod_{j=i}^{m-l}\frac{k_f}{k_j}b_j\right).$$

The function Q represents the following sum: It includes all products $\prod_{i=1}^{m}Q_i$ with $Q_i\in\{s_i,K_i\}$ such that there exist indices $1\le j<k<l\le m$ with $K_j s_k K_l$ being part of the product. In other words, this sum describes all index ordered products in which at least one substrate s_l is in between two constants K_j, K_l.

As can be easily seen, the growth rates (2.27) and (2.38) are of the same form if there exist model parameters that ensure $L(s_1,\dots,s_m)=0$.

[8]That this is a biologically reasonable choice follows from the fact that the resulting Monod constants equal the Michaelis constants (2.34).

In order to illustrate the mechanics of (2.38) and compare them with the proposed bacterial growth rates (2.27) in various concrete cases, we list below certain examples.

Example 3 ($m = 1$)**.** The purpose for deriving the general growth rate (2.38) was to consider enzymes that convert more than one substrate into a product. Nevertheless, it can be easily seen that the result is also applicable to bacteria whose growth limiting process is a single-substrate reaction. Hence, the specific growth rate of those bacteria is

$$\mu(s_1) = \mu_{max} \frac{s_1}{s_1 + K_1}$$

with

$$K_1 = \frac{k_{-1} + k_f}{k_1} b_1.$$

Due to the fact that $L(s_1) = 0$, both the growth rates (2.27) and (2.38) have the same structure and can be equalized by an appropriate choice of model parameters. This was already shown in section 2.2 under the assumption that in the enzymatic reaction only one molecule of substrate binds to an enzyme. Note that the above derivation generalizes this assumption: Taking into account the stoichiometric constant b_1 allows to consider enzymes that react with more than one molecule of substrate.

Example 4 ($m=2$)**.** The specific growth rate of bacteria whose growth depends on two substrates is

$$\mu(s_1, s_2) = \mu_{max} \frac{s_1 s_2}{(s_1 + K_1)(s_2 + K_2) + L(s_1, s_2)}$$

with

$$L(s_1, s_2) = \tilde{A}_1$$

and parameters

$$K_1 = \frac{k_f}{k_1} b_1 \qquad \tilde{A}_1 = \frac{(k_{-2} + k_f)(k_{-1} - k_f)}{k_1 k_2} b_1 b_2$$
$$K_2 = \frac{k_{-2} + k_f}{k_2} b_2.$$

This growth rate is identical in form to (2.27), which was suggested by Megee in [Meg72] for the growth of *Lactobacillus casei* by the availability of glucose and riboflavin, if $L(s_1, s_2) = 0$, and hence $k_{-1} = k_f$ (see also [Bad78]). In terms of enzyme kinetics, this equality means that in one time step as many complexes $S_1^* S_2^* E$ are converted into product as complexes $S_1^* E$ fall apart into S_1^* and E. This is consistent with the assumption $\frac{k_{-1}}{k_f} = O(1)$, which is made in the asymptotic analysis of the limiting enzymatic reactions in appendix A.2.

Example 5 ($m = 3$)**.** For dependency on three substrates we get the overall growth rate

$$\mu(s_1, s_2, s_3) = \mu_{max} \frac{s_1 s_2 s_3}{(s_1 + K_1)(s_2 + K_2)(s_3 + K_3) + L(s_1, s_2, s_3)}$$

with the function

$$L(s_1, s_2, s_3) = \tilde{A}_1 + \tilde{A}_2 s_1 - K_1 K_3 s_2 + \tilde{B}_{12} s_3$$

and the parameters

$$K_1 = \frac{k_f}{k_1} b_1 \qquad \tilde{A}_1 = \frac{(k_{-3} + k_f)(k_{-1}k_{-2} - k_f^2)}{k_1 k_2 k_3} b_1 b_2 b_3$$

$$K_2 = \frac{k_f}{k_2} b_2 \qquad \tilde{A}_2 = \frac{(k_{-3} + k_f)(k_{-2} - k_f)}{k_2 k_3} b_2 b_3$$

$$K_3 = \frac{k_{-3} + k_f}{k_3} b_3 \qquad K_1 K_3 = \frac{k_f (k_{-3} + k_f)}{k_1 k_3} b_1 b_3$$

$$\tilde{B}_{12} = \frac{k_f (k_{-1} - k_f)}{k_1 k_2} b_1 b_2.$$

This growth rate equals in form (2.27), which is used in [Wid88], if $L(s_1, s_2, s_3) = 0$. In order to ensure that all coefficients in the function L are zero, the rate constants have to satisfy

$$k_{-1} = -k_{-3} = k_f \quad \vee \quad k_{-2} = k_f = 0 \quad \vee \quad k_{-3} = k_f = 0,$$

which is inconsistent with the positivity of all rate constants k_i, $i \in \{\pm 1, \pm 2, \pm 3, f\}$. Consequently, the specific growth rates (2.27) and (2.38) cannot be equalized by a biologically reasonable choice of model parameters.

Considering the above examples and some further analyses, which are stated below, we can phrase the following results concerning the equivalence of the proposed model (2.25)-(2.27) and the model (2.25)/(2.26)/(2.37), derived in this chapter, for bacterial growth depending on $m \in \mathbb{N}$ substrates:

- $m = 1$: The bacterial growth rates (2.27) and (2.37) are of the same form and can be equalized by an appropriate choice of model parameters (see section 2.2 and example 3 in the current section).
- $m = 2$: The bacterial growth rates (2.27) and (2.37) are of the same form if, and only if, the rate constants of the growth limiting enzymatic reaction satisfy $k_{-1} = k_f$ (see example 4 in the current section).
- $m > 2$: The bacterial growth rates (2.27) and (2.37) are unequal (see example 5 for $m = 3$ in the current section).

Proof. The growth rates (2.27) and (2.37) have the same form if, and only if, there exist constants $K_i > 0$ $(i = 1, \ldots, m)$ such that the denominators only differ by a positive multiplier $a > 0$:

$$a \cdot \prod_{i=1}^{m}(s_i + K_i) = \sum_{i=1}^{m}\left(A_i \prod_{j=1}^{i-1} s_j\right) + \sum_{i=1}^{m-1}\sum_{l=2}^{m-i+1}\left(B_{il}\prod_{\substack{j=1\\ j\notin\{i,\ldots,m-l+1\}}}^{m} s_j\right) + \prod_{j=1}^{m} s_j.$$

This is not the case for $m > 2$ since the left-hand side of the equation includes every single s_i $(i = 1, \ldots, m)$ multiplied by positive constants, whereas on the right-hand side only s_1 and s_m occur without multiplication by other substrates. □

According to the above results, the assumptions 1-4 on page 15 generalized for m substrates are not sufficient to explain the bacterial growth model (2.25)-(2.27) for $m > 2$. Consequently, either the growth rate (2.27), which is used in various articles, is based on assumptions that differ fundamentally from the ones that are made in this thesis, or the additional simplification $L(s_1, \ldots, s_m) = 0$, which can not be justified from a biological or chemical point of view, is implicitly included in its derivation.

Remark 1. In the above derivation of the bacterial growth rate we assumed that the substrate uptake enzyme follows an ordered sequential kinetic mechanism. Assuming either a random ordered or a ping-pong mechanism yields much more complicated rate equations for the enzymatic reactions, and therefore more complex bacterial growth rates. According to [Bis08, Las87] the curves related to those rates differ in general fundamentally to those related to an ordered sequential mechanism. Nevertheless, making the additional assumption that in the enzymatic reaction all reaction steps except the product yielding ones are in equilibrium (*rapid equilibrium assumption*) yields simplified rate equations of similar structure to (2.33) (see [Bis08] for a random sequential mechanism for $m = 2$ and ping-pong mechanisms for $m = 2, 3$). The resulting bacterial growth rates are therefore similar to (2.38) with slightly different functions $L(s_1, \ldots, s_m)$. This might result in different statements about the equality of the proposed model (2.25)-(2.27) and the model based on a random sequential or ping-pong mechanism under the additional rapid equilibrium assumption for $m \in \mathbb{N}$.

2.4 Bioremediation

In the previous section we derived a mathematical model for the growth of bacteria and the associated degradation of their main food sources. The basic aspect of a bioremediation process is therefore described by this model so that just minor adjustments remain to be done in order to convert the bacterial growth model into a bioremediation model.

2.4.1 Expansion

Up to now we have only taken into account changes in time, i.e. we have assumed that the concentrations in the observed area are constant. Now, we will also consider spatial changes. More precisely, we consider the case of advection in which the substrates S_i are transported with a constant velocity u_i, while the bacteria are supposed to be immobile. If we assume that the concentrations are constant vertical to the direction of flow, it is sufficient to consider a one-dimensional model. The concentrations therefore depend on one space variable $x \in \mathbb{R}$ and time $t \in \mathbb{R}$. In connection with the spatial behavior we also take into account the porosity of the underlying medium via the porosity constant $\Phi \in [0,1]$.

Furthermore, we assume that the bacteria decay with rate R in the absence of the substrates.

These assumptions yield the bioremediation model

$$\Phi \frac{\partial}{\partial t} s_i + u_i \frac{\partial}{\partial x} s_i = -\frac{1}{Y_{n/s_i}} \mu(s_1, \ldots, s_m) n, \qquad i = 1, \ldots, m \tag{2.39}$$

$$\frac{\partial}{\partial t} n = \big(\mu(s_1, \ldots, s_m) - R\big) n \tag{2.40}$$

with growth rate (2.38).

2.4.2 Non-dimensionalization

For further analyses we will non-dimensionalize[9] the above bioremediation model. In order to obtain a specific structure of the dimensionless model, which will be specified later, we choose the scaling

$$s_i = K_i \bar{s}_i, \qquad t = t_r \bar{t},$$
$$n = \frac{\Phi}{\sum_{j=1}^{m} \frac{1}{K_j Y_{n/s_j}}} \bar{n}, \qquad x = x_r \bar{x}$$

with dimensionless variables denoted by bars and with reference parameters t_r and x_r. The scaled version of (2.39)/(2.40) reads

$$\frac{\partial}{\partial \bar{t}} \bar{s}_i + \bar{u}_i \frac{\partial}{\partial \bar{x}} \bar{s}_i = -\frac{1}{\bar{Y}_{\bar{n}/\bar{s}_i}} \bar{\mu}(\bar{s}_1, \ldots, \bar{s}_m) \bar{n}, \qquad i = 1, \ldots, m \tag{2.41}$$

$$\frac{\partial}{\partial \bar{t}} \bar{n} = \left(\sum_{j=1}^{m} \frac{1}{\bar{Y}_{\bar{n}/\bar{s}_j}} \bar{\mu}(\bar{s}_1, \ldots, \bar{s}_m) - \bar{R} \right) \bar{n} \tag{2.42}$$

with the dimensionless parameters

$$\bar{u}_i = \frac{t_r}{\Phi x_r} u_i, \qquad \frac{1}{\bar{Y}_{\bar{n}/\bar{s}_i}} = \frac{t_r \mu_{max}}{K_i \sum_{j=1}^{m} \frac{1}{K_j Y_{n/s_j}}} \frac{1}{Y_{n/s_i}}, \qquad \bar{R} = t_r R$$

[9] The units of all variables and parameters used in this process are stated in table 2.1.

and the notation

$$\bar{\mu}(\bar{s}_1,\ldots,\bar{s}_m)=\frac{\mu(K_1\bar{s}_1,\ldots,K_m\bar{s}_m)}{\mu_{max}}=\frac{\prod_{j=1}^m \bar{s}_j}{\prod_{j=1}^m(\bar{s}_j+1)+\bar{L}(\bar{s}_1,\ldots,\bar{s}_m)} \tag{2.43}$$

with

$$\bar{L}(\bar{s}_1,\ldots,\bar{s}_m)=\frac{L(K_1\bar{s}_1,\ldots,K_m\bar{s}_m)}{\prod_{j=1}^m K_j}. \tag{2.44}$$

The specific scaling $s_{ir}=K_i$ ensures that the dimensionless parameters $\frac{K_i}{s_{ir}}$ in the denominator of (2.43) are replaced by 1. This results in a reduction of the number of parameters that have to be considered, compared to other choices of s_{ir}. The scaling for n yields that the sum of the right-hand sides of all differential equations has the simple form $-\bar{R}\bar{n}$. The fact that the particular reference parameters are not necessarily estimates of the variables' maximum (see (i) in appendix A) does not present problems to further analyses since we will neither compare orders of magnitude of different parameters, nor neglect terms.

In the subsequent chapters we focus on the analysis of the bioremediation model (2.41)-(2.44) for $m=1$ and $m=2$ substrates. For this reason we state these two models explicitly in the following examples, where we omit the bars, which denote the dimensionless variables and parameters, for simplicity of notation.

Example 6 ($m=1$)**.** For bacterial growth depending on one substrate the dimensionless bioremediation model (2.41)-(2.44) is given by

$$\frac{\partial}{\partial t}s_1+u_1\frac{\partial}{\partial x}s_1=-\frac{1}{Y_{n/s_1}}\mu(s_1)n \tag{2.45}$$

$$\frac{\partial}{\partial t}n=\left(\frac{1}{Y_{n/s_1}}\mu(s_1)-R\right)n \tag{2.46}$$

with

$$\mu(s_1)=\frac{s_1}{s_1+1}. \tag{2.47}$$

Example 7 ($m=2$)**.** Bioremediation by bacteria whose growth depends on two substrates is described by the dimensionless model

$$\frac{\partial}{\partial t}s_1+u_1\frac{\partial}{\partial x}s_1=-\frac{1}{Y_{n/s_1}}\mu(s_1,s_2)n \tag{2.48}$$

$$\frac{\partial}{\partial t}s_2+u_2\frac{\partial}{\partial x}s_2=-\frac{1}{Y_{n/s_2}}\mu(s_1,s_2)n \tag{2.49}$$

$$\frac{\partial}{\partial t}n=\left(\left(\frac{1}{Y_{n/s_1}}+\frac{1}{Y_{n/s_2}}\right)\mu(s_1,s_2)-R\right)n. \tag{2.50}$$

From now on we assume $k_{-1} = k_f$ for the rate constants of the underlying enzymatic reaction so that the dimensional specific growth rates (2.27) and (2.37) are equal (for more details we refer to example 4 on page 24). The dimensionless growth rate is therefore given by

$$\mu(s_1, s_2) = \frac{s_1}{s_1 + 1} \frac{s_2}{s_2 + 1}. \tag{2.51}$$

This model is very similar to the one proposed in [Ode93] if we neglect diffusion. The main difference is the assumption of Odencrantz et al. that there exists a positive background concentration of bacteria, which causes an additional term in the last differential equation. The impact of this term is so far reaching that the traveling wave analyses in [Mur98, Log01] are not applicable to our model such that independent studies are required.

2.5 Conclusions

The main component of any bioremediation model is given by the growth rate of the bacteria that are involved in the degradation process. This growth rate is in turn closely linked to the rate of particular enzymatic reactions taking place inside the bacterial cells. For this reason the first step in deriving a bioremediation model is the analysis of enzymatic reactions and bacterial growth.

As a consequence of the above correlations we first derived the rate equation of specific enzymatic reactions that involve a general number $m \in \mathbb{N}$ of substrates. For $m = 1$, this has already been done by Michaelis and Menten, as well as by Briggs and Haldane, whose results are very similar, although they are based on different assumptions (see [Mic13, Bri25]). For $m > 1$, a number of approaches exist in the literature to compute the rate equation of complex enzymatic mechanisms, which usually attempt to avoid the direct solution of equations. These approaches have been used to derive rate equations for specific kinetic mechanisms and for various fixed numbers of substrates. In addition, a general rate equation for an arbitrary number of substrates occurs in the literature; see [Hem07]. However, the derivation of this formula, as well as the underlying assumptions, and in particular the specification of the kinetic mechanism under consideration, are missing. In the present chapter we derived the rate equation of a specific kinetic mechanism, namely of an ordered sequential one, satisfying a generalization of the quasi-steady-state assumption by Briggs and Haldane, by solving a set of equations directly. The resulting formula is of similar structure to the one proposed in [Hem07], but they differ for $m > 2$ (for conclusions about this fact see the discussion below).

In addition to the derivation of the rate equation, we studied the enzymatic reactions under consideration by means of asymptotic analyses in order to specify the meaning and the validity of the rate equations based on the different

assumptions of Michaelis/Menten and Briggs/Haldane. Various asymptotic approaches related to the quasi-steady-state assumption of Briggs and Haldane for single-substrate reactions can be found in the literature; see for example [Seg88, Seg89, Din08] and the references therein. However, to the best of our knowledge, neither asymptotic analyses concerning the equilibrium assumption of Michaelis and Menten, nor asymptotic analyses of multi-substrate reactions currently exist in the literature. These analyses show that the equations derived by Michaelis/Menten and Briggs/Haldane, as well as the equation derived for multi-substrate reactions, hold after a short initial layer, as long as the substrate concentrations are large enough.

Based on the rate equation of the underlying multi-substrate enzyme reaction, a bacterial growth rate could be determined, and a bacterial growth model set up. For $m = 1$ involved substrate, [Pir90] presented certain assumptions that explain the empirically found growth rate proposed in [Mon42]. For $m > 1$, growth rates for various fixed numbers, as well as for a general number of involved substrates, have been presented by different authors; see for example [Meg72, Wid88, Ben84, Hem07]. They are typically based on a simple multiplication of single-substrate growth rates, but explanations and specific assumptions that back this suggestion up are not declared. Based on a generalization of Pirt's assumptions for the single-substrate case, and concentrating on a specific kinetic mechanism of the limiting enzymatic reaction, namely an ordered sequential one, we propose a bacterial growth rate that is applicable to any number of involved substrates. This formula is similar to the multiplicative one mentioned above, but while both growth rates can be equalized for $m = 2$ by stating certain assumptions on the rate constants in the underlying enzymatic reaction (see [Bad78]), they are different for $m > 2$. This leads us to the conclusion that the growth rates suggested by [Wid88, Ben84, Hem07] and others are either based on assumptions that differ from the ones made in this chapter, or alternatively that these authors implicitly include a simplification, namely neglecting an additional term, which cannot be justified by biological or chemical arguments.

In the final step we extended the derived bacterial growth model to a bioremediation model by taking into account spatial changes and environmental properties. In order to compare the resulting model to others, we note that a variety of different bioremediation models exist in the literature; see for example [Bor86, Ode93, Xin98, Cir99, Klö02, Che06] and the references therein. Most of these models describe a degradation of $m = 2$, a few of $m = 3, 4$ substrates, where the commonly used bacterial growth rate is given by the multiplication of single-substrate growth rates mentioned above. The model derived in this thesis therefore differs from other models for $m > 2$, at least with respect to the growth rates, but as a matter of fact also in relation to other factors, such as consideration of diffusion or specific properties of particular bacteria. In general,

the bioremediation models in the literature show a large variation in complexity, where the model presented in [Ode93] for $m = 2$ substrates is outstanding for its relative simplicity while capturing the main aspects of bioremediation. If we neglect diffusion in that model and take into account a specific assumption about the rate constants in the limiting enzymatic reaction, this model bears a close resemblance to the model presented in this thesis for $m=2$. But nevertheless, the remaining small difference, namely the assumption of a positive background concentration of bacteria, and hence the occurrence of an additional term in the rate equation for the biomass, has a large impact on the analysis of the two models and requires different studies.

	description	units
N	bacteria	cells
S_i	substrate	mol
S_i^*	b_i molecules of substrate S_i ($S_i^* = b_i S_i$)	mol
P	intermediate product in the metabolism	mol
E	free enzyme	mol
E_0	total enzyme	mol
$S_1^* \dots S_i^* E$	complex of one enzyme and one unit of $S_1^*, \dots, S_i^*$	mol
n	concentration of bacteria	$\frac{\text{cells}}{\text{m}^3}$
s_i	concentration of substrate S_i	$\frac{\text{mol}}{\text{m}^3}$
s_i^*	concentration of S_i^* ($s_i^* = 1/b_i s_i$)	$\frac{\text{mol}}{\text{m}^3}$
p	concentration of product	$\frac{\text{mol}}{\text{m}^3}$
e	concentration of free enzyme	$\frac{\text{mol}}{\text{m}^3}$
e_0	concentration of total enzyme	$\frac{\text{mol}}{\text{m}^3}$
c_i	concentration of the substrate enzyme complex $S_1^* \dots S_i^* E$ ($c_0 := e$)	$\frac{\text{mol}}{\text{m}^3}$
K_i	half saturation concentration of substrate S_i (Michaelis/Monod constant)	$\frac{\text{mol}}{\text{m}^3}$
K_i^d	dissociation constant of complex $S_1^* \dots S_i^* E$	$\frac{\text{mol}}{\text{m}^3}$
v	reaction rate of the enzymatic reaction	$\frac{1}{\text{s}} \frac{\text{mol}}{\text{m}^3}$
v_{max}	maximum reaction rate of the enzymatic reaction	$\frac{1}{\text{s}} \frac{\text{mol}}{\text{m}^3}$
μ	specific growth rate of the bacteria	$\frac{1}{\text{s}}$
μ_{max}	maximum specific growth rate of the bacteria	$\frac{1}{\text{s}}$
b_i	stoichiometric coefficient of substrate S_i	1
Y_{n/s_i}	yield constant of substrate S_i	$\frac{\text{cells}}{\text{mol}}$
α	fraction enzyme of bacteria	$\frac{\text{mol}}{\text{cells}}$
k_i	rate constant for $S_1^* \dots S_{i-1}^* E + S_i^* \to S_1^* \dots S_i^* E$	$\frac{1}{\text{s}} \frac{\text{m}^3}{\text{mol}}$
k_{-i}	rate constant for $S_1^* \dots S_{i-1}^* E + S_i^* \leftarrow S_1^* \dots S_i^* E$	$\frac{1}{\text{s}}$
k_f	rate constant for $S_1^* \dots S_m^* E \to P + E$	$\frac{1}{\text{s}}$
Φ	porosity constant ($\Phi \in [0, 1]$)	1
u_i	transportation speed of substrate S_i	$\frac{\text{m}}{\text{s}}$
R	death rate of the bacteria	$\frac{1}{\text{s}}$
x	space	m
t	time	s

Table 2.1: Notation used in chapter 2

Chapter 3

Existence of traveling waves

This chapter is devoted to the existence of special solutions of the bioremediation model (2.41)-(2.43), namely *traveling waves*. These solutions progress with a constant speed and an unmodified shape. Consequently, they are constant along linear functions in time t and space x, the so-called *characteristics* $x = x_0 + st$, where s denotes the *wave speed*. We can therefore introduce a new "moving" variable $z = x - st$, which represents these linear functions, and write $Q(z) := q(x,t)$ for the traveling wave solution, where $Q(z)$ is called *wave form* or *profile*. The profile can appear in different shapes: If $Q(z)$ is a smooth function that converges to constant values at $\pm\infty$, then the traveling wave is said to be a *wave front*. If the rest states are the same at $\pm\infty$, the traveling wave is called a *pulse*. Furthermore, we refer to spatially-periodic traveling waves as *wave trains*. For more information see [Gri91, Log01, San02].

In the following we will think of injecting constant concentrations of substrates, and hence search for bounded non-negative traveling wave solutions with constant values at plus and minus infinity. In other words, we are interested in the existence of non-negative wave fronts in the bioremediation model (2.41)-(2.43).

Below we will concentrate on the analysis of the single-substrate and double-substrate case, but we will also give an outlook on how to study the existence of traveling waves if an arbitrary number of substrates is involved.

3.1 Single-substrate bioremediation model

In this section we will be concerned with the existence of non-negative traveling wave front solutions of the single-substrate bioremediation model (2.45)-(2.47):

$$\begin{pmatrix} c \\ n \end{pmatrix}_t + \begin{pmatrix} u & 0 \\ 0 & 0 \end{pmatrix} \begin{pmatrix} c \\ n \end{pmatrix}_x = \begin{pmatrix} -\nu\mu_1(c)n \\ (\nu\mu_1(c) - R)\, n \end{pmatrix}, \qquad \mu_1(c) = \frac{c}{c+1}. \tag{3.1}$$

For simplifying reasons we changed the notation slightly compared to chapter 2. The notation used throughout this section is listed in table 3.1 on page 38.

3.1.1 Ansatz

First, we specify the mathematical model that has to be studied for the intended existence analysis. This will be done by a change of variables and the declaration of some assumptions concerning the model parameters.

Traveling wave ansatz

As stated above we change the variables to the "moving" ones

$$z := x - st \quad \text{and} \quad (C, N)(z) = (C, N)(x - st) := (c, n)(x, t).$$

With respect to these variables model (3.1) reads

$$\begin{pmatrix} u - s & 0 \\ 0 & -s \end{pmatrix} \begin{pmatrix} C \\ N \end{pmatrix}_z = \begin{pmatrix} -\nu\mu_1(C)N \\ (\nu\mu_1(C) - R)\, N \end{pmatrix}. \tag{3.2}$$

Its solutions describe any traveling wave solution in (3.1). But due to our specific application we are interested in a particular wave form, namely in non-negative wave fronts. Taking into account that the constant states at $\pm\infty$ have to be critical points of (3.2), we therefore add the constraints

$$0 \leq C, N < \infty \tag{3.3}$$

$$(C, N)(\pm\infty) = (c_\pm, 0) \tag{3.4}$$

with arbitrary values $c_\pm \in \mathbb{R}_0^+$.

In this way we have reduced the problem of finding non-negative wave front solutions of (3.1) to the problem of solving (3.2)-(3.4) for s and (C, N) on $\mathbb{R}$.

Assumptions

For further analyses we will concentrate on a certain case, which is specified by the following assumptions:

(A1) The substrate is injected on the left side and transported to the right, i.e.

$$u > 0.$$

(A2) Due to the biological meaning the substrate concentration that is asymptotically approached for large z shall be smaller than the concentration of the injection. We thus assume

$$c_- > c_+.$$

(A3) We are only interested in traveling but not standing waves[1], i.e.

$$s \neq 0.$$

[1] For standing waves see remark 2 on page 39.

3.1.2 Analysis

Since (3.2) is a planar autonomous system of ordinary differential equations, we can study its solutions in the phase plane. In this way we will show the existence of a solution of (3.2)-(3.4) by demonstrating that for certain concentrations[2] $c_- =: \bar{c}_-$ there exist values of s that are related to a unique non-negative trajectory connecting the two critical points $(\bar{c}_-, 0)$ and $(c_+, 0)$.

In order to simplify the subsequent phase plane analysis, we will first present a *necessary condition* for the existence of a solution of (3.2)-(3.4): If there exists a non-negative connection of two different critical points, then the biomass concentration asymptotically decays from positive values to zero, i.e.

$$\begin{aligned} N_z &> 0 \quad \text{as } z \to -\infty \\ N_z &< 0 \quad \text{as } z \to +\infty. \end{aligned}$$

With respect to the assumptions and constraints we get the equivalent conditions

$$s < 0 \quad \wedge \quad \mu_1(c_+) < \frac{R}{\nu} < \mu_1(\bar{c}_-) \tag{3.5}$$

and

$$s < 0 \quad \wedge \quad 0 < \nu - R \quad \wedge \quad 0 \leq c_+ < \frac{R}{\nu - R} < \bar{c}_-. \tag{3.6}$$

Their meaning can be clarified by means of figure 3.1.

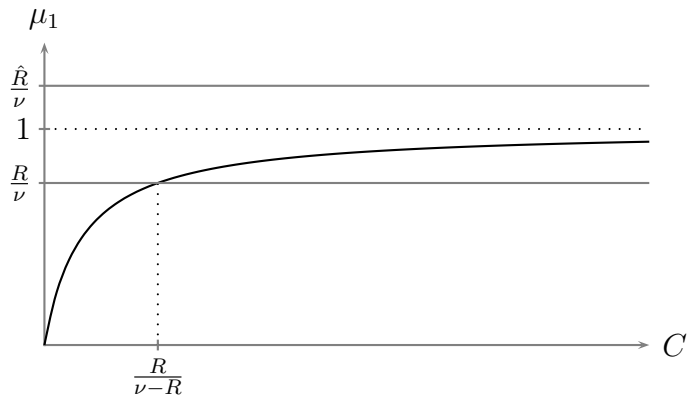

Figure 3.1: Specific growth rate μ_1 for different values of R

For studying the solutions of (3.2) in the phase plane we analyze the differential equation

$$\frac{dN}{dC} = \frac{u - s}{s} \left(1 - \frac{R}{\nu} \frac{C + 1}{C} \right).$$

[2]Throughout this chapter we label limit concentrations that are predefined boundary values by bars, while limit concentrations without bars have to be determined.

The trajectories that have a root in $C = \bar{c}_-$ are given by

$$N(C) := \frac{u-s}{s}\frac{R}{\nu}\left(\frac{\nu-R}{R}(C-\bar{c}_-) - \ln\left|\frac{C}{\bar{c}_-}\right|\right).$$

Considering the assumptions and the first and second part of necessary condition (3.6) yields that the trajectories are strictly concave on $\mathbb{R}^+$ with a non-negative maximum. Selected trajectories for two different values of s are visualized in figure 3.2, where the arrows indicate the direction of flow.

As can be verified by means of figure 3.2, for $\bar{c}_- > \frac{R}{\nu-R}$ there exist heteroclinic orbits representing solutions of (3.2) that satisfy the constraints (3.3) and (3.4). The necessary condition (3.6), without the requirement on c_+, is therefore a *sufficient condition* for the existence of solutions of (3.2)-(3.4) with respect to (A1)-(A3). The shape of these solutions, and hence the profile of the corresponding traveling wave in (3.1), is shown in figure 3.3 and specified in the following two propositions.

Proposition 1. *Consider model* (3.2)-(3.4) *with* $u > 0$, $\nu > R$ *and a predefined limit* $\bar{c}_- > \frac{R}{\nu-R} =: c^0$. *Then there exists a unique solution of* (3.2)-(3.4) *for every* $s < 0$. *This solution has the following properties:*

(i) $C(z)$ *is monotonically decreasing from* $\bar{c}_-$ *to* c_+, *which is the unique root of* $N(C)$ *in* $(0, c^0)$.

(ii) $N(z)$ *is monotonically increasing on the left and monotonically decreasing on the right of the maximum value and has the limits* $N(\pm\infty) = 0$.

(iii) The total biomass is given by $N_{tot} := \int_{-\infty}^{\infty} N(z)\,dz = \frac{u-s}{R}(\bar{c}_- - c_+)$.

Proof. Statements (i) and (ii) follow directly from the curve sketching of $N(C)$, as indicated above. The formula in (iii) is computed by integrating the sum of both differential equations of model (3.2) from minus to plus infinity and using $N(\pm\infty) = 0$. □

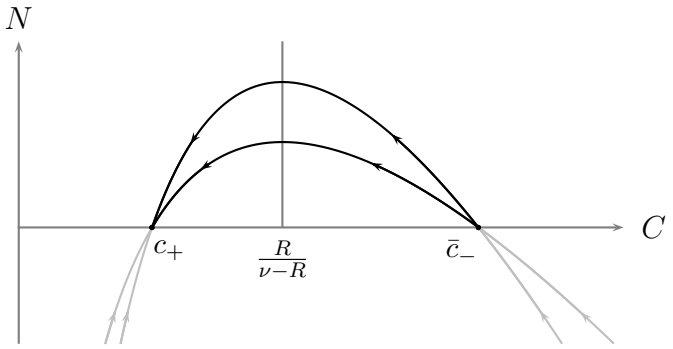

Figure 3.2: Trajectories of (3.2) for $u > 0$, $\nu - R > 0$, $\bar{c}_- > \frac{R}{\nu-R}$ and different values $s < 0$. The black orbits satisfy the constraints (3.3) and (3.4).

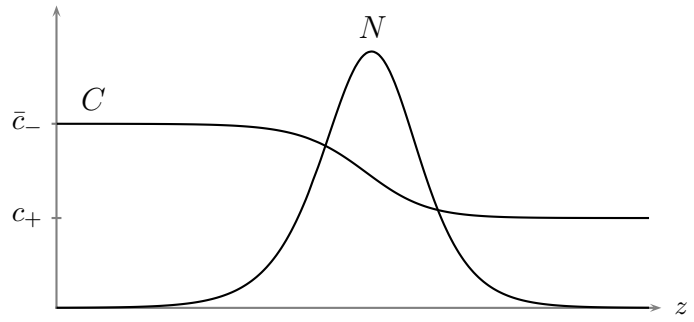

Figure 3.3: Profile of a non-negative traveling wave front in (3.1)

The next proposition specifies the profile $N(z)$, and hence statement (ii) of the above proposition:

Proposition 2. *$N(z)$ is bounded from above by exponentially increasing and decreasing functions. Furthermore, $N(z)$ asymptotically approaches the least of these upper bounds as $z \to \pm\infty$. More precisely, there exist positive constants $K_\pm$ such that*

$$N(z) < K_\pm e^{-\alpha_\pm z}$$

for all $z \in \mathbb{R}$ and

$$N(z) \sim K_\pm e^{-\alpha_\pm z} \tag{3.7}$$

as z tends to $\pm\infty$ with

$$\alpha_\pm = \frac{1}{s}\big(\nu\mu_1(c_\pm) - R\big),$$

where $\alpha_+ > 0$ and $\alpha_- < 0$.

Proof. For the proof, as well as an illustrating figure, we refer to appendix B. □

To sum up, proposition 1 describes the existence of an infinite number of solutions of (3.2)-(3.4) under specific assumptions on the model parameters, each solution related to a pair (s, N_{tot}) satisfying

$$s = u - \frac{R}{\bar{c}_- - c_+} N_{tot} < 0.$$

These solutions represent non-negative traveling wave fronts in model (3.1) that travel with speed s and have the total biomass N_{tot}.

Example 8. Consider model (3.2)-(3.4) with the following parameters[3]:

$$u = 7.81, \qquad \nu = 1.12,$$
$$R = 0.34, \qquad \bar{c}_- = 0.76.$$

[3]In the current and subsequent examples the sets of parameters are chosen to result in qualitative statements, but they are not necessarily close to realistic application data.

Then the unique root of $N(C)$ in $(0, c^0) = (0, 0.44)$ is $c_+ = 0.22$. With respect to proposition 1 there exist solutions related to any combination (s, N_{tot}) satisfying

$$s = 7.81 - 0.63 N_{tot} < 0.$$

These combinations are represented by the black line in figure 3.4.

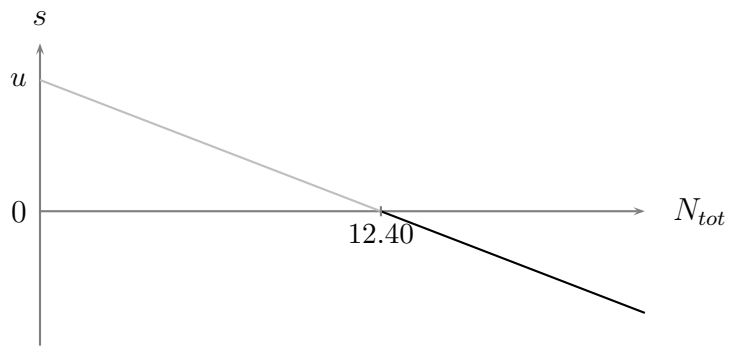

Figure 3.4: Occurring combinations (s, N_{tot}) in example 8

	description[4]
$c(x,t)$	concentration of substrate
$n(x,t)$	concentration of biomass
$C(z)$	concentration of substrate (traveling wave)
$N(z)$	concentration of biomass (traveling wave)
$c_\pm$	limit concentrations of $C(z)$ as z tends to $\pm\infty$
$\bar{c}_-$	predefined limit concentration c_-
$N(C)$	trajectories in the C-N phase plane that have a root in $C = \bar{c}_-$
N_{tot}	total biomass in the wave profile: $N_{tot} = \int_{-\infty}^{\infty} N(z)\,dz$
$-\alpha_\pm$	asymptotic growth rates of $N(z)$ as z tends to $\pm\infty$
u	transportation speed of the substrate
s	traveling wave speed
$\mu_1(c)$	specific growth rate of the biomass
ν	inverse yield constant of the substrate ($\nu = 1/Y_{n/c}$)
R	death rate of the biomass
x	space
z	space along the characteristics: $z = x - st$
t	time

Table 3.1: Notation used in section 3.1

[4]Note that according to subsection 2.4.2 the model under consideration is dimensionless. The descriptions thus correspond to the related dimensional variables and parameters.

Remark 2. Because they require a different treatment, we excluded standing waves, i.e. waves that travel with speed $s = 0$, from the above analysis. It should be mentioned that by a change of variables the problem of finding non-negative standing wave fronts in (3.1) is reduced to the problem of solving (3.2)-(3.4) with $s = 0$ for C and N on $\mathbb{R}$. Analysis in the phase plane yields that the solutions are $(C, N)(z) = (\bar{c}, 0)$ with any $\bar{c} \in \mathbb{R}_0^+$. The profile of the only standing wave fronts in (3.1) is therefore given by constant functions C and N that are related to no biomass in the system, and hence no reduction of the substrate concentration.

3.2 Double-substrate bioremediation model

In this section we will study the existence of non-negative traveling wave fronts in the double-substrate bioremediation model (2.48)-(2.51):

$$\begin{pmatrix} c_o \\ c_s \\ n \end{pmatrix}_t + \begin{pmatrix} u & 0 & 0 \\ 0 & v & 0 \\ 0 & 0 & 0 \end{pmatrix} \begin{pmatrix} c_o \\ c_s \\ n \end{pmatrix}_x = \begin{pmatrix} -\nu_o \mu_2(c_o, c_s) n \\ -\nu_s \mu_2(c_o, c_s) n \\ \big((\nu_o + \nu_s)\, \mu_2(c_o, c_s) - R \big) n \end{pmatrix} \tag{3.8}$$

with dimensionless growth rate

$$\mu_2(c_o, c_s) = \frac{c_o}{c_o + 1} \frac{c_s}{c_s + 1}.$$

Again, for simplifying reasons we changed the notation[5] compared to chapter 2. The notation used throughout this section is listed in table 3.2 on page 54.

3.2.1 Ansatz

In order to detect non-negative traveling wave front solutions of model (3.8), we follow the same approach as in the previous section. First, we will therefore specify the mathematical model that has to be analyzed.

Traveling wave ansatz

With respect to traveling wave solutions we introduce the new variables

$$z := x - st \quad \text{and} \quad (C_o, C_s, N)(z) = (C_o, C_s, N)(x - st) := (c_o, c_s, n)(x, t).$$

We are thus interested in solutions of the model

$$\begin{pmatrix} u - s & 0 & 0 \\ 0 & v - s & 0 \\ 0 & 0 & -s \end{pmatrix} \begin{pmatrix} C_o \\ C_s \\ N \end{pmatrix}_z = \begin{pmatrix} -\nu_o \mu_2(C_o, C_s) N \\ -\nu_s \mu_2(C_o, C_s) N \\ \big((\nu_o + \nu_s)\, \mu_2(C_o, C_s) - R \big) N \end{pmatrix} \tag{3.9}$$

[5] In particular, we assume one substrate to be oxygen, i.e. we concentrate on aerobic bacteria that grow depending on one substrate in the presence of oxygen. For regarding anaerobic bacteria the oxygen can be replaced by any other substrate.

with the constraints

$$0 \leq C_o, C_s, N < \infty \tag{3.10}$$

$$(C_o, C_s, N)(\pm\infty) = (c_{o\pm}, c_{s\pm}, 0) \tag{3.11}$$

with arbitrary limits $c_{o\pm}, c_{s\pm} \in \mathbb{R}_0^+$.

In this manner the problem of finding non-negative traveling wave fronts in the bioremediation model (3.8) is reduced to the problem of solving (3.9)-(3.11) for s and (C_o, C_s, N) on $\mathbb{R}$.

Model reduction

The above model can be reduced by taking into account the conservation law

$$\frac{d}{dz}\left(\nu_s(u-s)C_o - \nu_o(v-s)C_s\right) = 0, \tag{3.12}$$

which involves the first and second differential equation. Integration yields an interdependence of C_o and C_s such that model (3.9)-(3.11) is represented by

$$\begin{pmatrix} u-s & 0 \\ 0 & -s \end{pmatrix}\begin{pmatrix} C_o \\ N \end{pmatrix}_z = \begin{pmatrix} -\nu_o\mu_2(C_o, \tilde{C}_s(C_o))N \\ \big(\left(\nu_o+\nu_s\right)\mu_2(C_o, \tilde{C}_s(C_o)) - R\big)N \end{pmatrix} \tag{3.13}$$

with

$$\tilde{C}_s(C_o) := -\frac{\nu_s(u-s)}{\nu_o(s-v)}(C_o - c_{o-}) + c_{s-} \tag{3.14}$$

and the constraints

$$0 \leq C_o, N < \infty, \quad 0 \leq \tilde{C}_s(C_o) \tag{3.15}$$

$$(C_o, N)(\pm\infty) = (c_{o\pm}, 0). \tag{3.16}$$

The missing conditions $\tilde{C}_s(C_o) < \infty$ and $\tilde{C}_s(c_{o\pm}) = c_{s\pm}$ are covered by the other constraints.

By this approach we could once more reduce the problem of finding non-negative traveling wave fronts in model (3.8): The solutions s and (C_o, N) of (3.13)-(3.16) plus $C_s(z) = \tilde{C}_s(C_o(z))$ represent non-negative wave fronts in (3.8).

Assumptions

For the further analysis we concentrate on the following special case:

(A1) The substrates are injected at opposite sides and transported in different directions. Therefore, u and v have different signs, and without loss of generality we assume an injection of oxygen on the left and of the remaining substrate on the right side, which corresponds to

$$v < 0 < u.$$

(A2) Due to their biological meaning the inflowing substrate concentrations shall be greater than the asymptotically approached ones on the other side. We thus assume

$$c_{o-} > c_{o+} > 0 \quad \text{and} \quad 0 < c_{s-} < c_{s+}.$$

(A3) We are only interested in traveling but not standing waves[6], i.e.

$$s \neq 0.$$

With respect to the above assumptions, as well as the integrated conservation law (3.12), we can state bounds for the wave speed s,

$$v < s < u, \tag{3.17}$$

and hence specify the functions $\tilde{C}_s(C_o)$ and $\tilde{\mu}_2(C_o) := \mu_2(C_o, \tilde{C}_s(C_o))$, which are shown in figure 3.5.

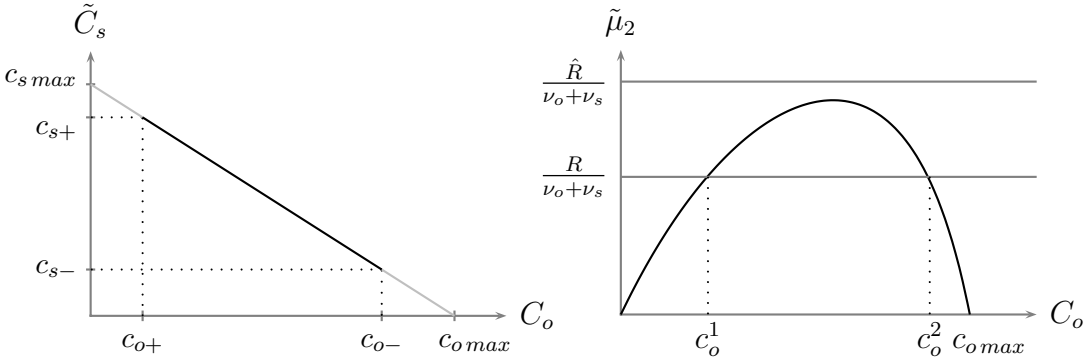

Figure 3.5: Functions $\tilde{C}_s$ and $\tilde{\mu}_2$ for different values of R

3.2.2 Analysis

Below we will analyze model (3.13)-(3.16) with respect to assumptions (A1)-(A3). For mathematical reasons we will first assume that the concentrations c_{o-} and c_{s-} are known, while the concentrations c_{o+} and c_{s+} have to be determined. But with respect to assumption (A1), namely that the substrates are injected at opposite sides, it is of more interest for practical use to study the more complicated case that c_{o-} and c_{s+} are predefined. This will be the objective in the subsequent paragraph.

[6]For standing waves see remark 6 on page 52.

Analysis for predefined values c_{o-}, c_{s-}

Analogous to subsection 3.1.2 we will first state a necessary condition for the existence of solutions of (3.13)-(3.16) with predefined concentrations $\bar{c}_{o-} := c_{o-} > 0$ and $\bar{c}_{s-} := c_{s-} > 0$. With respect to this condition, we will then study the solutions of the model described above in the phase plane.

A *necessary condition* for the existence of a non-negative heteroclinic orbit, and hence for the existence of a solution of (3.13)-(3.16), is

$$\begin{aligned} N_z &> 0 \quad \text{as } z \to -\infty \\ N_z &< 0 \quad \text{as } z \to +\infty. \end{aligned}$$

Due to the assumptions and constraints this condition is satisfied if

$$\begin{aligned} s < 0 \quad \wedge \quad \tilde{\mu}_2(c_{o+}) < \frac{R}{\nu_o + \nu_s} < \tilde{\mu}_2(\bar{c}_{o-}) \qquad \text{or} \\ s > 0 \quad \wedge \quad \tilde{\mu}_2(\bar{c}_{o-}) < \frac{R}{\nu_o + \nu_s} < \tilde{\mu}_2(c_{o+}), \end{aligned} \tag{3.18}$$

and equivalently if

$$\begin{aligned} s < 0 \quad \wedge \quad 0 < c_o^1 < c_o^2 \quad \wedge \quad 0 < c_{o+} < c_o^1 < \bar{c}_{o-} < c_o^2 \qquad \text{or} \\ s > 0 \quad \wedge \quad 0 < c_o^1 < c_o^2 \quad \wedge \quad 0 < c_o^1 < c_{o+} < c_o^2 < \bar{c}_{o-}, \end{aligned} \tag{3.19}$$

where $c_o^{1/2}$ represent the argument values of the intersections between $\tilde{\mu}_2$ and $\frac{R}{\nu_o+\nu_s}$ (see figure 3.5).

The solutions of (3.13) in the phase plane satisfy the differential equation

$$\frac{dN}{dC_o} = \frac{u-s}{s}\left(\frac{\nu_o+\nu_s}{\nu_o} - \frac{R}{\nu_o \tilde{\mu}_2(C_o)}\right).$$

The trajectories that have a root in $C_o = \bar{c}_{o-}$ are given by

$$\begin{aligned} N(C_o) := \frac{u-s}{s}\frac{R}{\nu_o}\Bigg[\left(\frac{\nu_o+\nu_s}{R} - 1\right)(C_o - \bar{c}_{o-}) - \left(1 + \frac{1}{\bar{c}_{s-} + a\bar{c}_{o-}}\right)\ln\left|\frac{c_o}{\bar{c}_{o-}}\right| \\ + \left(\frac{1}{a} + \frac{1}{\bar{c}_{s-} + a\bar{c}_{o-}}\right)\ln\left|1 - a\frac{C_o - \bar{c}_{o-}}{\bar{c}_{s-}}\right|\Bigg] \end{aligned} \tag{3.20}$$

with $-a$ denoting the derivative of $\tilde{C}_s(C_o)$.

Curve sketching of $N(C_o)$ with respect to the assumptions and the second parts of condition (3.19) yields the result that is visualized in figure 3.6. The arrows indicate the direction of flow.

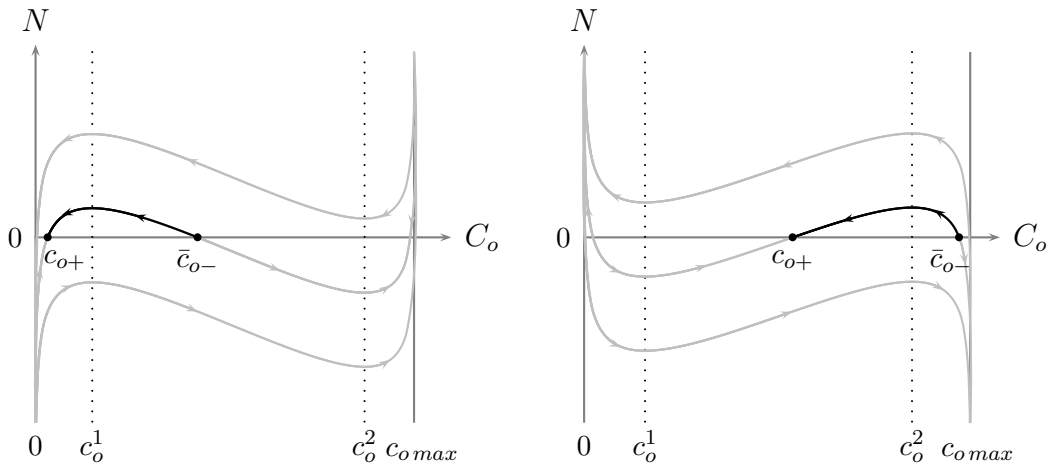

Figure 3.6: Trajectories of (3.13) for $v < 0 < u$ and specific values of $\bar{c}_{o-}, \bar{c}_{s-} > 0$, $v < s < 0$ (left) and $0 < s < u$ (right) such that $0 < c_o^1 < c_o^2$. The black orbits satisfy the constraints (3.15) and (3.16).[7]

The following statements can be verified by means of figure 3.6: If $\bar{c}_{o-}$ satisfies condition (3.19), then for $s < 0$ there exists a heteroclinic orbit representing a solution of (3.13) that satisfies the constraints (3.15) and (3.16). For $s > 0$, a solution like this does not necessarily exist. The first line of condition (3.19), without the requirement on the unknown value c_{o+}, is therefore a *sufficient condition* for the existence of solutions of (3.13)-(3.16) with respect to (A1)-(A3). By contrast, the second line is not sufficient without the requirement on c_{o+}.

The solutions mentioned above, and hence the profiles of the corresponding traveling wave solutions of (3.8), are visualized in figure 3.7.

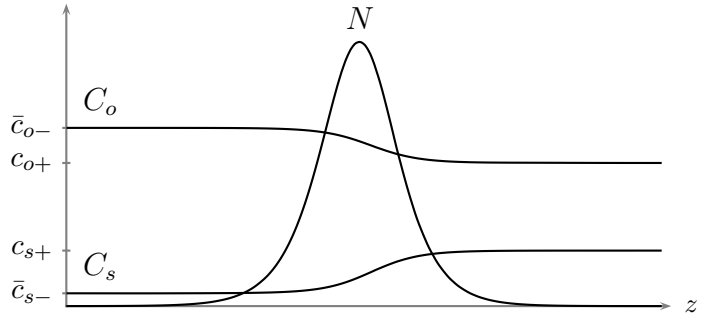

Figure 3.7: Profile of non-negative traveling wave fronts in (3.8)

[7]Note that $c_o^{1/2}$ depend on $\bar{c}_{o-}, \bar{c}_{s-}$ and s. Figure 3.6 shows selected trajectories that have the following property: For a fixed s these trajectories are related to different values $\bar{c}_{o-}, \bar{c}_{s-}$ that all result in the same functions $\tilde{C}_s$ and $\tilde{\mu}_2$, and hence in the same arguments $c_o^{1/2}$ of the intersections between $\tilde{\mu}_2$ and $R/(\nu_o + \nu_s)$.

With this information we can state the following propositions:

Proposition 3. *Consider model* (3.9)-(3.11) *with* $v < s < 0 < u$. *Assume that the limits* $\bar{c}_{o-}$ *and* $\bar{c}_{s-}$ *are given and satisfy* $0 < \bar{c}_{s-}$ *and* $0 < c_o^1 < \bar{c}_{o-} < c_o^2$. *Then there exists a unique solution of* (3.9)-(3.11). *This solution has the following properties:*

(i) $C_o(z)$ *is monotonically decreasing from* $\bar{c}_{o-}$ *to* c_{o+}, *which is the unique root of* $N(C_o)$ *in* $(0, c_o^1)$.

(ii) $C_s(z)$ *is monotonically increasing from* $\bar{c}_{s-}$ *to* c_{s+}, *which is determined by* $\tilde{C}_s(c_{o+})$.

(iii) $N(z)$ *is monotonically increasing on the left and monotonically decreasing on the right of the maximum value and has the limits* $N(\pm\infty) = 0$.

(iv) The total biomass is given by

$$N_{tot} = \frac{u-s}{R}\frac{\nu_o+\nu_s}{\nu_o}(\bar{c}_{o-} - c_{o+}) = \frac{s-v}{R}\frac{\nu_o+\nu_s}{\nu_s}(c_{s+} - \bar{c}_{s-}). \tag{3.21}$$

Proposition 4. *Consider model* (3.9)-(3.11) *with* $v < 0 < s < u$. *Assume that the limits* $\bar{c}_{o-}$ *and* $\bar{c}_{s-}$ *are given and satisfy* $0 < \bar{c}_{s-}$ *and* $0 < c_o^2 < \bar{c}_{o-}$. *Then there exists either no solution or a unique solution of* (3.9)-(3.11). *If there exists a solution, it has the following properties:*

(i) $C_o(z)$ *is monotonically decreasing from* $\bar{c}_{o-}$ *to* c_{o+}, *which is the unique root of* $N(C_o)$ *in* (c_o^1, c_o^2).

(ii) $C_s(z)$ *is monotonically increasing from* $\bar{c}_{s-}$ *to* c_{s+}, *which is determined by* $\tilde{C}_s(c_{o+})$.

(iii) $N(z)$ *is monotonically increasing on the left and monotonically decreasing on the right of the maximum value and has the limits* $N(\pm\infty) = 0$.

(iv) The total biomass is given by

$$N_{tot} = \frac{u-s}{R}\frac{\nu_o+\nu_s}{\nu_o}(\bar{c}_{o-} - c_{o+}) = \frac{s-v}{R}\frac{\nu_o+\nu_s}{\nu_s}(c_{s+} - \bar{c}_{s-}).$$

Proof. The following ideas of proof hold for both propositions 3 and 4: Statements (i)-(iii) follow directly from the curve sketching of $N(C_o)$, as indicated above. The first part of (3.21) is computed by integrating the first and substituting the result into the second differential equation of (3.13). Plugging this result into the integrated equation (3.12) yields the second part of (3.21). □

Analogous to section 3.1 we can specify the properties of $N(z)$:

Proposition 5. *$N(z)$ is bounded from above by exponentially increasing and decreasing functions. Furthermore, $N(z)$ asymptotically approaches the least of these upper bounds as $z \to \pm\infty$. More precisely, there exist positive constants $K_\pm$ such that*

$$N(z) < K_\pm e^{-\alpha_\pm z}$$

for all $z \in \mathbb{R}$ and

$$N(z) \sim K_\pm e^{-\alpha_\pm z}$$

as z tends to $\pm\infty$ with

$$\alpha_\pm = \frac{1}{s}\big((\nu_o + \nu_s)\mu_2(c_{o\pm}, c_{s\pm}) - R\big),$$

where $\alpha_+ > 0$ and $\alpha_- < 0$.

Proof. Based on the reduced model (3.13) the proof is analogous to the one of proposition 2, which is presented in appendix B. □

The solutions described in propositions 3-5 represent non-negative wave fronts in the bioremediation model (3.8) that travel with speed s.

Analysis for predefined values c_{o-}, c_{s+}

As indicated before, for practical use it is of more interest to state some results about traveling wave fronts if besides c_{o-} the concentration c_{s+}, but not c_{s-}, is predefined. This is the objective of the current paragraph.

With respect to (3.21) the traveling wave solutions under consideration satisfy

$$c_{o+} = c_{o-} - \frac{\nu_o}{\nu_o + \nu_s}\frac{R\, N_{tot}}{u - s} \tag{3.22}$$

$$c_{s-} = c_{s+} - \frac{\nu_s}{\nu_o + \nu_s}\frac{R\, N_{tot}}{s - v}. \tag{3.23}$$

The concentration c_{s-} in model (3.13) can therefore be replaced by (3.23), and hence be expressed by c_{s+}. Solving the model that results from this replacement yields information about traveling waves in (3.8) under fixation of c_{o-} and c_{s+}.

Note that by the replacement indicated above not only c_{s+}, but also the total biomass N_{tot} comes into the model. It follows that the integral of $N(z)$ appears in a non-linear way in both differential equations, which is an aggravating circumstance.

First, we will study this problem under fixation of N_{tot}. Afterwards, we will generalize the results and specify conditions for the existence of solutions if the total biomass N_{tot} is not fixed.

Fixation of N_{tot} The approach for solving the problem outlined above is to perceive N_{tot} initially just as a predefined positive model parameter that has to be equalized with the total biomass by an additional constraint:

$$\begin{pmatrix} u-s & 0 \\ 0 & -s \end{pmatrix} \begin{pmatrix} C_o \\ N \end{pmatrix}_z = \begin{pmatrix} -\nu_o \mu_2(C_o, C_s^*(C_o))N \\ \big((\nu_o+\nu_s)\,\mu_2(C_o, C_s^*(C_o)) - R \big) N \end{pmatrix} \tag{3.24}$$

with

$$C_s^*(C_o) = -\frac{\nu_s(u-s)}{\nu_o(s-v)}(C_o - \bar{c}_{o-}) + \underbrace{\left(\bar{c}_{s+} - \frac{\nu_s}{\nu_o+\nu_s}\frac{R\,N_{tot}^*}{s-v} \right)}_{=:c_{s-}^*} \tag{3.25}$$

and the constraints

$$(i) \quad 0 \le C_o, N < \infty, \quad 0 \le C_s^*(C_o) \tag{3.26}$$

$$(ii) \quad (C_o, N)(-\infty) = (\bar{c}_{o-}, 0), \quad (C_o, N)(+\infty) = (c_{o+}, 0), \quad c_{o+} \in \mathbb{R}^+ \tag{3.27}$$

$$(iii) \quad N_{tot} = \int_{-\infty}^{\infty} N(z)\,dz = \frac{u-s}{R}\frac{\nu_o+\nu_s}{\nu_o}(\bar{c}_{o-} - c_{o+}) \stackrel{!}{=} N_{tot}^* \tag{3.28}$$

$$\Leftrightarrow c_{o+} \stackrel{!}{=} \bar{c}_{o-} - \frac{\nu_o}{\nu_o+\nu_s}\frac{RN_{tot}^*}{u-s} =: c_{o+}^*. \tag{3.29}$$

As before, the bars denote the predefined concentrations, while N_{tot}^* is a given parameter[8], and c_{o+}^*, c_{s-}^* are parameters that result from N_{tot}^*. These parameters only have a biological meaning as total biomass and limit concentrations, respectively, if C_o and N satisfy constraint (3.29).

Remark 3. To shorten notation in the remainder of this chapter, we introduce the parameters

$$b_o^* := \frac{\nu_o}{\nu_o+\nu_s}\frac{RN_{tot}^*}{\bar{c}_{o-}}, \qquad d_o := \frac{\mu_2(\bar{c}_{o-}, \bar{c}_{s+}) - \frac{R}{\nu_o+\nu_s}\mu_1(\bar{c}_{o-})}{\mu_2(\bar{c}_{o-}, \bar{c}_{s+}) - \frac{R}{\nu_o+\nu_s}},$$

$$b_s^* := \frac{\nu_s}{\nu_o+\nu_s}\frac{RN_{tot}^*}{\bar{c}_{s+}}, \qquad d_s := \frac{\mu_2(\bar{c}_{o-}, \bar{c}_{s+}) - \frac{R}{\nu_o+\nu_s}\mu_1(\bar{c}_{s+})}{\mu_2(\bar{c}_{o-}, \bar{c}_{s+}) - \frac{R}{\nu_o+\nu_s}}.$$

By means of these parameters we define the following modifications of the transportation speeds u and v, whose precise meaning will be specified below:

$$u_1^* := u - b_o^*, \qquad v_1^* := v + b_s^*,$$
$$u_2^* := u - b_o^* d_o, \qquad v_2^* := v + b_s^* d_s.$$

[8] In the remainder of this chapter, parameters and functions that depend on the predefined value N_{tot}^* are labeled by stars.

In order to solve the above problem, we consider the C_o-N phase plane again. The solutions of (3.24) in the phase plane are given by (3.20), where $\bar{c}_{s-}$ is replaced by c^*_{s-}. For satisfaction of constraint (3.29) it is *necessary* to find a value s such that the trajectory $N^*(C_o)$ has a zero in $\bar{c}_{o-}$, as well as in c^*_{o+}, i.e.

$$N^*\left(\bar{c}_{o-} - \frac{\nu_o}{\nu_o+\nu_s}\frac{R\,N^*_{tot}}{u-s}\right) = 0. \tag{N1}$$

For this purpose we consider the function value $N^*(c^*_{o+})$ as a function of s. This function, denoted by $g^*(s)$, has a root if, and only if, the function

$$f^*(s) := \frac{s}{R}g^*(s) = \left(\frac{R}{\nu_o+\nu_s} - 1\right)N^*_{tot} + \frac{u-s}{\nu_o}\ln\left|\frac{1}{a^*_o(s)}\right| + \frac{s-v}{\nu_s}\ln\left|\frac{1}{a^*_s(s)}\right| + \frac{RN^*_{tot}}{\nu_o+\nu_s}\frac{1}{\bar{c}_{o-}\bar{c}_{s+}}\frac{1}{a^*_o(s)a^*_s(s)-1}\cdot\ln|a^*_o(s)a^*_s(s)|$$

with

$$a^*_o(s) := \frac{c^*_{o+}}{\bar{c}_{o-}} = 1 - \frac{b^*_o}{u-s} \qquad \text{and} \qquad a^*_s(s) := \frac{c^*_{s-}}{\bar{c}_{s+}} = 1 - \frac{b^*_s}{s-v}$$

has a root $s \neq 0$. For a certain set of parameters the functions g^* and f^* are shown in figure 3.8. With respect to the later result (3.31), the visualization, as well as the following remark, are restricted to the interval $I^*_{nc} := (v^*_1, u^*_1)$. Its endpoints correspond to the zeros of $a^*_s(s)$ and $a^*_o(s)$, and hence to the zeros of $c^*_{s-}(s)$ and $c^*_{o+}(s)$.

Remark 4. For $\bar{c}_{o-}$, $\bar{c}_{s+}$, $N^*_{tot} > 0$ and $v < u$, it can be proven that the function f^* is convex in I^*_{nc}. It follows that both f^* and g^* have at most two zeros in I^*_{nc} that might correspond to a solution of (3.24)-(3.29).

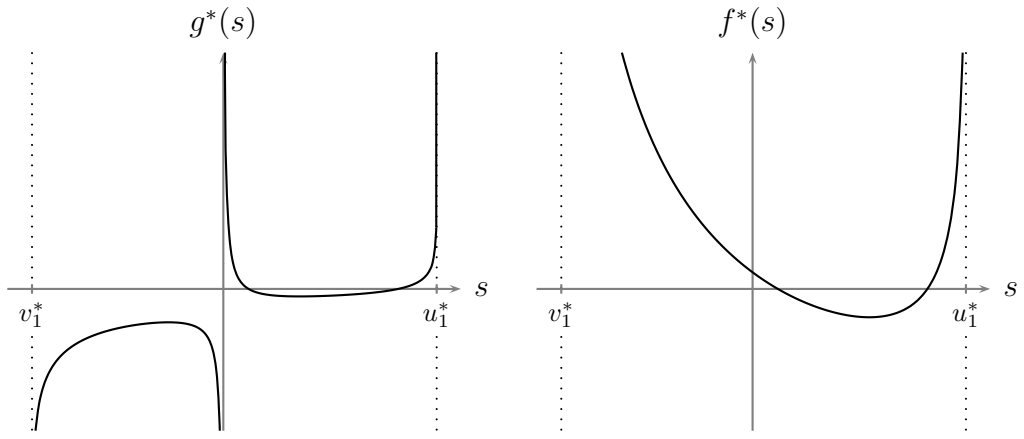

Figure 3.8: g^* and f^* with certain parameters $\bar{c}_{o-}$, $\bar{c}_{s+}$, $N^*_{tot} > 0$ and $v < 0 < u$

As can be verified by means of figure 3.6, not all zeros of $N^*(C_o)$ correspond to solutions of (3.24)-(3.29). For this reason it has to be tested whether the zeros of $N^*(C_o)$ that correspond to the values of s satisfying (N1), are located in the correct interval. For this survey previous results, namely condition (3.19) and propositions 3 and 4, can be used: Since $c^*_{s-} > 0$ is equivalent to $\bar{c}_{o-} < c^*_{o\,max}$, a sufficient condition for the existence of a solution of (3.24)-(3.27), i.e. the above model without the last-mentioned constraint, is

$$\begin{array}{llll} s<0 & \wedge & 0<c^*_{o+}<c^{1*}_o<\bar{c}_{o-}<c^{2*}_o<c^*_{o\,max} & \text{or} \\ s>0 & \wedge & 0<c^{1*}_o<c^*_{o+}<c^{2*}_o<\bar{c}_{o-}<c^*_{o\,max}. & \end{array} \tag{N2}$$

Since all concentrations, except the predefined one $\bar{c}_{o-}$, depend on s, we can determine intervals such that each s in the conjunction of these intervals satisfies (N2):

Proposition 6. *Consider $\bar{c}_{o-}$, $\bar{c}_{s+}$, $N^*_{tot} > 0$ and $v < 0 < u$. Then the following equivalences hold:*

1. *The condition* $s<0 \quad \wedge \quad 0<c^*_{o+}<c^{1*}_o<\bar{c}_{o-}<c^{2*}_o<c^*_{o\,max}$
   is satisfied if, and only if, $s \in \big(\max(v^*_2,u^*_2),\min(0,u^*_1)\big)$.
2. *The condition* $s>0 \quad \wedge \quad 0<c^{1*}_o<c^*_{o+}<c^{2*}_o<\bar{c}_{o-}<c^*_{o\,max}$
   is satisfied if, and only if, $s \in \big(\max(v^*_1,0),\min(v^*_2,u^*_2)\big)$.

Proof. The idea of proof of part 1 is the following: Note that the chain of inequalities is equivalent to

$$0<c^*_{o+}<\bar{c}_{o-}<c^*_{o\,max} \quad \wedge \quad \mu^*_2(c^*_{o+})<\frac{R}{\nu_o+\nu_s}<\mu^*_2(\bar{c}_{o-}) \tag{3.30}$$

with $\mu^*_2(C_o) := \mu_2(C_o, C^*_s(C_o))$. By solving inequalities for s it is shown that

$$0<c^*_{o+}<\bar{c}_{o-}<c^*_{o\,max} \quad \Leftrightarrow \quad s \in (v^*_1,u^*_1) = I^*_{nc}. \tag{3.31}$$

Curve sketching of $\mu^*_2(c^*_{o+})$ and $\mu^*_2(\bar{c}_{o-})$, perceived as functions of s, yields the equivalence of the second part of (3.30) and s being in a certain point set.

Combining both results yields statement 1. Statement 2 is proven analogously. □

From the above results it follows that finding a value s that satisfies (N1) and (N2) is *sufficient* for the existence of a solution of (3.24)-(3.29):

Proposition 7. *Consider model* (3.24)-(3.29) *with $\bar{c}_{o-}$, $\bar{c}_{s+}$, $N^*_{tot} > 0$ and $v < 0 < u$. This model has a solution if there exists a value s that satisfies*

1. $f^*(s) = 0$
2. $s \in \big(\max(v^*_2,u^*_2),\min(0,u^*_1)\big) := I^*_-$ *or*
   $s \in \big(\max(v^*_1,0),\min(v^*_2,u^*_2)\big) := I^*_+$.

The solutions of model (3.24)-(3.29) correspond to non-negative traveling wave fronts in the bioremediation model (3.8).

Example 9. Consider model (3.24)-(3.29) with the parameters

$$\begin{array}{llll} u = \ 4.000, & \nu_o = 1.170, & R = \ 0.360, & \bar{c}_{o-} = 2.240, \\ v = -9.780, & \nu_s = 1.550, & N^*_{tot} = 15.000, & \bar{c}_{s+} = 0.432. \end{array}$$

We seek for values s such that the above problem has a solution.

(i) In the interval $I^*_{nc} = (v^*_1, u^*_1) = (-2.657, 2.963)$ the function f^* has the roots

$$s_1 := 0.351 \quad \text{and} \quad s_2 := 2.427.$$

(ii) Since both roots are positive, they have to satisfy $s \in I^*_+ = (0, 2.407)$. The value s_1 meets the condition, while s_2 does not satisfy it.

Consequently, s_1 corresponds to a solution of (3.24)-(3.29) with the above parameters. This solution represents a traveling wave front in the bioremediation model (3.8) with $N_{tot} = N^*_{tot}$ and $c_{o+} = c^*_{o+} = 1.603$, as shown in figure 3.9 (left). By contrast, s_2 only corresponds to a solution of (3.24)-(3.27), the constraint (3.29) is not satisfied. More precisely, there exists a trajectory connecting $\bar{c}_{o-}$ with a value c_{o+}, namely $c_{o+} = 0.825$, but this limit concentration does not satisfy $c_{o+} = c^*_{o+} = 0.763$. Moreover, the total biomass $N_{tot} = 14.366$ in this solution is not given by the parameter N^*_{tot}. The values c^*_{o+} and N^*_{tot} are therefore just model parameters without applicable meaning.

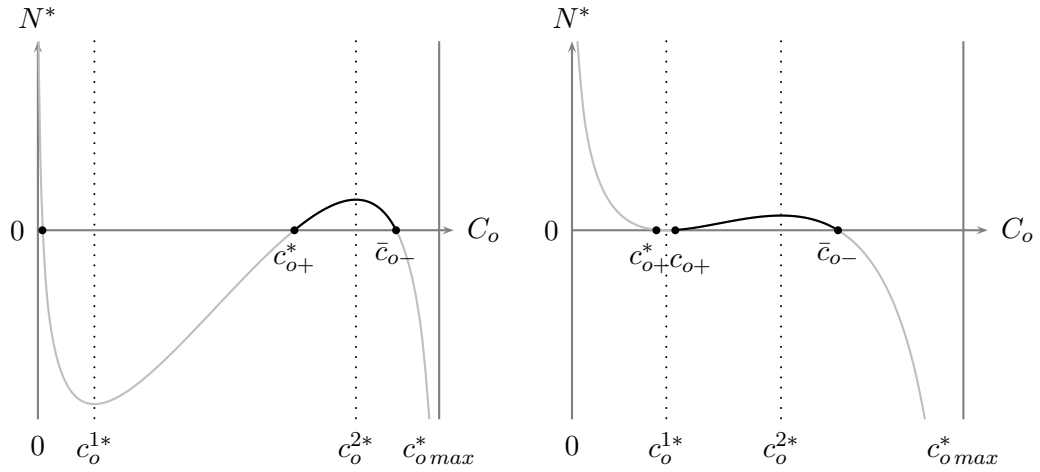

Figure 3.9: Trajectories related to model (3.24)-(3.29) with the parameters given in example 9, $s = s_1$ (left) and $s = s_2$ (right)

No fixation of N_{tot} Below we will generalize the previous results by abandoning the predefinition of total biomass. Accordingly, the issue is to state some results concerning the solutions of the subsequent model, where only the positive concentrations $\bar{c}_{o-}$ and $\bar{c}_{s+}$ are predefined:

$$\begin{pmatrix} u-s & 0 \\ 0 & -s \end{pmatrix} \begin{pmatrix} C_o \\ N \end{pmatrix}_z = \begin{pmatrix} -\nu_o \mu_2(C_o, \hat{C}_s(C_o))N \\ \big((\nu_o + \nu_s)\, \mu_2(C_o, \hat{C}_s(C_o)) - R \big) N \end{pmatrix} \tag{3.32}$$

with

$$\hat{C}_s(C_o) = -\frac{\nu_s(u-s)}{\nu_o(s-v)}(C_o - \bar{c}_{o-}) + \left(\bar{c}_{s+} - \frac{\nu_s}{\nu_o + \nu_s} \frac{R\, N_{tot}}{s-v} \right) \tag{3.33}$$

and the constraints

$$(i) \quad 0 \le C_o, N < \infty, \quad 0 \le \hat{C}_s(C_o) \tag{3.34}$$

$$(ii) \quad (C_o, N)(-\infty) = (\bar{c}_{o-}, 0), \quad (C_o, N)(+\infty) = (c_{o+}, 0), \quad c_{o+} \in \mathbb{R}^+. \tag{3.35}$$

Since proposition 7 is applicable to any positive parameter N^*_{tot}, we can generalize its conditions in order to state results about (3.32)-(3.35). This generalization will be done by regarding the conditions not only depending on s, but also on N_{tot}.

By $f(s, N_{tot})$ we denote the function $f^*(s)$, which now depends on s, as well as on N_{tot}. Thus, the first necessary condition is satisfied by values s and $N_{tot} > 0$ such that $f(s, N_{tot}) = 0$.

For meeting the second condition, and hence the sufficient condition for the existence of a solution, the zeros of f have to be in a restricted domain. This domain is determined by regarding the endpoints of the intervals $I^*_\pm$ as functions of N_{tot}. For example, the boundary v^*_1 for a fixed parameter N^*_{tot}, which is defined on page 46, is replaced by

$$s_{v_1}(N_{tot}) := v + \frac{\nu_s}{\nu_o + \nu_s} \frac{R}{\bar{c}_{s+}} N_{tot}$$

for a variable biomass N_{tot}. By transferring this notation to the other occurring boundaries[9] we can state the following result about the existence of solutions of (3.32)-(3.35), and hence about the existence of non-negative traveling wave fronts in the bioremediation model (3.8):

Proposition 8. *Consider model* (3.32)-(3.35) *with* $\bar{c}_{o-}$, $\bar{c}_{s+} > 0$ *and* $v < 0 < u$. *This model has a solution if there exist values* s *and* $N_{tot} > 0$ *that satisfy*

1. $f(s, N_{tot}) = 0$
2. $(s, N_{tot}) \in \big\{(a,b) : \max\big(s_{v_2}(b), s_{u_2}(b)\big) < a < \min\big(0, s_{u_1}(b)\big)\big\} =: D_-$ *or*
   $(s, N_{tot}) \in \big\{(a,b) : \max\big(s_{v_1}(b), 0\big) < a < \min\big(s_{v_2}(b), s_{u_2}(b)\big)\big\} =: D_+$.

[9] For a list of all occurring functions, as well as their intersections, see appendix B.

Remark 5. The set of points that satisfy the second condition of proposition 8 is on the same side of the N_{tot} axis as the intersection point P_{v_2,u_2} of s_{v_2} and s_{u_2}.

Example 10. Consider model (3.32)-(3.35) with the parameters

$$\begin{aligned} u &= \ \ 4.000, & \nu_o &= 1.170, & R &= 0.360, & \bar{c}_{o-} &= 2.240, \\ v &= -9.780, & \nu_s &= 1.550, & & & \bar{c}_{s+} &= 0.432. \end{aligned}$$

Note that this set of parameters equals the set given in example 9 with the difference that the total biomass N_{tot} is not fixed in this example.

We search for values s and N_{tot} such that the above model has a solution.

(i) The zeros of $f(s, N_{tot})$ in the domain

$$D_{nc} := \big\{(s, N_{tot}) : s_{v_1}(N_{tot}) < s < s_{u_1}(N_{tot})\big\}$$

are represented by black and white dots in figure 3.10, while the domain D_{nc} is illustrated by the entire gray set.

(ii) Since the intersection point $P_{v_2,u_2} = (11.911, 2.735)$ of s_{v_2} and s_{u_2} is above the N_{tot} axis, the set of points satisfying the second condition of proposition 8 is D_+, which is represented by the dark gray set in figure 3.10.

All black and white dots in the dark gray set in figure 3.10 therefore correspond to a solution of (3.32)-(3.35). These solutions represent non-negative traveling wave fronts in (3.8) that travel with speed s and have the total biomass N_{tot}.

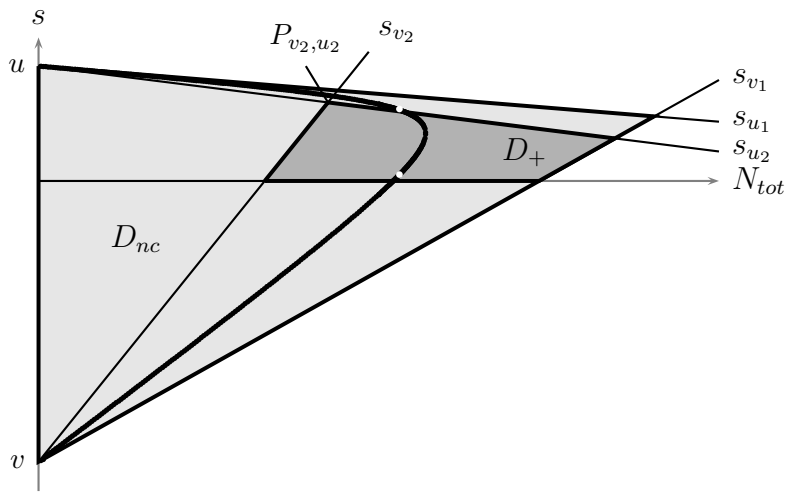

Figure 3.10: Domains D_{nc}, D_+ and zeros of f with parameters given in example 10 (comparable to example 9: white zeros for $N_{tot} = 15$)

Remark 6. Just as in section 3.1, standing waves were excluded from the above analysis. By a change of variables the problem of finding non-negative standing wave fronts in (3.8) can be reduced to the problem of solving (3.13)-(3.16) with $s = 0$ for C_o, N and $C_s = \tilde{C}_s(C_o)$ on $\mathbb{R}$. Phase plane analysis for $v < 0 < u$ yields the solutions $(C_o, C_s, N)(z) = (\bar{c}_o, \bar{c}_s, 0)$ with any $\bar{c}_o, \bar{c}_s \in \mathbb{R}_0^+$. The profile of standing wave fronts in (3.8) is therefore given by constant functions that are related to no biomass in the system, and hence no substrate reduction.

Remark 7. This remark is intended to give an outlook on how to generalize the analysis of traveling wave solutions in the double-substrate bioremediation model to the general case of an arbitrary number of involved substrates.

To simplify notation we first omit the bars in the multi-substrate bioremediation model (2.41)-(2.43) and introduce the notation $\nu_i := Y_{n/s_i}^{-1}$. With respect to the "moving" variables

$$z := x - st \quad \text{and} \quad (C_1, \ldots, C_m, N)(z) := (s_1, \ldots, s_m, n)(x, t)$$

model (2.41)-(2.43) then reads

$$\begin{pmatrix} u_1 - s & & & 0 \\ & \ddots & & \\ & & u_m - s & \\ 0 & & & -s \end{pmatrix} \begin{pmatrix} C_1 \\ \vdots \\ C_m \\ N \end{pmatrix}_z = \begin{pmatrix} -\nu_1 \mu(C_1, \ldots, C_m) N \\ \vdots \\ -\nu_m \mu(C_1, \ldots, C_m) N \\ \big((\nu_1 + \ldots + \nu_m)\mu(C_1, \ldots, C_m) - R\big) N \end{pmatrix}.$$

As easily seen, the above model induces in particular the $m-1$ conservation laws

$$\frac{d}{dz}\big(\nu_i(u_1 - s)C_1 - \nu_1(u_i - s)C_i\big) = 0, \qquad i = 2, \ldots, m.$$

If we integrate these equations, we can express all concentrations by C_1, and hence reduce the model above to

$$\begin{pmatrix} u_1 - s & 0 \\ 0 & -s \end{pmatrix} \begin{pmatrix} C_1 \\ N \end{pmatrix}_z = \begin{pmatrix} -\nu_1 \mu(C_1, \tilde{C}_2(C_1), \ldots, \tilde{C}_m(C_1)) N \\ \big((\nu_1 + \ldots + \nu_m)\mu(C_1, \tilde{C}_2(C_1), \ldots, \tilde{C}_m(C_1)) - R\big) N \end{pmatrix}$$

with

$$\tilde{C}_i(C_1) := \frac{\nu_i}{\nu_1} \frac{u_1 - s}{u_i - s}(C_1 - c_{1-}) + c_{i-}, \qquad i = 2, \ldots, m.$$

For concentrating on non-negative traveling wave fronts we add the constraints

$$0 \le C_1, N < \infty, \qquad 0 \le \tilde{C}_i(C_1), \quad i = 2, \ldots, m$$
$$(C_1, N)(\pm\infty) = (c_{1\pm}, 0)$$

with arbitrary limits $c_{1\pm} \in \mathbb{R}_0^+$.

Thus, the problem of finding non-negative traveling wave fronts in the bioremediation model (2.41)-(2.43) is reduced to the problem of solving the above model. With appropriate assumptions on the speeds u_i and limits $c_{i\pm}$, and hence by a specification of the functions $\tilde{C}_i$ and μ, the solutions of the problem can be studied in the C_1-N phase plane, as presented in the current section for $m = 2$.

3.3 Conclusions

Provided that the model parameters satisfy certain conditions, traveling wave fronts exist in the single-substrate model, related to any speed $s < 0$. They all show the same qualitative profile, namely a monotonically decreasing substrate concentration and a bacteria concentration which is bounded from above by monotonically increasing, as well as decreasing, functions. Beyond these similarities, each wave profile is in particular characterized by a unique value of total biomass, and a characteristic asymptotic behavior of the biomass function.

Likewise, we could establish sufficient conditions on the parameters in the double-substrate model that ensure the occurrence of traveling wave fronts. Here we distinguished two cases that differ in the selection of predefined limit concentrations. Of particular interest for practical use is the case in which the inflowing substrate concentrations are known, while the outflowing ones are not known. All waves resulting from the sufficient condition in this case travel in the same direction with speeds out of a specific interval. Just as in the single-substrate case, the profiles of these solutions have the same quality, i.e. while the oxygen concentration decreases and the substrate concentration increases monotonically, the biomass is bounded from above by monotonically increasing and decreasing functions. But the profiles differ in their asymptotic behavior and total biomass, where each value of total biomass at most occurs twice.

	description[4]
$c_o(x,t)$	concentration of oxygen
$c_s(x,t)$	concentration of substrate
$n(x,t)$	concentration of biomass
$C_o(z)$	concentration of oxygen (traveling wave)
$C_s(z)$	concentration of substrate (traveling wave)
$N(z)$	concentration of biomass (traveling wave)
$\tilde{C}_s(C_o)$	function that expresses C_s depending on C_o
$C_s^*(C_o)$	$\tilde{C}_s(C_o)$ including the predefined parameter N_{tot}^*
$\hat{C}_s(C_o)$	$\tilde{C}_s(C_o)$ including the total biomass N_{tot}
$c_{o\pm}, c_{s\pm}$	limit concentrations of $C_o(z)$ and $C_s(z)$ as z tends to $\pm\infty$
$\bar{c}_{o\pm}, \bar{c}_{s\pm}$	predefined limit concentrations $c_{o\pm}, c_{s\pm}$
$c_o^{1/2}$	argument value of the intersections between $\tilde{\mu}_2(C_o)$ and $\frac{R}{\nu_o+\nu_s}$
$c_{o\,max}$	root of the function $\tilde{C}_s(C_o)$
$c_{s\,max}$	$c_{s\,max} = \tilde{C}_s(0)$
$(\cdot)^*$	concentrations that depend on the predefined parameter N_{tot}^*
$N(C_o)$	trajectories in the C_o-N phase plane that have a root in $C_o = \bar{c}_{o-}$
$N^*(C_o)$	$N(C_o)$ including the predefined parameter N_{tot}^*
$g^*(s)$	$N^*(c_{o+}^*)$ considered as a function of s
$f^*(s)$	$f^*(s) = \frac{s}{R} g^*(s)$
$f(s, N_{tot})$	$f^*(s)$ considered as a function of s, as well as of N_{tot}
N_{tot}	total biomass in the wave profile: $N_{tot} = \int_{-\infty}^{\infty} N(z)\,dz$
N_{tot}^*	predefined parameter
$-\alpha_\pm$	asymptotic growth rates of $N(z)$ as z tends to $\pm\infty$
u	transportation speed of oxygen
v	transportation speed of substrate
s	traveling wave speed
u_i^*, v_i^*	endpoints of admissible intervals for s, depending on N_{tot}^*
$s_{u_i}(N_{tot})$	u_i^* considered as a function of N_{tot}
$s_{v_i}(N_{tot})$	v_i^* considered as a function of N_{tot}
$I_{nc}^*, I_\pm^*$	admissible intervals for s, depending on N_{tot}^*
$D_{nc}, D_\pm$	admissible domains for (s, N_{tot})
$\mu_2(c_o, c_s)$	specific growth rate of the biomass
$\tilde{\mu}_2(C_o)$	$\tilde{\mu}_2(C_o) = \mu_2(C_o, \tilde{C}_s(C_o))$
$\mu_2^*(C_o)$	$\mu_2^*(C_o) = \mu_2(C_o, C_s^*(C_o))$
ν_o	inverse yield constant of oxygen ($\nu_o = 1/Y_{n/c_o}$)
ν_s	inverse yield constant of substrate ($\nu_s = 1/Y_{n/c_s}$)
R	death rate of the biomass
x	space
z	space along the characteristics: $z = x - st$
t	time

Table 3.2: Notation used in section 3.2

Chapter 4

Stability of traveling waves

In this chapter we will study the stability of the traveling waves that have been determined in chapter 3 for the bioremediation models (3.1) and (3.8). The issue is to describe the effect of a small perturbation of the wave front to the further development of the solution, i.e. to find out whether the system will tend to the original traveling wave front or whether a small perturbation causes a drastic change of the solution.

There exist various approaches to investigate the stability of traveling waves. In this context we concentrate on *linearized stability*, i.e. we assume that the perturbations about the traveling waves are sufficiently small such that nonlinear terms are negligible. This approach yields understanding of the evolution of small perturbations to the wave front. In this way it provides a strong indication of (in-)stability, but for rigorous results the studies stated below have to be complemented by a nonlinear stability analysis.

The following linearized stability analysis, which is related to the spectral analysis of specific differential operators, will be supplemented with numerical results.

4.1 Linear perturbation model

Oriented by [Log01], we will stepwise derive a linearized perturbation model that describes the evolution of small perturbations of traveling wave fronts. In order to judge its solutions in terms of stability of the traveling waves, we will subsequently specify the meaning of linearized stability.

In order to discuss both models (3.1) and (3.8) at the same time, we introduce the notation

$$q_t + \tilde{D} q_x = F(q), \tag{4.1}$$

where $q(x,t)$ denotes the concentration vector, $\tilde{D}$ the diagonal velocity matrix and $F(q)$ the function that contains the nonlinear growth terms.[1]

[1] For a list of notations that are used throughout this chapter we refer to table 4.1 on page 94.

Moving coordinate system For looking at model (4.1) in a coordinate system that moves with the speed s of the traveling wave, we regard the solution depending on the variables $z = x - st$ and t:

$$q_t + \big(\tilde{D} - sI\big)q_z = F(q). \tag{4.2}$$

The traveling wave $Q(z)$ is a stationary solution in this coordinate system and satisfies

$$DQ_z = F(Q),$$

where we use the notation $D := \tilde{D} - sI$ for the diagonal matrix, which represents the velocities in the moving coordinate system.

Nonlinear perturbation model Regarding the solution of (4.2) as sum of the traveling wave solution and a small perturbation $p(z,t)$,

$$q(z,t) = Q(z) + p(z,t)$$

with a given initial perturbation $p(z,0)$, we get a nonlinear model for the perturbation:

$$p_t + Dp_z = F(Q+p) - F(Q) \tag{4.3}$$
$$p(z,0) = u(z). \tag{4.4}$$

The solutions $p(z,t)$ of this model represent the evolution of any small initial perturbation $u(z)$ of the traveling wave front $Q(z)$. Hence, for studying the stability of traveling wave fronts, these solutions have to be characterized.

Linear perturbation model Making the assumption that the perturbations $p(z,t)$ of the traveling wave are sufficiently small such that the nonlinear terms are negligible, we can simplify equation (4.3) by linearization around the traveling wave solution $q(z,t) = Q(z)$ or $p(z,t) = 0$, respectively. This yields

$$p_t = \big(J_F(Q) - D\partial_z\big)p =: \mathfrak{L}p \tag{4.5}$$
$$p(z,0) = u(z), \tag{4.6}$$

where J_F denotes the Jacobian matrix of F. The solutions $p(z,t)$ describe the evolution of small initial perturbations $u(z)$ of the traveling wave $Q(z)$ in the linearized system, and hence in a small neighborhood of the wave front. For a linearized stability analysis of the traveling waves, we thus have to characterize these solutions.

According to [Log01] we use the following definition as a measure for stability:

Definition 1. A traveling wave $Q(z)$ is called *stable in a norm* $\|\cdot\|_X$ if there exists a positive constant $\delta > 0$ such that the following statement holds:

$$\|q(z,0) - Q(z)\|_X = \|u(z)\|_X < \delta \quad \Rightarrow \quad \|q(z,t) - Q(z+h)\|_X \xrightarrow{t\to\infty} 0$$

for some $h \in \mathbb{R}$.

Hence, if the solution $q(z,t)$ for all sufficiently small initial perturbations asymptotically approaches some translate of the traveling wave front $Q(z)$, we call the traveling wave *stable*, otherwise *unstable in the norm* $\|\cdot\|_X$.

If $q(z,t)$ and $p(z,t)$, respectively, are the solutions of linearized models, we call the traveling wave *linearly stable* or *linearly unstable in the norm* $\|\cdot\|_X$.

As we will see in the remainder of this chapter, the choice of the norm that measures the closeness is a crucial issue. Related to this problem is the choice of the function space X of admissible perturbations. Two typical options for the function space X and the related norm $\|\cdot\|_X$ are the following:

- $X = L^2(\mathbb{R}, \mathbb{C}^n)$: The Hilbert space $L^2(\mathbb{R}, \mathbb{C}^n)$, equipped with the norm $\|\cdot\|_{L^2}$, consists of square-integrable functions, i.e. of functions that satisfy

$$\|u\|_{L^2}^2 = \int_{-\infty}^{\infty} |u(z)|^2 \, dz < \infty.$$

- $X = L^2_w(\mathbb{R}, \mathbb{C}^n)$: The weighted space $L^2_w(\mathbb{R}, \mathbb{C}^n)$, equipped with the norm $\|\cdot\|_{L^2_w}$, consists of functions that satisfy

$$\|u_w\|_{L^2_w}^2 = \int_{-\infty}^{\infty} |u_w(z)|^2 \bar{w}(z) \, dz < \infty,$$

  where $\bar{w}(z)$ is a positive weight function. Note that by definition this space consists of those functions $u_w(z)$ for which $u(z) := u_w(z)\sqrt{\bar{w}(z)}$ is in $L^2(\mathbb{R}, \mathbb{C}^n)$.

In the following two sections we will study perturbations in both function spaces $L^2(\mathbb{R}, \mathbb{C}^n)$ and $L^2_w(\mathbb{R}, \mathbb{C}^n)$, and hence derive results about the linearized stability of the traveling waves in the norm $\|\cdot\|_{L^2}$, as well as in the norm $\|\cdot\|_{L^2_w}$.

Remark 8. Due to the interpretation of $q(z,t)$ and $p(z,t)$ as concentration vectors, we are particularly interested in real-valued solutions $q(z,t)$ and perturbations $p(z,t)$. We will keep this in mind in the analysis below and interpret the results with respect to this request.

4.2 Perturbations in L^2

The solutions of the linearized perturbation model (4.5)/(4.6), and hence the linearized stability properties of the traveling waves, are characterized by the spectrum of the linear differential operator[2] $\mathfrak{L}$: In particular, a spectral value with positive real part yields instability, while we have stability if all spectral values are localized in the open left half plane. Therefore, the issue of this section is to determine the spectrum of $\mathfrak{L} : L^2(\mathbb{R}, \mathbb{C}^n) \to L^2(\mathbb{R}, \mathbb{C}^n)$ for the bioremediation models (3.1) and (3.8). The approach that is presented below for studying the spectrum of $\mathfrak{L}$ is based on [San02] and the references therein.

4.2.1 Theory

The spectrum of an operator $\mathfrak{L} : X \to Y$ is defined by solvability properties of the equation

$$(\mathfrak{L} - \lambda I)x = y \tag{4.7}$$

for a given $y \in Y$. Since the Fredholm index of a Fredholm operator is also a measure for the solvability of equation (4.7), we can define the spectrum by using Fredholm properties.

To this end we first recall the definition of a Fredholm operator and refer to [San01, Sch02] for further information.

Definition 2 (Fredholm operator)**.** Let X, Y be Banach spaces. A closed, densely defined linear operator $\mathfrak{L} : X \to Y$ is said to be a *Fredholm operator* if

- the range $R(\mathfrak{L})$ is closed in Y,
- the dimension of the nullspace $N(\mathfrak{L})$ is finite: $\dim N(\mathfrak{L}) < \infty$,
- the codimension of the range $R(\mathfrak{L})$ is finite: $\operatorname{codim} R(\mathfrak{L}) < \infty$.

The difference

$$\operatorname{ind}(\mathfrak{L}) := \dim N(\mathfrak{L}) - \operatorname{codim} R(\mathfrak{L})$$

is called the *Fredholm index* of $\mathfrak{L}$.

With respect to definition 2, the spectrum of a closed, densely defined linear operator $\mathfrak{L}$ acting on a Banach space X is defined as follows (see [San02]):

Definition 3 (Spectrum)**.** We say that λ is in the *spectrum* $\sigma(\mathfrak{L})$ of $\mathfrak{L} : X \to X$ if $\mathfrak{L} - \lambda I$ is not invertible, i.e. if the inverse operator does not exist or is not bounded. We say that $\lambda \in \sigma(\mathfrak{L})$ is in the *point spectrum* $\sigma_{pt}(\mathfrak{L})$ if $\mathfrak{L} - \lambda I$ is a Fredholm operator with index zero. The complement $\sigma_{ess}(\mathfrak{L}) := \sigma(\mathfrak{L}) \setminus \sigma_{pt}(\mathfrak{L})$ is called the *essential spectrum* of $\mathfrak{L}$. The complement $\rho(\mathfrak{L}) := \mathbb{C} \setminus \sigma(\mathfrak{L})$ of the spectrum in the complex plane $\mathbb{C}$ is the *resolvent set* of $\mathfrak{L}$.

[2] The operator $\mathfrak{L}$, as well as all operators that will be defined in the remainder of this chapter, are specified in appendix C for both the bioremediation models (3.1) and (3.8).

Remark 9. While there exists a standard definition of the spectrum of an operator $\mathfrak{L}$, i.e. all values λ such that $\mathfrak{L} - \lambda I$ is not invertible, the two subsets of the spectrum, namely the point and essential spectrum, are not uniformly defined. The definitions differ in the classification of the eigenvalues.

Note that all eigenvalues λ of $\mathfrak{L}$, i.e. all values λ such that

$$(\mathfrak{L} - \lambda I)u = 0 \tag{4.8}$$

has a nontrivial solution $u \in X$, belong to the spectrum. Different definitions of the point spectrum include for example either all eigenvalues, or alternatively all isolated eigenvalues with finite multiplicity, while the complement in the set of eigenvalues belongs to the essential spectrum.

According to the particular definition 3 of the spectrum, there is no distinction between isolated and not isolated eigenvalues but a distinction in terms of Fredholm properties (see [San02, Sch02] and figure 4.1). Here, the point spectrum entirely consists of eigenvalues, either isolated or not, while all eigenvalues in the essential spectrum are not isolated.

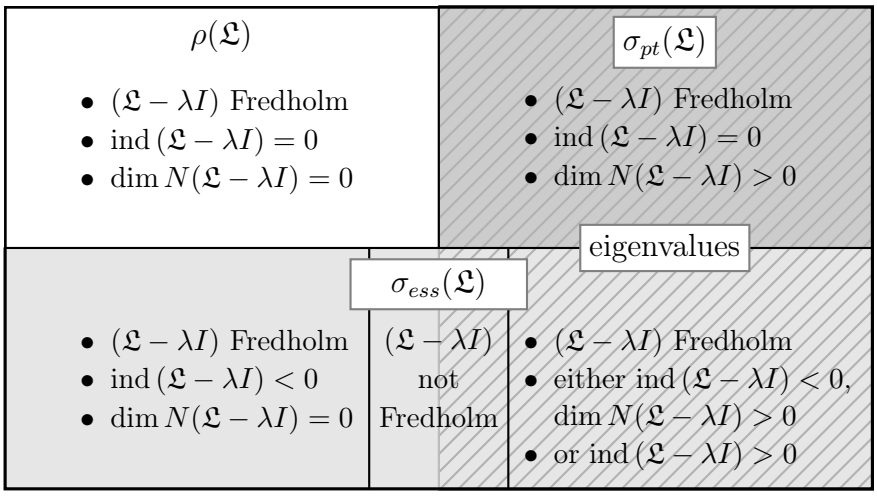

Figure 4.1: Spectrum of $\mathfrak{L}$ according to definition 3

Due to the fact that D is invertible, $Q(z)$ smooth and $J_F(Q(z))$ bounded, the linear differential operator $\mathfrak{L}$ defined by (4.5) is closed and densely defined in $L^2(\mathbb{R}, \mathbb{C}^n)$(for more details see appendix C) such that we can apply definition 3 to determine its spectrum by Fredholm properties.

For practical computation of the spectrum we will take advantage of a special property of $\mathfrak{L}$, which is related to the fact that the operator results from the linearization about a traveling wave front. Taking this into account, we will first introduce a problem that is equivalent to the eigenvalue equation (4.8), and afterwards present a reformulation of the entire spectrum.

Reformulation of the eigenvalue problem

The eigenvalue equation (4.8), which determines whether the linearized perturbation model (4.5) has solutions of the form

$$p(z,t) = e^{\lambda t}u(z), \tag{4.9}$$

is equivalent to the ordinary differential equation

$$u' = D^{-1}\big(J_F(Q(z)) - \lambda I\big)u =: A(z,\lambda)u. \tag{4.10}$$

Since the only z dependency in $A(z,\lambda)$ is related to the traveling wave front $Q(z)$, which connects two stationary points, $A(z,\lambda)$ asymptotically approaches constant matrices as $z \to \pm\infty$. The differential equation (4.10) can therefore be written as

$$\begin{aligned} u' &= A(z,\lambda)u \\ &= \left(\lim_{z\to\pm\infty} A(z,\lambda) + \Big(A(z,\lambda) - \lim_{z\to\pm\infty} A(z,\lambda)\Big)\right) u \\ &= \Big(D^{-1}\big(J_F(Q_\pm) - \lambda I\big) + D^{-1}\big(J_F(Q(z)) - J_F(Q_\pm)\big)\Big)u \\ &=: \big(A^\pm(\lambda) + R^\pm(z)\big)\, u, \end{aligned} \tag{4.11}$$

where $R^\pm(z)$ tends to zero as z tends to $\pm\infty$.

In a second step of reformulation we introduce the family of differential operators $\mathfrak{T}(\lambda)$, which are determined by differential equation (4.11):

$$\mathfrak{T}(\lambda)u := \left(\frac{d}{dz} - A(z,\lambda)\right) u = \left(\frac{d}{dz} - \big(A^\pm(\lambda) + R^\pm(z)\big)\right) u = 0. \tag{4.12}$$

All pairs (λ, u) with $u \in L^2(\mathbb{R},\mathbb{C}^n)$ that solve the equivalent problems (4.8)-(4.12) are eigenvalues and eigenfunctions of $\mathfrak{L}$, and the eigenfunctions u represent all possible initial perturbations of the wave front in $L^2(\mathbb{R},\mathbb{C}^n)$ that evolve according to (4.9). The norm of these perturbations is

$$\|p(z,t)\|_{L^2}^2 = \int_{-\infty}^{\infty} |e^{\lambda t}u(z)|^2\, dz = e^{2\mathrm{Re}(\lambda)t} \int_{-\infty}^{\infty} |u(z)|^2\, dz = e^{2\mathrm{Re}(\lambda)t}\|u\|_{L^2}^2,$$

which yields the following statements about the stability of the traveling waves:

(i) If there exists an eigenvalue λ of $\mathfrak{L}$ with $\mathrm{Re}(\lambda) > 0$, the related eigenfunction u represents an initial perturbation of the traveling wave whose norm increases in time. In particular, for $\lambda \in \mathbb{R}$, i.e. an eigenvalue on the real axis, and a related real-valued eigenvector $u(z) \in \mathbb{R}^n$, the perturbation increases in time in every point $z \in \mathbb{R}$ in the linearized system. The traveling wave front is therefore linearly unstable under perturbations $u \in L^2(\mathbb{R},\mathbb{C}^n)$.

(ii) If there only exist eigenvalues λ of $\mathfrak{L}$ with negative real part, i.e. $\mathrm{Re}(\lambda) < 0$, the norm of all perturbations that are given by related eigenfunctions u decreases in time. Consequently, there exist no initial perturbations in $L^2(\mathbb{R}, \mathbb{C}^n)$ evolving according to (4.9) that prevent the traveling wave front from being linearly stable. In this case, the determination of the non-eigenvalues in the spectrum is needed in order to find out whether there exist other initial perturbations $p(z, 0)$ that evolve differently to (4.9) and cause instability.

Reformulation of the entire spectrum

Since we have the relation

$$(\mathfrak{L} - \lambda I) = -D\mathfrak{T}(\lambda)$$

between the differential operators $\mathfrak{L}$ and $\mathfrak{T}(\lambda)$, the spectrum of $\mathfrak{L}$ is equal to the set of values λ for which the operator $\mathfrak{T}(\lambda)$ is not invertible. We call this set the *spectrum*[3] of $\mathfrak{T}$, which is specified by definition 3 if we replace $\mathfrak{L} - \lambda I$ by $\mathfrak{T}(\lambda)$.

For computing the spectrum of $\mathfrak{T}$ in practice, we will take advantage of the fact that the involved matrix $A(z, \lambda)$ tends to constant matrices as z tends to $\pm\infty$. By using this fact we can relate Fredholm properties of $\mathfrak{T}(\lambda)$ to properties of the asymptotic matrices $A^{\pm}(\lambda)$. This results in a practical relation between spectral values of $\mathfrak{T}$ and characteristics of $A^{\pm}(\lambda)$, as will be seen in theorem 2.

Before stating the final theorems, we will name the properties of the matrices $A^{\pm}(\lambda)$ that will be of interest to us by recalling the definition of hyperbolicity of a matrix and introducing the instability index of a matrix:

Definition 4 (Hyperbolicity of a matrix)**.** Consider a matrix $A \in \mathbb{C}^{n\times n}$. We call A *hyperbolic* if all eigenvalues of A have non-zero real part, i.e. if no eigenvalue lies on the imaginary axis. We refer to eigenvalues of A with positive (negative) real part as *unstable (stable) eigenvalues*. Furthermore, we refer to the number of unstable eigenvalues of a hyperbolic matrix A, counted with its algebraic multiplicity, as its *instability index*.

Using definition 4, we can formulate relations between Fredholm properties of $\mathfrak{T}(\lambda)$ and its asymptotic matrices $A^{\pm}(\lambda)$:

Theorem 1. *Consider a family $\mathfrak{T}$ of linear differential operators defined by*

$$\mathfrak{T}(\lambda) : L^2(\mathbb{R}, \mathbb{C}^n) \longrightarrow L^2(\mathbb{R}, \mathbb{C}^n)$$
$$u \longmapsto \frac{du}{dz} - A(z, \lambda)u$$

[3]Note that we are not interested in the spectrum of the individual operators $\mathfrak{T}(\lambda)$ for fixed values of λ.

with $\lambda \in \mathbb{C}$. Let $A(z,\lambda)$ be piecewise continuous and bounded for any fixed λ, and let it asymptotically approach constant matrices $\lim_{z\to\pm\infty} A(z,\lambda) = A^{\pm}(\lambda)$.[4] *Then, $\mathfrak{T}(\lambda)$ is Fredholm if, and only if, $A^{\pm}(\lambda)$ are both hyperbolic. The Fredholm index of $\mathfrak{T}(\lambda)$ is then equal to the difference of the instability indices of $A^{-}(\lambda)$ and $A^{+}(\lambda)$:*

$$ind\,(\mathfrak{T}(\lambda)) = i_{-}(\lambda) - i_{+}(\lambda). \tag{4.13}$$

Proof. The case of operators $\mathfrak{T}(\lambda)$ acting on $C^0(\mathbb{R},\mathbb{R}^n)$ with continuous matrices $A(z,\lambda)$ was proven by Palmer and Coppel: See [Pal84] and [Pal88] for the equivalence of Fredholm properties of $\mathfrak{T}(\lambda)$ and the existence of exponential dichotomies for $u' = A(z,\lambda)u$, and [Cop78] for the relation between exponential dichotomies and hyperbolicity of the asymptotic matrices $A^{\pm}(\lambda)$. In order to consider the operators on the function space $L^2(\mathbb{R},\mathbb{C}^n)$, we take the results of [Ben92, San93] into account. For a summary of the results we refer to [San00, San02]. □

By means of theorem 1 we can formulate a characterization of the spectrum of $\mathfrak{T}$ by properties of the matrices $A^{\pm}(\lambda)$ (for a visualization of these results see figure 4.2):

Theorem 2. *Consider a family $\mathfrak{T}$ of linear differential operators defined by*

$$\begin{aligned} \mathfrak{T}(\lambda) : L^2(\mathbb{R},\mathbb{C}^n) &\longrightarrow L^2(\mathbb{R},\mathbb{C}^n) \\ u &\longmapsto \frac{du}{dz} - A(z,\lambda)u \end{aligned}$$

with $\lambda \in \mathbb{C}$. Let $A(z,\lambda)$ be piecewise continuous and bounded for any fixed λ, and let it asymptotically approach constant matrices $\lim_{z\to\pm\infty} A(z,\lambda) = A^{\pm}(\lambda)$. Then the following statements are true:

- *λ is in the resolvent set $\rho(\mathfrak{T})$ if, and only if, $A^{\pm}(\lambda)$ are both hyperbolic with same instability index $i_{+}(\lambda) = i_{-}(\lambda)$ and $\dim N(\mathfrak{T}(\lambda)) = 0$.*
- *λ is in the point spectrum $\sigma_{pt}(\mathfrak{T})$ if, and only if, the asymptotic matrices $A^{\pm}(\lambda)$ are both hyperbolic with identical instability index $i_{+}(\lambda) = i_{-}(\lambda)$ and $\dim N(\mathfrak{T}(\lambda)) > 0$.*
- *λ is in the essential spectrum $\sigma_{ess}(\mathfrak{T})$ if, and only if,*
  - *either at least one of the asymptotic matrices $A^{\pm}(\lambda)$ is not hyperbolic*
  - *or else both matrices $A^{\pm}(\lambda)$ are hyperbolic but their instability indices differ, so that $i_{+}(\lambda) \neq i_{-}(\lambda)$.*

[4] These properties of $A(z,\lambda)$ ensure in particular that the operators $\mathfrak{T}(\lambda)$ are closed and densely defined in $L^2(\mathbb{R},\mathbb{C}^n)$. The proof is analogous to the one concerning the operator $\mathfrak{L}$, which is presented in appendix C.

Proof. This theorem is proven by relating the results of theorem 1 to definition 3. To this end we consider figure 4.1, which illustrates definition 3 in more detail with respect to Fredholm properties of the involved operator. As stated above, we define the spectrum of $\mathfrak{T}$ to be the set of values λ for which $\mathfrak{T}(\lambda)$ is not invertible such that in definition 3, as well as in figure 4.1, the operator $\mathfrak{L} - \lambda I$ has to be replaced by $\mathfrak{T}(\lambda)$. Since, according to theorem 1, the operator $\mathfrak{T}(\lambda)$ is Fredholm if, and only if, $A^{\pm}(\lambda)$ are both hyperbolic, figure 4.1 changes to figure 4.2. With respect to correlation (4.13) this proves the above theorem. □

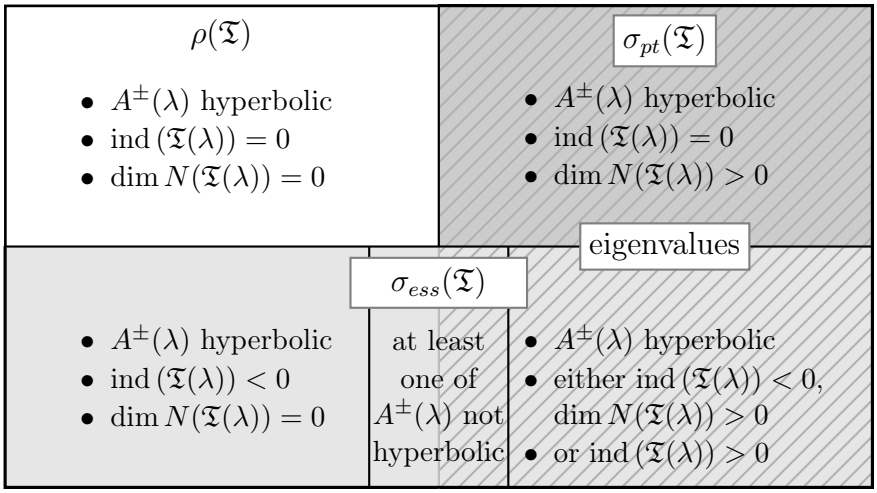

Figure 4.2: Spectrum of $\mathfrak{T}$ according to definition 3 with respect to theorem 2 (note that the Fredholm index is given by ind $(\mathfrak{T}(\lambda)) = i_-(\lambda) - i_+(\lambda)$)

To sum up, the spectrum of an operator $\mathfrak{T}$ defined as in theorem 2 is related to the eigenvalues of the asymptotic matrices $A^{\pm}(\lambda)$. As can easily be verified by (4.10), the particular matrix $A(z, \lambda)$ in our application satisfies the requirements such that we can apply theorem 2 for computing the spectrum of the operator $\mathfrak{T}$, and hence of the operator $\mathfrak{L}$. This computation will be done separately for the single- and double-substrate bioremediation model in the following subsections.

4.2.2 Single-substrate bioremediation model

For studying the stability of traveling waves in the bioremediation model (3.1), we have to determine the spectrum of $\mathfrak{T}$ defined by the family

$$\begin{aligned}\mathfrak{T}(\lambda) &= \frac{d}{dz} - A(z, \lambda) \\ &= \frac{d}{dz} - \begin{pmatrix} -\frac{1}{d_1}\big(f'(C)N + \lambda\big) & -\frac{1}{d_1} f(C) \\ \frac{1}{d_2} f'(C)N & \frac{1}{d_2}\big(f(C) - R - \lambda\big) \end{pmatrix},\end{aligned}$$

where $d_1 = u - s > 0$ and $d_2 = -s > 0$ denote the velocities in the diagonal matrix $D = \mathrm{diag}(d_1, d_2)$, and $f(C) = \nu\mu_1(C)$.

In order to identify the spectrum of $\mathfrak{T}$ by means of theorem 2, we compute the eigenvalues of the asymptotic matrices

$$A^{\pm}(\lambda) = \begin{pmatrix} -\frac{\lambda}{d_1} & -\frac{1}{d_1} f(c_{\pm}) \\ 0 & \frac{1}{d_2}\big(f(c_{\pm}) - R - \lambda\big) \end{pmatrix}, \tag{4.14}$$

which are

$$\mu_1^{\pm}(\lambda) = -\frac{\lambda}{d_1} \tag{4.15}$$

$$\mu_2^{\pm}(\lambda) = \frac{1}{d_2}\big(f(c_{\pm}) - R - \lambda\big). \tag{4.16}$$

By denoting the zeros of $\mathrm{Re}(\mu_2^{\pm}(\lambda))$ by

$$\lambda_2^{\pm} := f(c_{\pm}) - R$$

and taking into account the relation $\lambda_2^+ < 0 < \lambda_2^-$, following from (3.5), we can determine the signs of $\mathrm{Re}(\mu_i^{\pm}(\lambda))$, as well as the Fredholm indices of $\mathfrak{T}(\lambda)$, which are visualized in figure 4.3.

With this information we can, according to theorem 2, make the following classification of the values λ, as illustrated in figures 4.3 and 4.4:

$$\sigma_{ess}(\mathfrak{T}) = \{\lambda \in \mathbb{C} : \mathrm{Re}(\lambda) \in [\lambda_2^+, \lambda_2^-]\}$$
$$\rho(\mathfrak{T}) \cup \sigma_{pt}(\mathfrak{T}) = \{\lambda \in \mathbb{C} : \mathrm{Re}(\lambda) \in \big(-\infty, \lambda_2^+\big) \cup \big(\lambda_2^-, \infty\big)\}.$$

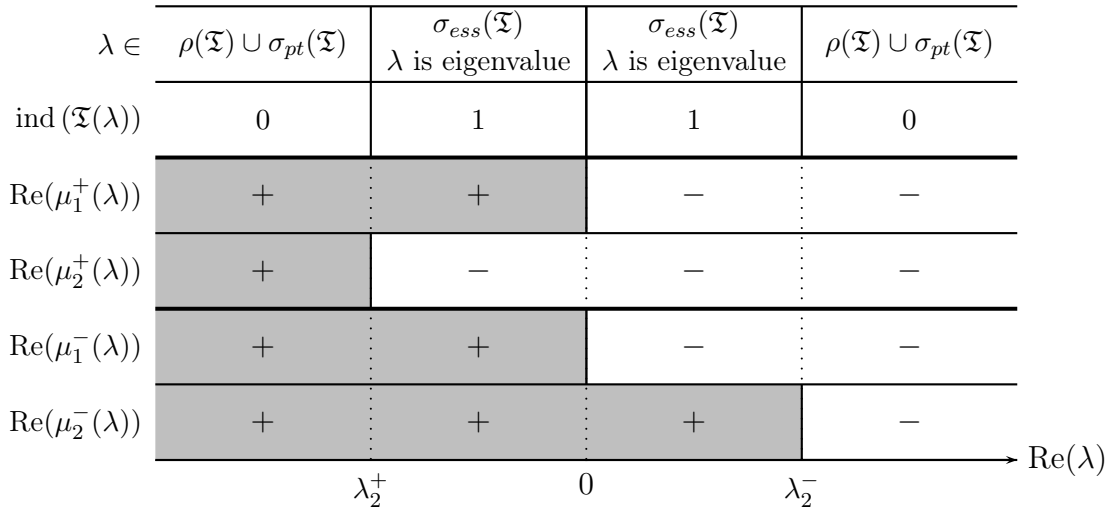

Figure 4.3: Signs of $\mathrm{Re}(\mu_i^{\pm}(\lambda))$, Fredholm indices $\mathrm{ind}\,(\mathfrak{T}(\lambda)) = i_-(\lambda) - i_+(\lambda)$, and classification of λ with respect to theorem 2. Unstable eigenvalues are labeled by gray sets.

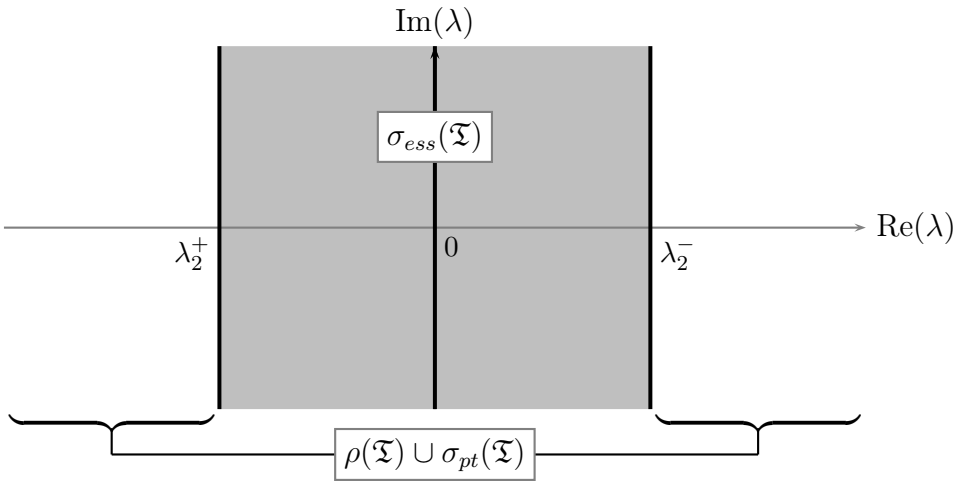

Figure 4.4: Classification of λ for $\mathfrak{T}$ on $L^2(\mathbb{R}, \mathbb{C}^2)$

Due to $\lambda_2^- > 0$, the essential spectrum (and in particular the set of eigenvalues) crosses the imaginary axis, which yields the following instability result:

Proposition 9. *The traveling wave fronts in the bioremediation model* (3.1) *are linearly unstable under initial perturbations* $u \in L^2(\mathbb{R}, \mathbb{C}^2)$.

Since the essential spectrum already causes instability, no further distinction between resolvent set and point spectrum is needed for stating stability results[5].

Remark 10 (Real-valued perturbations). Related to the eigenvalues in the essential spectrum, there exist perturbations of the form $p(z,t) = e^{\lambda t}u(z)$. These perturbations are real-valued if, and only if, either λ and u are both real-valued or else if λ has a non-zero imaginary part and $u \equiv 0$.

Every complex eigenvector $u = u_R + iu_I$ ($u_I \neq 0$) of $\mathfrak{L}$ that is related to $\lambda \in \mathbb{R}$ satisfies

$$\lambda u = \lambda u_R + i\lambda u_I = \mathfrak{L}u_R + i\mathfrak{L}u_I = \mathfrak{L}u.$$

Since from $u \in L^2(\mathbb{R}, \mathbb{C}^n)$ follows $u_R, u_I \in L^2(\mathbb{R}, \mathbb{R}^n) \subset L^2(\mathbb{R}, \mathbb{C}^n)$, the real and imaginary part of u belong to the function space under consideration, and therefore, for $u_{R/I} \neq 0$, the pairs $(\lambda, u_{R/I})$ are real-valued eigenvalue-eigenvector pairs of $\mathfrak{L}$.

From the above it follows that for the positive real eigenvalues $\lambda \in (0, \lambda_2^-)$ in the essential spectrum real-valued perturbations $p(z,t)$ exist that cause instability of the traveling wave by growing in every point $z \in \mathbb{R}$ in the linearized perturbation model.

[5] In subsection 4.3.2 and appendix C.3 we will present an approach that enables us to distinct between resolvent set and point spectrum in certain cases by studying the asymptotic behavior of the solutions of (4.10). Applied to the differential operator $\mathfrak{T}$ in the current section, this theory yields that the point spectrum of $\mathfrak{T}$ is empty, i.e. $\mathbb{C} = \sigma_{ess}(\mathfrak{T}) \cup \rho(\mathfrak{T})$.

4.2.3 Double-substrate bioremediation model

In order to study the stability of traveling waves in the bioremediation model (3.8), we will compute the spectrum of $\mathfrak{T}$ given by

$$\begin{aligned}\mathfrak{T}(\lambda) &= \frac{d}{dz} - A(z,\lambda)\\ &= \frac{d}{dz} - \begin{pmatrix} -\frac{1}{d_1}(\nu_o f_{c_o} N + \lambda) & -\frac{1}{d_1}\nu_o f_{c_s} N & -\frac{1}{d_1}\nu_o f \\ -\frac{1}{d_2}\nu_s f_{c_o} N & -\frac{1}{d_2}(\nu_s f_{c_s} N + \lambda) & -\frac{1}{d_2}\nu_s f \\ \frac{1}{d_3}(\nu_o+\nu_s) f_{c_o} N & \frac{1}{d_3}(\nu_o+\nu_s) f_{c_s} N & \frac{1}{d_3}\big((\nu_o+\nu_s) f - R - \lambda\big) \end{pmatrix}.\end{aligned}$$

Here, we use the notation

$$f_{c_o} = \frac{d}{dc_o} f(C_o, C_s) \qquad \text{and} \qquad f_{c_s} = \frac{d}{dc_s} f(C_o, C_s)$$

with $f(C_o, C_s) = \mu_2(C_o, C_s)$, and $d_1 = u - s > 0$, $d_2 = v - s < 0$ and $d_3 = -s$ denote the velocities in the diagonal matrix $D = \operatorname{diag}(d_1, d_2, d_3)$.

In order to identify the spectrum of $\mathfrak{T}$ by applying theorem 2, we note that the eigenvalues of the asymptotic matrices

$$A^{\pm}(\lambda) = \begin{pmatrix} -\frac{\lambda}{d_1} & 0 & -\frac{1}{d_1}\nu_o f(c_{o\pm}, c_{s\pm}) \\ 0 & -\frac{\lambda}{d_2} & -\frac{1}{d_2}\nu_s f(c_{o\pm}, c_{s\pm}) \\ 0 & 0 & \frac{1}{d_3}\big((\nu_o+\nu_s) f(c_{o\pm}, c_{s\pm}) - R - \lambda\big) \end{pmatrix} \tag{4.17}$$

are

$$\begin{aligned}\mu_1^{\pm}(\lambda) &= -\frac{\lambda}{d_1}\\ \mu_2^{\pm}(\lambda) &= -\frac{\lambda}{d_2}\\ \mu_3^{\pm}(\lambda) &= \frac{1}{d_3}\big((\nu_o+\nu_s) f(c_{o\pm}, c_{s\pm}) - R - \lambda\big).\end{aligned}$$

Since there exist traveling waves with negative as well as traveling waves with positive wave speeds s, we have to distinct both cases in the process of determining the signs of the real parts of $\mu_i^{\pm}(\lambda)$. By denoting the zeros of $\operatorname{Re}(\mu_3^{\pm}(\lambda))$ by

$$\lambda_3^{\pm} := (\nu_o + \nu_s) f(c_{o\pm}, c_{s\pm}) - R$$

and taking into account the relations $\lambda_3^{+} < 0 < \lambda_3^{-}$ for $s < 0$ and $\lambda_3^{-} < 0 < \lambda_3^{+}$ for $s > 0$, which follow from condition (3.18), we can identify the signs of $\operatorname{Re}(\mu_i^{\pm})$ and Fredholm indices of $\mathfrak{T}(\lambda)$ and classify λ, as visualized in figures 4.5 and 4.6. We thus have

$$\begin{aligned}\sigma_{ess}(\mathfrak{T}) &= \{\lambda \in \mathbb{C} : \operatorname{Re}(\lambda) \in [\lambda_3^{\pm}, \lambda_3^{\mp}]\}\\ \rho(\mathfrak{T}) \cup \sigma_{pt}(\mathfrak{T}) &= \{\lambda \in \mathbb{C} : \operatorname{Re}(\lambda) \in \big(-\infty, \lambda_3^{\pm}\big) \cup \big(\lambda_3^{\mp}, \infty\big)\},\end{aligned}$$

where the upper signs are related to $s < 0$ and the lower signs to $s > 0$.

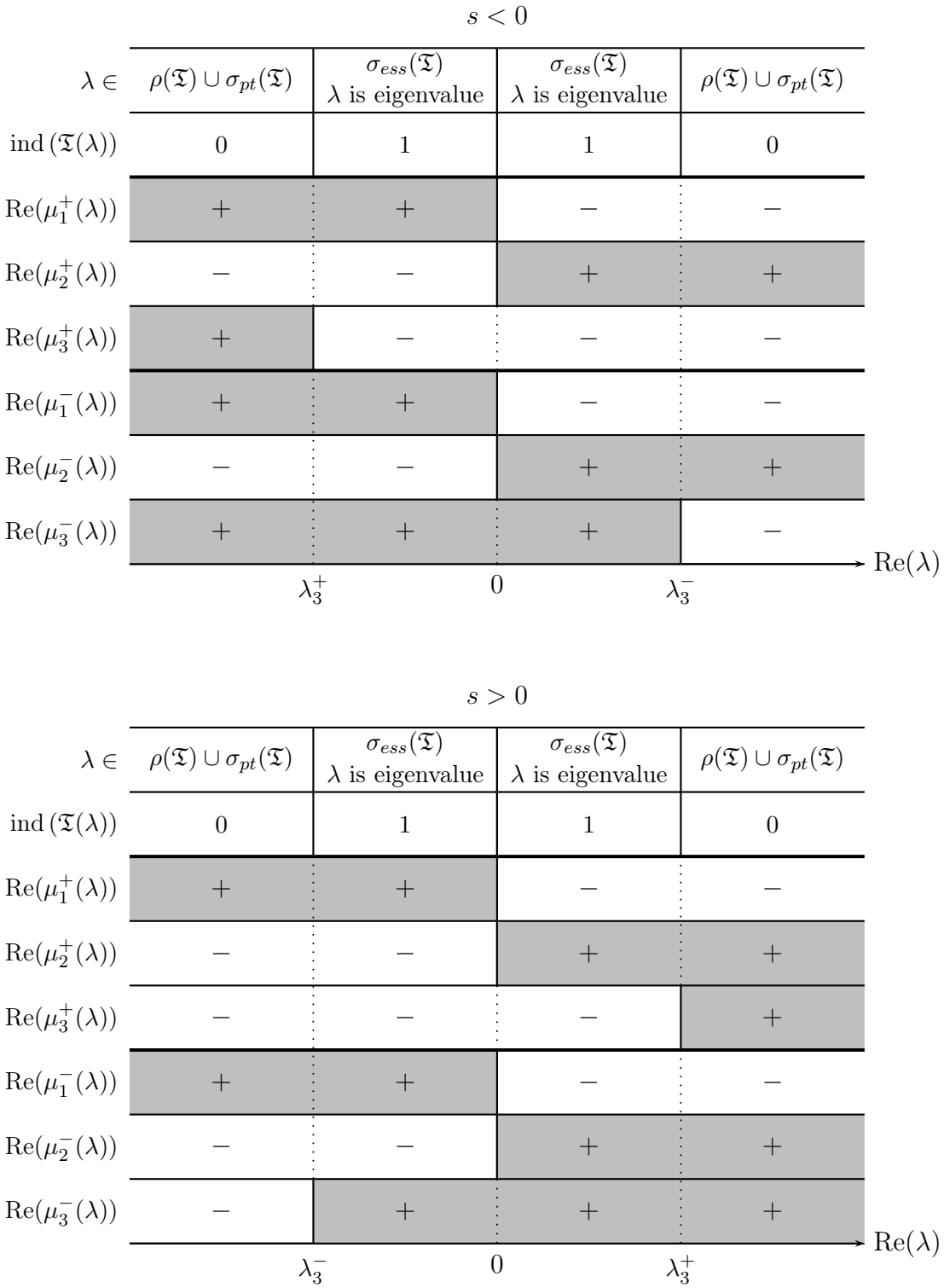

Figure 4.5: Signs of $\operatorname{Re}(\mu_i^{\pm}(\lambda))$, Fredholm indices $\operatorname{ind}(\mathfrak{T}(\lambda)) = i_-(\lambda) - i_+(\lambda)$, and classification of λ with respect to theorem 2. Unstable eigenvalues are labeled by gray sets.

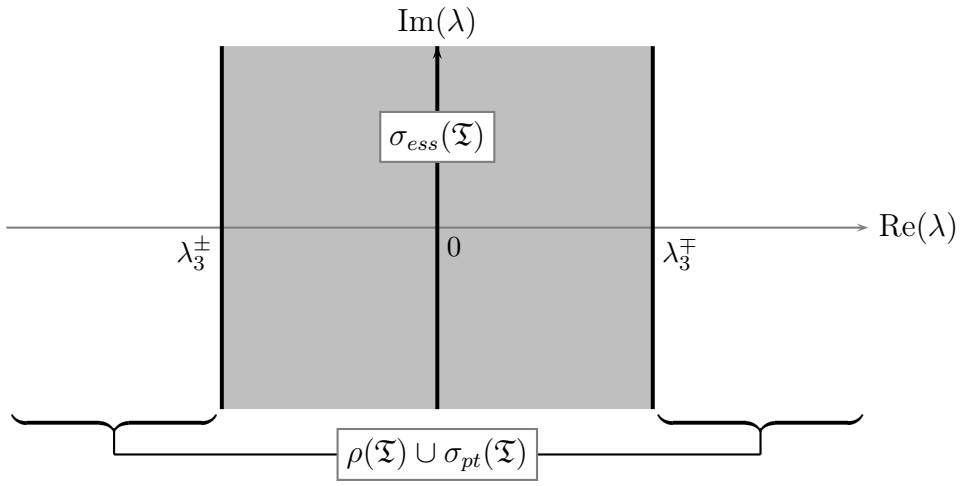

Figure 4.6: Classification of λ for $\mathfrak{T}$ on $L^2(\mathbb{R}, \mathbb{C}^3)$ for $s < 0$ (upper signs) and $s > 0$ (lower signs)

Because of $\lambda_3^{\mp} > 0$, a subset of the essential spectrum (and in particular a subset of the set of eigenvalues) lies in the positive half plane, which yields the following instability result:

Proposition 10. *The traveling wave fronts in the bioremediation model* (3.8) *are linearly unstable under initial perturbations* $u \in L^2(\mathbb{R}, \mathbb{C}^3)$.

Similar to subsection 4.2.2, a distinction between resolvent set and point spectrum does not yield any further instability results and is therefore not necessary.

Remark 11 (Real-valued perturbations). With the same argument as in remark 10, for every real positive eigenvalue $\lambda \in (0, \lambda_3^{\mp})$ there exist real-valued perturbations $p(z, t)$ that cause instability of the traveling wave by growing in every point $z \in \mathbb{R}$ with respect to the linearization.

4.3 Perturbations in weighted L^2 spaces

As discussed in section 4.2, for both bioremediation models (3.1) and (3.8) there exist initial perturbations $p(z,0) = u(z) \in L^2(\mathbb{R}, \mathbb{R}^n)$ that cause instability of the traveling wave solutions $Q(z)$. But does there maybe exist another function space X that the differential operator $\mathfrak{L}$ acts on such that the spectrum of $\mathfrak{L}$ lies in the negative half plane and the traveling waves are linearly stable under perturbations $p(z,0) = u(z) \in X$? In order to search for a function space X with these properties, we transform the problem to a weighted L^2 space (where the weight function has to be determined) and study the spectrum of the operator $\mathfrak{L}$ acting on this space for the bioremediation models (3.1) and (3.8).

4.3.1 Theory

In the following we will introduce the conventional weighted L^2 spaces and present a procedure to determine the spectrum of $\mathfrak{L}$ acting on these spaces, which will be applied to the bioremediation models in the subsequent subsections. Since some of the later results will suggest a certain generalization of the conventional weighted L^2 spaces, we will introduce this theory as well in this context.

Conventional weighted L^2 spaces

At first, we will study perturbations in general weighted spaces, and concentrate afterwards on spaces that are defined by exponential weight functions.

Let $L^2_w(\mathbb{R}, \mathbb{C}^n)$ denote the space of functions that satisfy

$$\|u_w\|^2_{L^2_w} = \int_{-\infty}^{\infty} |u_w(z)|^2 \bar{w}(z)\, dz < \infty,$$

where $\bar{w}(z)$ is a positive weight function. For simplicity of notation, and similar to [Log01], we introduce the function $w(z) := \sqrt{\bar{w}(z)}$ so that the weighted space $L^2_w(\mathbb{R}, \mathbb{C}^n)$ can be defined by functions that satisfy

$$\|u_w\|^2_{L^2_w} = \int_{-\infty}^{\infty} |u_w(z)w(z)|^2\, dz < \infty.$$

In addition to its positivity we initially assume $w(z)$ to be differentiable.

The objective now is to identify the spectrum of the operator $\mathfrak{L}$ on the weighted space defined above. For practical computation of the spectral values we will take advantage of the identity of the spectra of $\mathfrak{L}$ acting on $L^2_w(\mathbb{R}, \mathbb{C}^n)$ and a related operator $\mathfrak{B}$ acting on the already known function space $L^2(\mathbb{R}, \mathbb{C}^n)$. Referring to [Log01], we will first derive the operator $\mathfrak{B}$ from the eigenvalue problem and give afterwards some information about the essential spectrum.

Eigenvalues: It is easily seen that $u_w \in L^2_w(\mathbb{R},\mathbb{C}^n)$ satisfies the eigenvalue equation

$$\mathfrak{L}u_w = \lambda u_w$$

if, and only if, $u = u_w w \in L^2(\mathbb{R},\mathbb{C}^n)$ satisfies

$$\mathfrak{B}u = \lambda u \tag{4.18}$$

with

$$\mathfrak{B} = w\mathfrak{L}\frac{1}{w} = \mathfrak{L} + D\frac{w'}{w}.$$

For finding the eigenvalues λ of the differential operator $\mathfrak{L}$ acting on $L^2_w(\mathbb{R},\mathbb{C}^n)$, we therefore have to determine the eigenvalues λ of $\mathfrak{B}$ acting on $L^2(\mathbb{R},\mathbb{C}^n)$.

Analogous to subsection 4.2.1 we will rephrase the eigenvalue equation (4.18) and present two equivalent problems: Based on the assumption that the fraction $w'(z)/w(z)$ approaches constant values at $\pm\infty$, equation (4.18) is equivalent to

$$\begin{aligned} u' &= \left(A(z,\lambda) + \frac{w'(z)}{w\,(z)}I\right)u \qquad (4.19)\\ &= \left(\left[A^{\pm}(\lambda) + \left(\frac{w'}{w}\right)_{\pm} I\right] + \left[R^{\pm}(z) + \left(\frac{w'(z)}{w\,(z)} - \left(\frac{w'}{w}\right)_{\pm}\right) I\right]\right) u \\ &=: \left(A^{\pm}_w(\lambda) + R^{\pm}_w(z)\right) u \qquad (4.20) \end{aligned}$$

and

$$\mathfrak{T}_{\mathfrak{B}}(\lambda)u := \left(\frac{d}{dz} - A_w(z,\lambda)\right)u = \left(\frac{d}{dz} - \left(A^{\pm}_w(\lambda) + R^{\pm}_w(z)\right)\right)u = 0, \tag{4.21}$$

where $R^{\pm}_w(z)$ tends to zero as z tends to $\pm\infty$.

All solutions (λ, u) of the equivalent problems (4.18)-(4.21) with $u \in L^2(\mathbb{R},\mathbb{C}^n)$ are eigenvalues and eigenvectors of $\mathfrak{B}$, while (λ, u_w) with $u_w = u/w \in L^2_w(\mathbb{R},\mathbb{C}^n)$ are eigenvalues and eigenvectors of $\mathfrak{L}$. The eigenfunctions u_w represent initial perturbations in the function space $L^2_w(\mathbb{R},\mathbb{C}^n)$ that evolve according to (4.9) and satisfy

$$\begin{aligned} \|p(z,t)\|^2_{L^2_w} &= \int_{-\infty}^{\infty} |e^{\lambda t}u_w(z)w(z)|^2\,dz = e^{2\mathrm{Re}(\lambda)t}\int_{-\infty}^{\infty} |u_w(z)w(z)|^2\,dz \\ &= e^{2\mathrm{Re}(\lambda)t}\|u_w\|^2_{L^2_w}. \end{aligned}$$

It follows that the stability of traveling waves in the norm $\|\cdot\|_{L^2_w}$ is related to the real parts of the eigenvalues of $\mathfrak{B}$ and $\mathfrak{L}$ in the same way as described on page 60.

Essential spectrum: Not only the eigenvalues but also their complements in the essential spectra of $\mathfrak{L}$ and $\mathfrak{B}$ are identical. This follows from the equivalence of

$$(\mathfrak{L} - \lambda I)g_w = f_w, \quad g_w, f_w \in L^2_w(\mathbb{R},\mathbb{C}^n)$$

and

$$(\mathfrak{B} - \lambda I)g = f, \quad g := g_w w, f := f_w w \in L^2(\mathbb{R}, \mathbb{C}^n).$$

The determination of the essential spectrum of $\mathfrak{B}$ on $L^2(\mathbb{R}, \mathbb{C}^n)$ thus results in knowing the essential spectrum of $\mathfrak{L}$ on $L^2_w(\mathbb{R}, \mathbb{C}^n)$.

Due to the relation

$$(\mathfrak{B} - \lambda I) = -D\mathfrak{T}_{\mathfrak{B}}(\lambda)$$

the spectra of $\mathfrak{B}$ and $\mathfrak{T}_{\mathfrak{B}}$ are identical such that we can apply theorem 2 again for computing the spectrum of $\mathfrak{B}$, and hence the spectrum of $\mathfrak{L}$ on the weighted space $L^2_w(\mathbb{R}, \mathbb{C}^n)$.

It is often convenient to consider exponentially weighted spaces such that in the remainder of this section $L^2_w(\mathbb{R}, \mathbb{C}^n)$ will be defined by exponential weight functions[6]

$$w(z) = \begin{cases} e^{k_+ z}, & z \geq 0 \\ e^{k_- z}, & z < 0 \end{cases} \tag{4.22}$$

with growth rates

$$k(z) = \begin{cases} k_+, & z \geq 0 \\ k_-, & z < 0 \end{cases}$$

and $k_\pm \in \mathbb{R}$ (see [San00]). The matrices in (4.20) and (4.21) thus read

$$A^\pm_w(\lambda) = A^\pm(\lambda) + k_\pm I$$
$$R^\pm_w(z) = R^\pm(z) + \big(k(z) - k_\pm\big)I.$$

Generalization of the conventional weighted L^2 spaces

In the above definition of weighted spaces we chose the same weight function $w(z)$ for each component of the perturbation vector $u_w(z) = (u_{w1}, \ldots, u_{wn})(z)$. A generalization of this approach is to allow different weight functions for each component, i.e. we define the weighted space $\tilde{L}^2_w(\mathbb{R}, \mathbb{C}^n)$ by

$$\|u_w\|^2_{\tilde{L}^2_w} = \int_{-\infty}^{\infty} \left(\sum_{i=1}^{n} |u_{wi}(z) w_i(z)|^2 \right) dz < \infty$$

with differentiable, positive weight functions $w_i(z)$, $i = 1, \ldots, n$. In order to compute the spectrum of $\mathfrak{L}$ acting on this more general weighted space, we follow the above procedure and derive related operators $\tilde{\mathfrak{B}}$ and $\mathfrak{T}_{\tilde{\mathfrak{B}}}$ that act on $L^2(\mathbb{R}, \mathbb{C}^n)$ and have the same spectrum as $\mathfrak{L}$.

[6] Alternatively, we could choose $w(z)$ in such a way that it smoothly connects the asymptotic functions $e^{k_\pm z}$, but since this neither changes the norm nor the results, we will concentrate on the simpler weight functions (4.22) and replace the term $\frac{w'(z)}{w(z)}$ in the above derivation by $k(z)$.

Due to the equivalence

$$u_w = \begin{pmatrix} u_{w1} \\ \vdots \\ u_{wn} \end{pmatrix} \in \tilde{L}^2_w(\mathbb{R}, \mathbb{C}^n) \;\Leftrightarrow\; u = \begin{pmatrix} w_1 & & 0 \\ & \ddots & \\ 0 & & w_n \end{pmatrix} \begin{pmatrix} u_{w1} \\ \vdots \\ u_{wn} \end{pmatrix} = W u_w \in L^2(\mathbb{R}, \mathbb{C}^n),$$

λ and $u_w \in \tilde{L}^2_w(\mathbb{R}, \mathbb{C}^n)$ satisfy the eigenvalue equation

$$\mathfrak{L} u_w = \lambda u_w$$

if, and only if, λ and $u = W u_w \in L^2(\mathbb{R}, \mathbb{C}^n)$ satisfy

$$\tilde{\mathfrak{B}} u = \lambda u$$

with

$$\tilde{\mathfrak{B}} = W \mathfrak{L} W^{-1} = W J_F(Q) W^{-1} - DW(W^{-1})' - D\partial_z.$$

Furthermore, the above eigenvalue equations are equivalent to the problems

$$u' = \tilde{A}_w(z, \lambda) u,$$

$$\mathfrak{T}_{\tilde{\mathfrak{B}}}(\lambda) u = \left(\frac{d}{dz} - \tilde{A}_w(z, \lambda) \right) u = 0$$

with

$$\tilde{A}_w(z, \lambda) = D^{-1} W J_F(Q) W^{-1} - W(W^{-1})' - \lambda D^{-1}.$$

With the same argumentation as before, the entire spectra of $\mathfrak{L}$ on $\tilde{L}^2_w$ and $\mathfrak{T}_{\tilde{\mathfrak{B}}}$ on L^2 are identical such that the problem of finding the spectrum of $\mathfrak{L}$ on the weighted space is transformed to the problem of computing the spectrum of $\mathfrak{T}_{\tilde{\mathfrak{B}}}$ on the well known function space L^2.

In order to apply theorem 2 for computing the spectral values of $\mathfrak{T}_{\tilde{\mathfrak{B}}}$, we have to choose the weight matrix W such that $\tilde{A}_w(z, \lambda)$ asymptotically approaches constant matrices $\tilde{A}^{\pm}_w(\lambda)$ as $z \to \pm\infty$. If we concentrate again on exponential weight functions, i.e.

$$w_i(z) = \begin{cases} e^{k^i_+ z}, & z \geq 0 \\ e^{k^i_- z}, & z < 0 \end{cases}, \qquad i = 1, \ldots, n,$$

this requirement results in restrictions on the growth rates $k^i_{\pm}$. If these restrictions are satisfied, the eigenvalues of $\tilde{A}^{\pm}_w(\lambda)$ allow conclusions about the spectrum of $\mathfrak{T}_{\tilde{\mathfrak{B}}}$ on L^2, and hence of $\mathfrak{L}$ on $\tilde{L}^2_w$.

The issue of the subsequent subsections is to determine exponential weight functions such that the traveling waves in the bioremediation models (3.1) and (3.8) are stable in the associated weighted norms. To this end we will study the spectrum of $\mathfrak{L}$ depending on the weight function, and try to deduce sufficient conditions on its growth rates that yield stability of the traveling waves in the related weighted norm. According to the above derivation, the spectrum of $\mathfrak{L}$ on the weighted spaces will be determined by studying the related operators $\mathfrak{B}$ and $\tilde{\mathfrak{B}}$ on $L^2(\mathbb{R}, \mathbb{C}^n)$.

4.3.2 Single-substrate bioremediation model

In order to study the stability of traveling waves in the bioremediation model (3.1) in exponentially weighted spaces, we will first study the spectra of $\mathfrak{L}$ in the conventional weighted spaces $L^2_w(\mathbb{R},\mathbb{C}^2)$ and supplement these results with notes about the spectra of $\mathfrak{L}$ in the more general spaces $\tilde{L}^2_w(\mathbb{R},\mathbb{C}^2)$.

Perturbations in $L^2_w(\mathbb{R},\mathbb{C}^2)$

According to [Hen81, San02], the essential spectrum of $\mathfrak{B}$ is bounded by values for which at least one of the asymptotic matrices

$$A^{\pm}_w(\lambda) = \begin{pmatrix} -\frac{\lambda}{d_1} + k_\pm & -\frac{1}{d_1} f(c_\pm) \\ 0 & \frac{1}{d_2}\big(f(c_\pm) - R - \lambda\big) + k_\pm \end{pmatrix}$$

is not hyperbolic, i.e. by values λ such that

$$\mathrm{Re}(\mu^{\pm}_{1w}(\lambda)) = -\frac{\mathrm{Re}(\lambda)}{d_1} + k_\pm = 0 \qquad \Leftrightarrow \mathrm{Re}(\lambda) = d_1 k_\pm$$

$$\mathrm{Re}(\mu^{\pm}_{2w}(\lambda)) = \frac{1}{d_2}\big(f(c_\pm) - R - \mathrm{Re}(\lambda)\big) + k_\pm = 0 \Leftrightarrow \mathrm{Re}(\lambda) = f(c_\pm) - R + d_2 k_\pm.$$

It follows that a sufficient condition for the essential spectrum of $\mathfrak{B}$ to lie strictly in the left half plane is given by the requirement that all values λ that are related to a not hyperbolic matrix $A^{\pm}_w(\lambda)$ have negative real part $\mathrm{Re}(\lambda) < 0$:

> *Sufficient condition for* $\sigma_{ess}(\mathfrak{B}) \subseteq \{x \in \mathbb{C} : Re(x) < 0\}$: For
>
> $$k_- < -\frac{1}{d_2}\big(f(c_-) - R\big) \quad \text{and} \quad k_+ < 0$$
>
> the essential spectrum $\sigma_{ess}(\mathfrak{B})$ lies strictly in the left half plane.[7]

Consequently, the traveling waves might be linearly stable under perturbations in weighted spaces $L^2_w(\mathbb{R},\mathbb{C}^2)$ whose weight functions satisfy the sufficient condition stated above, but for a final stability result also the point spectrum has to be localized.

Instead of computing the kernel of $\mathfrak{T}_{\mathfrak{B}}(\lambda)$, which would be necessary for distinguishing between point spectrum and resolvent set by means of theorem 2, we will follow an alternative approach: We will compute the set of eigenvalues, which includes the point spectrum, by finding those values λ such that (4.20) has a solution in $L^2(\mathbb{R},\mathbb{C}^2)$. To this end we will first study the differential equation (4.20) separately on $\mathbb{R}^+$ and $\mathbb{R}^-$, and characterize the asymptotic behavior of the solutions $u \in C^1(\mathbb{R}^\pm,\mathbb{C}^2)$ depending on the parameter λ. From these results we will deduce conclusions about solutions of (4.20) in $L^2(\mathbb{R},\mathbb{C}^2)$.

[7] For an interpretation of this condition see page 78.

In order to characterize the solutions of (4.20), we will apply the following theorem of [Cod55] to the model of interest:

Theorem 3. *Consider the linear system*

$$y' = \big(A + R(z)\big)y, \tag{4.23}$$

where A is a constant matrix.

(i) It is assumed that the Jordan normal form J similar to A is diagonal. Let R be an integrable matrix such that

$$\int_1^\infty |R(z)|\, dz < \infty.$$

If μ_j is a characteristic root of A and g_j is the characteristic vector, so that $Ag_j = \mu_j g_j$, then (4.23) has a solution y_j such that

$$\lim_{z\to\infty} y_j(z)e^{-\mu_j z} = g_j, \qquad j = 1, \dots, n.$$

In other words, for large z the solution acts like the corresponding one for the case $R(z) \equiv 0$.

(ii) It is assumed that the Jordan normal form J similar to A has non-diagonal submatrices J_k, $k \geq 1$, where $r+1$ is the maximum number of rows in any matrix J_k, $k \geq 1$. Assume furthermore that

$$\int_1^\infty z^r |R(z)|\, dz < \infty.$$

Let μ_j be a characteristic root of A, and let $\bar{y}' = A\bar{y}$ have a solution of the form $\bar{y}(z) = e^{\mu_j z} z^l g + O(e^{\mu_j z} z^{l-1})$, where g is a vector and clearly, $0 \leq l \leq r$. Then (4.23) has a solution

$$\lim_{z\to\infty} y(z)e^{-\mu_j z} z^{-l} - g = 0.$$

Proof. See [Cod55]. □

Remark 12. In order to characterize the asymptotic behavior of solutions as z tends to $-\infty$, we study the reflection along the vertical axis: Instead of

$$y'(z) = \big(A + R(z)\big)y(z), \qquad z \to -\infty$$

we investigate

$$\hat{y}'(z) = \big(\hat{A} + \hat{R}(z)\big)\hat{y}(z), \qquad z \to +\infty$$

with $\hat{y}(z) = y(-z)$, $\hat{A} = -A$ and $\hat{R}(z) = -R(-z)$.

Applying theorem 3 to (4.20) thus means that we have to study

$$u'(z) = \big(A_w^+(\lambda) + R_w^+(z)\big)u(z) \quad \text{and} \quad \hat{u}'(z) = \big(\hat{A}_w^-(\lambda) + \hat{R}_w^-(z)\big)\hat{u}(z)$$

with $\hat{u}(z) = u(-z)$, $\hat{A}_w^-(\lambda) = -A_w^-(\lambda)$ and $\hat{R}_w^-(z) = -R_w^-(-z)$ for $z \to +\infty$.

For λ fixed, the upper triangular matrices $A_w^\pm(\lambda)$ are constant with the following eigenvalues $\mu_{iw}^\pm(\lambda)$ and eigenvectors $g_{iw}^\pm(\lambda)$:

$$\mu_{1w}^\pm(\lambda) = -\frac{\lambda}{d_1} + k_\pm, \qquad g_{1w}^\pm(\lambda) = \begin{pmatrix} 1 \\ 0 \end{pmatrix},$$
$$\mu_{2w}^\pm(\lambda) = \frac{1}{d_2}\big(f(c_\pm) - R - \lambda\big) + k_\pm, \qquad g_{2w}^\pm(\lambda) = \begin{pmatrix} \frac{1}{d_1} f(c_\pm) \\ \mu_1^\pm(\lambda) - \mu_2^\pm(\lambda) \end{pmatrix}.$$

The eigenvalues of $A_w^-(\lambda)$ and $\hat{A}_w^-(\lambda)$ just differ by their signs, while the sets of corresponding eigenvectors are identical.

As proven in appendix C.2, for every fixed $\lambda \in \mathbb{C}$ each pair of matrices $A_w^+(\lambda)/R_w^+(\lambda)$ and $\hat{A}_w^-(\lambda)/\hat{R}_w^-(\lambda)$ satisfies the assumptions of theorem 3 (i) or (ii). With the notation $\bar{\lambda}^\pm := \frac{d_1}{d_1 - d_2}(f(c_\pm) - R)$, theorem 3 yields the following results:

- For $\lambda \in \mathbb{C} \setminus \{\bar{\lambda}^-, \bar{\lambda}^+\}$, system (4.20) has solutions with the asymptotic behavior

$$u_i^-(z) \sim e^{\mu_{iw}^-(\lambda)z} g_{iw}^-(\lambda), \quad i = 1, 2 \quad \text{as } z \to -\infty$$
$$u_i^+(z) \sim e^{\mu_{iw}^+(\lambda)z} g_{iw}^+(\lambda), \quad i = 1, 2 \quad \text{as } z \to +\infty.$$

- For $\lambda = \bar{\lambda}^+$, system (4.20) has solutions with the asymptotic behavior

$$u_i^-(z) \sim \quad e^{\mu_{iw}^-(\lambda)z} g_{iw}^-(\lambda), \quad i = 1, 2 \quad \text{as } z \to -\infty$$
$$u_1^+(z) \sim \quad e^{\mu_{1w}^+(\lambda)z} g_{1w}^+(\lambda)$$
$$u_2^+(z) \sim z e^{\mu_{1w}^+(\lambda)z} g_{1w}^+(\lambda) \qquad \text{as } z \to +\infty.$$

- For $\lambda = \bar{\lambda}^-$, system (4.20) has solutions with the asymptotic behavior

$$u_1^-(z) \sim \quad e^{\mu_{1w}^-(\lambda)z} g_{1w}^-(\lambda)$$
$$u_2^-(z) \sim -z e^{\mu_{1w}^-(\lambda)z} g_{1w}^-(\lambda) \qquad \text{as } z \to -\infty$$
$$u_i^+(z) \sim \quad e^{\mu_{iw}^+(\lambda)z} g_{iw}^+(\lambda), \quad i = 1, 2 \quad \text{as } z \to +\infty.$$

The asymptotic behavior of all solutions of (4.20) is therefore given by the eigenvalues and eigenvectors of the asymptotic matrices $A_w^\pm(\lambda)$. In particular, the signs of the real parts of the eigenvalues determine whether the solutions asymptotically decrease or increase.

Since we are interested in solutions $u \in L^2(\mathbb{R}, \mathbb{C}^2)$, we have to concentrate on solutions that disappear at both ends. All functions $u(z)$ that are a combination of a decaying solution $u_i^-(z)$ of (4.20) for z negative and $u_j^+(z)$ for z positive are solutions of (4.20) in $L^2(\mathbb{R}, \mathbb{C}^2)$. The related pair (λ, u) thus represents an eigenvalue and eigenvector of $\mathfrak{B}$.

In order to detect functions u with the above properties, we first select solutions u_i^+ and u_j^- with $\mathrm{Re}(\mu_{iw}^+(\lambda)) < 0$ and $\mathrm{Re}(\mu_{jw}^-(\lambda)) > 0$, respectively. We then have to decide whether these decaying solutions for z negative and positive are connected, and hence form a solution on $\mathbb{R}$ that disappears at both ends.

The real parts of the eigenvalues $\mu_{iw}^{\pm}(\lambda)$ satisfy

$$\mathrm{Re}(\mu_{1w}^{\pm}(\lambda))\begin{pmatrix}>\\=\\<\end{pmatrix}0 \quad \Leftrightarrow \quad \mathrm{Re}(\lambda)\begin{pmatrix}<\\=\\>\end{pmatrix}d_1 k_{\pm} =: \lambda_{1w}^{\pm}$$

$$\mathrm{Re}(\mu_{2w}^{\pm}(\lambda))\begin{pmatrix}>\\=\\<\end{pmatrix}0 \quad \Leftrightarrow \quad \mathrm{Re}(\lambda)\begin{pmatrix}<\\=\\>\end{pmatrix}f(c_{\pm}) - R + d_2 k_{\pm} =: \lambda_{2w}^{\pm}.$$

From these properties we can particularly deduce the following statements, which can be verified by means of figure 4.7:

- *Necessary condition for the existence of solutions of* (4.20) *that vanish at both ends*, and hence for λ being an eigenvalue of $\mathfrak{B}$: For

  $$\min(\lambda_{1w}^+, \lambda_{2w}^+) < \mathrm{Re}(\lambda) < \max(\lambda_{1w}^-, \lambda_{2w}^-)$$

  there exists at least one solution $u_i^-(z)$ that disappears as $z \to -\infty$ and at least one solution $u_j^+(z)$ that disappears as $z \to \infty$.

- *Sufficient condition for the existence of solutions of* (4.20) *that vanish at both ends*, and hence for λ being an eigenvalue of $\mathfrak{B}$: For

  $$\begin{aligned}\max(\lambda_{1w}^+, \lambda_{2w}^+) < \mathrm{Re}(\lambda) < \max(\lambda_{1w}^-, \lambda_{2w}^-) \quad \vee \\ \min(\lambda_{1w}^+, \lambda_{2w}^+) < \mathrm{Re}(\lambda) < \min(\lambda_{1w}^-, \lambda_{2w}^-)\end{aligned}$$

  on one side both linearly independent solutions disappear, and on the other side at least one solution disappears. Therefore, there must be a connection between two solutions vanishing on either side.

- *Sufficient condition for the non-existence of a solution of* (4.20) *that vanishes at both ends*, and hence for λ being no eigenvalue of $\mathfrak{B}$: For

  $$\mathrm{Re}(\lambda) < \min(\lambda_{1w}^+, \lambda_{2w}^+) \quad \vee \quad \max(\lambda_{1w}^-, \lambda_{2w}^-) < \mathrm{Re}(\lambda)$$

  there either exists no solution of (4.20) that disappears as $z \to \infty$ or no solution that disappears as $z \to -\infty$.

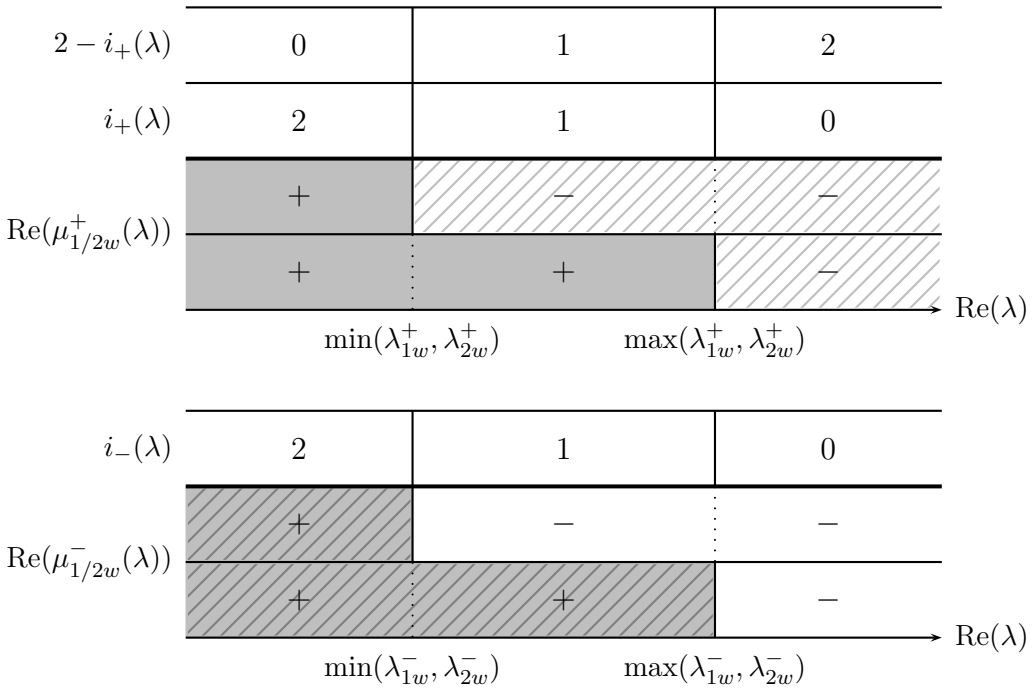

Figure 4.7: Signs of $\mathrm{Re}(\mu^{\pm}_{iw}(\lambda))$, instability indices $i_{\pm}(\lambda)$, and number of disappearing solutions ($2-i_+(\lambda)$ for $z \to +\infty$, $i_-(\lambda)$ for $z \to -\infty$). Unstable eigenvalues $\mu^{\pm}_{iw}(\lambda)$ are labeled by gray sets, disappearing solutions by hatched ones.

Remark 13. The above necessary and sufficient conditions for λ being an eigenvalue or no eigenvalue of the differential operator $\mathfrak{B}$ are characteristic for the model under consideration. But the idea of counting linearly independent decaying solutions at each end in order to study eigenvalues can be applied to a more general class of problems (see appendix C.3).

For stability investigations we are particularly interested whether there exist eigenvalues λ of $\mathfrak{B}$ with non-negative real part. From the last condition we can deduce that for

$$\max(\lambda^-_{1w}, \lambda^-_{2w}) < 0,$$

or equivalently

$$k_- < -\frac{1}{d_2}\big(f(c_-) - R\big), \tag{4.24}$$

no such eigenvalue exists. This yields the following statement about the point spectrum, which is a subset of the set of eigenvalues:

Sufficient condition for $\sigma_{pt}(\mathfrak{B}) \subseteq \{x \in \mathbb{C} : Re(x) < 0\}$: For

$$k_- < -\frac{1}{d_2}\big(f(c_-) - R\big) \quad \text{and} \quad k_+ \in \mathbb{R}$$

the point spectrum $\sigma_{pt}(\mathfrak{B})$ is either empty or else lies strictly in the left half plane.

Taking into account the sufficient conditions for both $\sigma_{ess}(\mathfrak{B})$ and $\sigma_{pt}(\mathfrak{B})$, and hence for the entire spectrum $\sigma(\mathfrak{B})$, to lie in the open left half plane, we can deduce the following stability result:

Proposition 11. *A traveling wave front in the bioremediation model* (3.1) *is linearly stable under initial perturbations* $u_w \in L^2_w(\mathbb{R}, \mathbb{C}^2)$ *if the weighted space is defined by an exponential weight function*

$$w(z) = \begin{cases} e^{k_+ z}, & z \geq 0 \\ e^{k_- z}, & z < 0 \end{cases}$$

that satisfies

$$k_- < -\frac{1}{d_2}\big(f(c_-) - R\big) \quad \textit{and} \quad k_+ < 0. \tag{4.25}$$

Interpretation of the stability condition In the following we will present an interpretation of the sufficient stability condition (4.25) by specifying properties of the functions in the associated weighted spaces. To this end we will first consider arbitrary exponentially weighted spaces and subsequently take into account the sufficient stability condition.

With respect to our application we restrict our concentration on real-valued perturbations, i.e. on functions $u_w \in L^2_w(\mathbb{R}, \mathbb{R}^2)$. Since $u_w \in L^2_w(\mathbb{R}, \mathbb{R}^2)$ is equivalent to $u_{wi} \in L^2_w(\mathbb{R}, \mathbb{R})$ for $i = 1, 2$, we can study the components individually.

For simplification we think of u_{wi} as an exponential function such that we are concerned with the functions

$$u_{wi}(z) = \begin{cases} e^{a_+ z}, & z \geq 0 \\ e^{a_- z}, & z < 0 \end{cases} \qquad \text{and} \qquad w(z) = \begin{cases} e^{k_+ z}, & z \geq 0 \\ e^{k_- z}, & z < 0. \end{cases}$$

As mentioned before, u_{wi} belongs to the function space $L^2_w(\mathbb{R}, \mathbb{R})$ if, and only if,

$$u_i(z) = u_{wi}(z)w(z) = \begin{cases} e^{(a_+ + k_+)z}, & z \geq 0 \\ e^{(a_- + k_-)z}, & z < 0 \end{cases}$$

is an element of $L^2(\mathbb{R}, \mathbb{R})$. In order to ensure that $u_i \in L^2(\mathbb{R}, \mathbb{R})$, the functions $u_i(z)$ have to decay exponentially as z tends to $\pm\infty$, and hence the growth rates $a_\pm$ of u_{wi} have to satisfy

$$\begin{aligned} a_+ + k_+ < 0 \quad &\Leftrightarrow \quad a_+ < -k_+ \\ a_- + k_- > 0 \quad &\Leftrightarrow \quad a_- > -k_-. \end{aligned}$$

Thus, for a given weight function w with growth rates $k_\pm$, the weighted space $L^2_w(\mathbb{R}, \mathbb{R})$ contains those functions u_{wi} whose exponential growth rates $a_\pm$ satisfy the above conditions.

The stability condition (4.25) is a limitation of allowed weight functions, and hence of admissible growth rates of u_{wi}, which have to satisfy

$$a_+ < -k_+ \quad \wedge \quad k_+ < 0$$
$$a_- > -k_- > \frac{1}{d_2}\big(f(c_-) - R\big) = -\alpha_-.$$

In particular, for $z < 0$ the stability condition (4.25) represents a lower bound for the growth rate a_- of u_{wi}. With respect to the result (3.7), this ensures that all functions $u_{wi} \in L^2_w(\mathbb{R}, \mathbb{R})$ decay faster than the traveling wave front $N(z)$ as z tends to $-\infty$, which asymptotically decays with the rate $-\alpha_-$.

In other words, a traveling wave front is stable under initial perturbations $u_w(z)$ that decay in both components faster than the biomass concentration $N(z)$ as z tends to $-\infty$, while they are allowed to decay or even grow exponentially with any rate less than $-k_+ > 0$ as z tends to $+\infty$ (see figure 4.8).

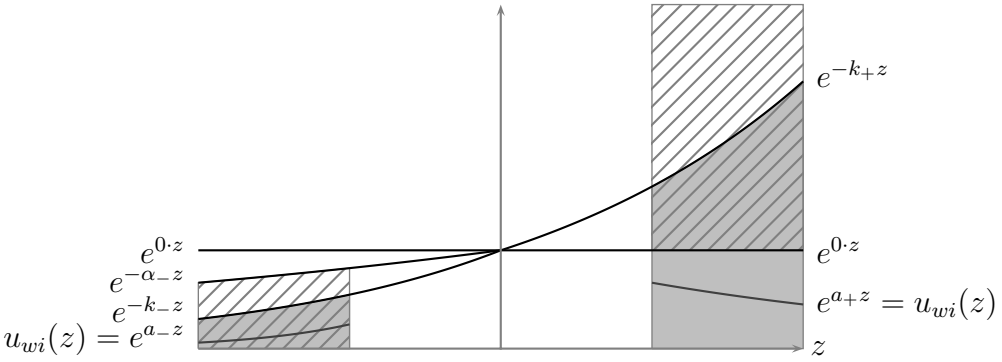

Figure 4.8: If the upper bounds $e^{-k_\pm z}$ of u_{wi} at $\pm\infty$ are in the hatched sets, then the traveling wave is stable under initial perturbations $u_w \in L^2_w(\mathbb{R}, \mathbb{R}^2)$, where L^2_w is defined as the set of functions whose components show asymptotic behavior in the gray sets (for a better comparison of the growth rates no multipliers of the exponential functions are taken into account)

In the following example we will consider a special case of exponential weight functions, namely the case $k_- = k_+$.

Example 11. We are interested in the stability of traveling waves under perturbations $u_w \in L^2_w(\mathbb{R}, \mathbb{C}^2)$, where the weighted space is defined by the exponential weight function

$$w(z) = e^{kz}$$

with $k \in \mathbb{R}$. For

$$k < -\frac{1}{d_2}\big(f(c_-) - R\big) = \alpha_- < 0$$

the sufficient condition for the spectrum $\sigma(\mathfrak{B})$ to lie in the left half plane is met. The traveling waves of (3.1) are therefore linearly stable in function spaces that satisfy the above condition.

The special case

$$\frac{1}{d_1 - d_2}\big(f(c_+) - R\big) < k < -\frac{1}{d_2}\big(f(c_-) - R\big) < 0, \tag{4.26}$$

which is equivalent to $\lambda_{2w}^+ < \lambda_{1w}^+ = \lambda_{1w}^- < \lambda_{2w}^- < 0$, is shown in the figures 4.9 and 4.10.

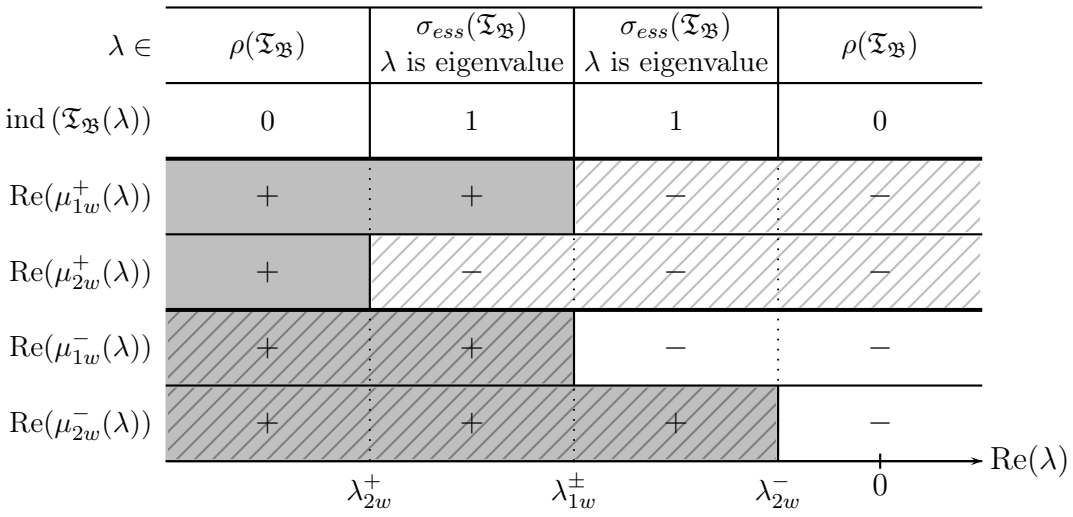

Figure 4.9: Example 11 for k satisfying (4.26): Signs of $\mathrm{Re}(\mu_{iw}^{\pm}(\lambda))$, Fredholm indices $\mathrm{ind}\,(\mathfrak{T}_{\mathfrak{B}}(\lambda)) = i_-(\lambda) - i_+(\lambda)$, and classification of λ with respect to theorem 2 and the conditions following from theorem 3. Unstable eigenvalues $\mu_{iw}^{\pm}(\lambda)$ are labeled by gray sets, disappearing solutions by hatched ones.

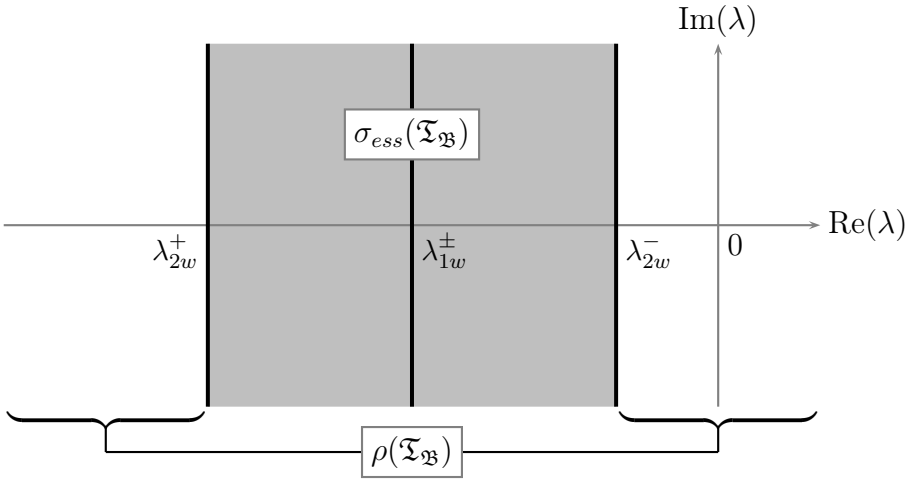

Figure 4.10: Example 11 for k satisfying (4.26): Classification of λ for $\mathfrak{T}_{\mathfrak{B}}$ on $L_w^2(\mathbb{R}, \mathbb{C}^2)$ according to theorem 2 and the conditions following from theorem 3

The spectrum of $\mathfrak{B}$ and $\mathfrak{T}_\mathfrak{B}$ is given by

$$\sigma(\mathfrak{T}_\mathfrak{B}) = \sigma_{ess}(\mathfrak{T}_\mathfrak{B}) = \{\lambda \in \mathbb{C} : \mathrm{Re}(\lambda) \in [\lambda_{2w}^+, \lambda_{2w}^-]\} \subset \{\lambda \in \mathbb{C} : \mathrm{Re}(\lambda) < 0\}.$$

The point spectrum is empty.

Perturbations in $\tilde{L}_w^2(\mathbb{R}, \mathbb{C}^2)$

In order to examine whether the sufficient stability condition (4.25) can be relaxed by allowing different weight functions for both components of the perturbation vector, we will study the operator $\mathfrak{L}$ on the exponentially weighted spaces $\tilde{L}_w^2(\mathbb{R}, \mathbb{C}^2)$.

In order to apply theorem 2, we have to ensure that the matrix

$$\tilde{A}_w(z, \lambda) = \begin{pmatrix} -\frac{1}{d_1}(f'(C)N + \lambda) + \frac{w_1'}{w_1} & -\frac{1}{d_1}\frac{w_1}{w_2}f(C) \\ \frac{1}{d_2}\frac{w_2}{w_1}f'(C)N & \frac{1}{d_2}(f(C) - R - \lambda) + \frac{w_2'}{w_2} \end{pmatrix}$$

asymptotically approaches constant matrices $\tilde{A}_w^\pm(\lambda)$, which is equivalent to the following restrictions on the growth rates of the weight functions:

$$0 \le k_+^2 - k_+^1 \le \alpha_+ \qquad \text{and} \qquad \alpha_- \le k_-^2 - k_-^1 \le 0. \tag{4.27}$$

Due to the fact that the asymptotic growth rates of $N(z)$ satisfy $\alpha_- < 0 < \alpha_+$, at least one of the secondary diagonal elements of each asymptotic matrix is zero so that the eigenvalues of all asymptotic matrices equal their diagonal entries:

$$\tilde{\mu}_{1w}^\pm(\lambda) = -\frac{\lambda}{d_1} + k_\pm^1$$
$$\tilde{\mu}_{2w}^\pm(\lambda) = \frac{1}{d_2}\big(f(c_\pm) - R - \lambda\big) + k_\pm^2.$$

A necessary and sufficient condition for the essential spectrum $\sigma_{ess}(\tilde{\mathfrak{B}})$ to lie in the open left half plane is that the real parts of all values λ that satisfy at least one of the equations $\mathrm{Re}\big(\tilde{\mu}_{1/2w}^\pm(\lambda)\big) = 0$ have to be less than zero. This is equivalent to the restrictions

$$k_\pm^1 < 0 \qquad \text{and} \qquad k_\pm^2 < \alpha_\pm. \tag{4.28}$$

For studying the point spectrum $\sigma_{pt}(\tilde{\mathfrak{B}})$ we note that the upper triangular matrices $\tilde{A}_w^\pm(\lambda)$, as well as the related matrices $\tilde{R}_w^\pm(z)$, more precisely $\tilde{A}_w^+(\lambda)/\tilde{R}_w^+(z)$ and $-\tilde{A}_w^-(\lambda)/-\tilde{R}_w^-(-z)$, meet the requirements of theorem 3. Information about the eigenvalues of $\tilde{\mathfrak{B}}$ can therefore be deduced from the eigenvalues of $\tilde{A}_w^\pm(\lambda)$: A sufficient condition for the existence of no eigenvalues λ of $\tilde{\mathfrak{B}}$ with non-negative real part is that both eigenvalues $\tilde{\mu}_{1/2w}^-(\lambda)$ of $\tilde{A}_w^-(\lambda)$ have negative real parts if $\mathrm{Re}(\lambda) \ge 0$. This condition is equivalent to

$$k_-^1 < 0 \qquad \text{and} \qquad k_-^2 < \alpha_-. \tag{4.29}$$

Combining the requirements (4.27)-(4.29) we have the following stability result:

Proposition 12. *A traveling wave front in model* (3.1) *is linearly stable in the norm* $\|\cdot\|_{\tilde{L}^2_w}$ *defined by a weight matrix* $W(z) = diag\big(w_1(z), w_2(z)\big)$ *with*

$$w_i(z) = \begin{cases} e^{k^i_+ z}, & z \geq 0 \\ e^{k^i_- z}, & z < 0 \end{cases}$$

satisfying

$$\begin{aligned} k^2_- \leq k^1_- < 0 \quad &\wedge \quad k^2_- < \alpha_- < k^2_- - k^1_-, \\ k^1_+ \leq k^2_+ < \alpha_+ \quad &\wedge \quad k^1_+ < 0 \leq k^2_+ - k^1_+ < \alpha_+. \end{aligned} \tag{4.30}$$

Closing the analysis of the single-substrate bioremediation model, we relate the stability results concerning the weighted spaces $\tilde{L}^2_w$ to the results concerning L^2_w. Clearly, the exponentially weighted spaces L^2_w, defined by the same weight function for all components, are special cases of $\tilde{L}^2_w$, and consequently the stability condition (4.25) is a special case of (4.30): If we choose the weight matrix $W(z)$ such that $w_1(z) = w_2(z)$, and hence $k^1_\pm = k^2_\pm =: k_\pm$, the sufficient stability condition (4.30) is reduced to $k_- < \alpha_-$ and $k_+ < 0$.

The consideration of the more general function spaces $\tilde{L}^2_w$ does not yield a relaxation of the constraints on the biomass perturbations, i.e. in order to ensure stability of the traveling waves, the perturbations in the second component have to decay faster than the biomass wave profile as z tends to $-\infty$. In contrast, the perturbations of $C(z)$ in $\tilde{L}^2_w$ are allowed to decay slower than the wave profile $N(z)$ as z tends to $-\infty$, i.e. the weight function does not necessarily have to satisfy $k^1_- < \alpha_-$ in order to yield stability of the traveling wave in the associated norm.

Remark 14. In section 3.1 we proved that for a given set of parameters there exists an infinite number of traveling wave front solutions of model (3.1). These waves differ in their propagation speed, total biomass and in particular in the decay rate of the biomass at $-\infty$. In this section we proved that each of these traveling waves is linearly stable under perturbations that decay faster than the biomass as z tends to $-\infty$. Consequently, the decay of any perturbed biomass profile at $-\infty$ is dominated by the biomass itself, and hence any perturbed profile is uniquely related to a particular wave front. This roughly clarifies the apparent inconsistency of an infinite number of stable traveling wave fronts.

4.3.3 Double-substrate bioremediation model

Analogous to the previous subsection the issue is to derive sufficient conditions on the weight functions such that the traveling waves in the bioremediation model (3.8) are stable in the associated weighted norm. For this we will consider again perturbations in the conventional exponentially weighted spaces L^2_w, as well as in the generalized function spaces $\tilde{L}^2_w$.

Perturbations in $L^2_w(\mathbb{R},\mathbb{C}^3)$

Since the essential spectrum of $\mathfrak{B}$ is bounded by values for which

$$A^{\pm}_w(\lambda) = \begin{pmatrix} -\frac{\lambda}{d_1} + k_\pm & 0 & -\frac{1}{d_1}\nu_o f(c_{o\pm}, c_{s\pm}) \\ 0 & -\frac{\lambda}{d_2} + k_\pm & -\frac{1}{d_2}\nu_s f(c_{o\pm}, c_{s\pm}) \\ 0 & 0 & \frac{1}{d_3}\big((\nu_o+\nu_s) f(c_{o\pm}, c_{s\pm}) - R - \lambda\big) + k_\pm \end{pmatrix}$$

is not hyperbolic, a necessary and sufficient condition for the essential spectrum of $\mathfrak{B}$ to lie in the closed left half plane is that all values λ that are related to a not hyperbolic matrix $A^{\pm}_w(\lambda)$ have non-positive real part. This means, all values λ that solve at least one of the equations

$$\begin{aligned} \mathrm{Re}(\mu^{\pm}_{1w}(\lambda)) &= -\frac{\mathrm{Re}(\lambda)}{d_1} + k_\pm = 0 \quad \Leftrightarrow \quad \mathrm{Re}(\lambda) = d_1 k_\pm =: \lambda^{\pm}_{1w} \\ \mathrm{Re}(\mu^{\pm}_{2w}(\lambda)) &= -\frac{\mathrm{Re}(\lambda)}{d_2} + k_\pm = 0 \quad \Leftrightarrow \quad \mathrm{Re}(\lambda) = d_2 k_\pm =: \lambda^{\pm}_{2w} \\ \mathrm{Re}(\mu^{\pm}_{3w}(\lambda)) &= \frac{1}{d_3}\big((\nu_o+\nu_s) f(c_{o\pm},c_{s\pm}) - R - \mathrm{Re}(\lambda)\big) + k_\pm = 0 \\ &\qquad \Leftrightarrow\ \mathrm{Re}(\lambda) = (\nu_o+\nu_s) f(c_{o\pm}, c_{s\pm}) - R + d_3 k_\pm =: \lambda^{\pm}_{3w} \end{aligned}$$

have to satisfy $\mathrm{Re}(\lambda) \leq 0$.

It is easily seen that there does not exist any set of parameters $k_\pm$ such that this necessary stability condition is satisfied: Due to $d_2 < 0 < d_1$, for any $k_+ \neq 0$ the values λ^+_{1w} and λ^+_{2w} have opposite signs. Analogously we can argue for $k_- \neq 0$, and according to subsection 4.2.3 either λ^+_{3w} or λ^-_{3w} is positive in the remaining case $k_- = k_+ = 0$. It follows that the essential spectrum crosses the imaginary axis for any choice of $k_\pm \in \mathbb{R}$, which yields the following instability result:

Proposition 13. *The traveling wave fronts in the bioremediation model* (3.8) *are linearly unstable under initial perturbations $u_w \in L^2_w(\mathbb{R},\mathbb{C}^3)$ defined by an exponential weight function*

$$w(z) = \begin{cases} e^{k_+ z}, & z \geq 0 \\ e^{k_- z}, & z < 0 \end{cases}$$

with $k_\pm \in \mathbb{R}$.

The above results indicate that moving the entire essential spectrum into the left half plane requires a different treatment of the different components of the perturbation vector. The asymptotic behavior of the perturbations in all three components has to be restricted in a way that cannot be captured by a scalar weight function. We will therefore study perturbations in the weighted spaces $\tilde{L}^2_w(\mathbb{R},\mathbb{C}^3)$, which are defined by different weight functions for each component of the perturbation vector.

Perturbations in $\tilde{L}^2_w(\mathbb{R}, \mathbb{C}^3)$

In order to apply theorem 2 for studying the spectrum of $\tilde{\mathfrak{B}}$, we will restrict our concentration on weight functions such that the matrix

$$\tilde{A}_w(z,\lambda) = \begin{pmatrix} -\frac{1}{d_1}(\nu_o f_{c_o} N + \lambda) + \frac{w_1'}{w_1} & -\frac{1}{d_1}\frac{w_1}{w_2}\nu_o f_{c_s} N & -\frac{1}{d_1}\frac{w_1}{w_3}\nu_o f \\ -\frac{1}{d_2}\frac{w_2}{w_1}\nu_s f_{c_o} N & -\frac{1}{d_2}(\nu_s f_{c_s} N + \lambda) + \frac{w_2'}{w_2} & -\frac{1}{d_2}\frac{w_2}{w_3}\nu_s f \\ \frac{1}{d_3}\frac{w_3}{w_1}(\nu_o+\nu_s) f_{c_o} N & \frac{1}{d_3}\frac{w_3}{w_2}(\nu_o+\nu_s) f_{c_s} N & \frac{1}{d_3}\big((\nu_o+\nu_s) f - R - \lambda\big) + \frac{w_3'}{w_3} \end{pmatrix}$$

asymptotically approaches constant matrices $\tilde{A}^{\pm}_w(\lambda)$, i.e. we consider weight functions whose growth rates satisfy

$$\begin{aligned} -\alpha_+ \le k^2_+ - k^1_+ \le \alpha_+ \qquad & \alpha_- \le k^2_- - k^1_- \le -\alpha_- \\ 0 \le k^3_+ - k^1_+ \le \alpha_+ \qquad & \alpha_- \le k^3_- - k^1_- \le \quad 0 \\ 0 \le k^3_+ - k^2_+ \le \alpha_+ \qquad & \alpha_- \le k^3_- - k^2_- \le \quad 0. \end{aligned} \tag{4.31}$$

It is easily verified that due to $\alpha_- < 0 < \alpha_+$ the components of each asymptotic matrix satisfy $a_{ij} \neq 0 \Rightarrow a_{ji} = 0$ for $i \neq j$, and that furthermore the eigenvalues of each asymptotic matrix are given by its diagonal elements:

$$\begin{aligned} \tilde{\mu}^{\pm}_{1w}(\lambda) &= -\frac{\lambda}{d_1} + k^1_{\pm} \\ \tilde{\mu}^{\pm}_{2w}(\lambda) &= -\frac{\lambda}{d_2} + k^2_{\pm} \\ \tilde{\mu}^{\pm}_{3w}(\lambda) &= \frac{1}{d_3}\big((\nu_o+\nu_s) f(c_{o\pm}, c_{s\pm}) - R - \lambda\big) + k^3_{\pm}. \end{aligned} \tag{4.32}$$

The essential spectrum $\sigma_{ess}(\tilde{\mathfrak{B}})$ lies in the open left half plane if, and only if, all λ satisfying $\mathrm{Re}(\tilde{\mu}^{\pm}_{iw}(\lambda)) = 0$ also satisfy $\mathrm{Re}(\lambda) < 0$, which is equivalent to

$$k^1_{\pm} < 0, \qquad k^2_{\pm} > 0, \qquad k^3_{\pm} \begin{cases} < \alpha_{\pm}, & s < 0 \\ > \alpha_{\pm}, & s > 0. \end{cases} \tag{4.33}$$

This condition ensures that in each component the associated weighted norm tolerates perturbations on the downstream side, while it penalizes them on the upstream side. This means for example for the first component, which is related to the transportation speed $d_1 > 0$, that the weighted norm by $k^1_{\pm} < 0$ tolerates perturbations at $+\infty$ and penalizes them at $-\infty$.

But these restrictions are not compatible with (4.31): Combining the restrictions (4.31) and (4.33) yields in particular the contradictions

$$\begin{aligned} k^3_- - k^2_- < \alpha_- \le k^3_- - k^2_- \qquad & \text{for } s < 0 \\ k^3_+ - k^1_+ \le \alpha_+ < k^3_+ - k^1_+ \qquad & \text{for } s > 0. \end{aligned}$$

Consequently, there does not exist any weight matrix $W(z)$ consisting of exponential weight functions such that the asymptotic matrices $\tilde{A}_w^{\pm}(\lambda)$ exist and the essential spectrum is bounded to the left of the imaginary axis. We can therefore not directly formulate a sufficient condition on the weight functions that ensures the stability of the traveling waves in the associated weighted norm.

In a second stage we will study a necessary condition which, if it is met, requires further analyses to deduce stability or instability results. A necessary stability condition is that the spectrum of $\mathfrak{T}_{\tilde{\mathfrak{B}}}$ lies in the closed left half plane, i.e. the imaginary axis is allowed to be contained in the essential spectrum:

$$k_{\pm}^1 \leq 0, \qquad k_{\pm}^2 \geq 0, \qquad k_{\pm}^3 \begin{cases} \leq \alpha_{\pm}, & s < 0 \\ \geq \alpha_{\pm}, & s > 0. \end{cases} \tag{4.34}$$

While in this case perturbations in the first and second component are not necessarily penalized by a weight function, the perturbations in the third component are still restricted on the upstream side by the biomass growth.

Indeed, there exist weight functions with the required properties, namely which on the one hand ensure the existence of constant asymptotic matrices and which on the other hand meet condition (4.34): The growth rates

$$k_{\pm}^1 = k_{\pm}^2 = k_{+}^3 = 0, \quad k_{-}^3 = \alpha_{-}, \tag{4.35}$$

for example, are related to an upper triangular matrix $\tilde{A}_w^{+}(\lambda)$ and a lower triangular matrix $\tilde{A}_w^{-}(\lambda)$. By means of theorem 2 we can deduce from the eigenvalues (4.32) the following statements about the spectrum of $\mathfrak{T}_{\tilde{\mathfrak{B}}}$ for $s < 0$ (see figures 4.11 and 4.12):

$$\begin{aligned} \sigma_{ess}(\mathfrak{T}_{\tilde{\mathfrak{B}}}) &= \{\lambda \in \mathbb{C} : \mathrm{Re}(\lambda) \in [\lambda_3^+, 0]\} \\ \rho(\mathfrak{T}_{\tilde{\mathfrak{B}}}) \cup \sigma_{pt}(\mathfrak{T}_{\tilde{\mathfrak{B}}}) &= \{\lambda \in \mathbb{C} : \mathrm{Re}(\lambda) \in (-\infty, \lambda_3^+) \cup (0, \infty)\}. \end{aligned}$$

The essential spectrum of $\mathfrak{T}_{\tilde{\mathfrak{B}}}$ contains the imaginary axis but does not cross it. We note furthermore that neither theorem 2 nor theorem 3 enables us to distinct the point spectrum from the resolvent set without further information. Thus, in order to deduce a final stability or instability result in this special case, as well as in any other case satisfying the necessary condition (4.34), further analyses are needed, which will not be part of this thesis.

The growth rates presented in (4.35) can be interpreted as follows: The weighted space $\tilde{L}_w^2(\mathbb{R}, \mathbb{C}^3)$ defined by a weight matrix $W(z)$ satisfying (4.35) consists of functions that are elements of $L^2(\mathbb{R}, \mathbb{C})$ in the first and second component, and that decay faster than $N(z)$ as z tends to $-\infty$ in the third one. The traveling waves are therefore possibly stable under perturbations in $L^2(\mathbb{R}, \mathbb{C}^3)$ that are restricted in the third component on the upstream side.

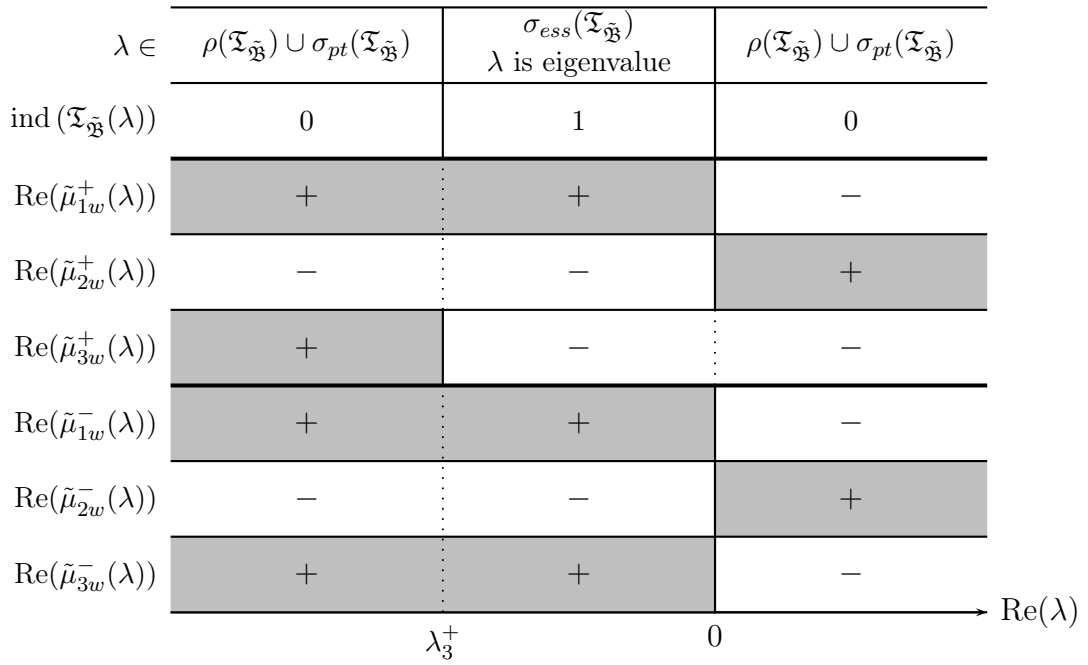

Figure 4.11: Signs of $\operatorname{Re}(\tilde{\mu}^{\pm}_{iw}(\lambda))$, Fredholm indices, and classification of λ with respect to theorem 2 for weight functions that satisfy (4.35) ($s < 0$)

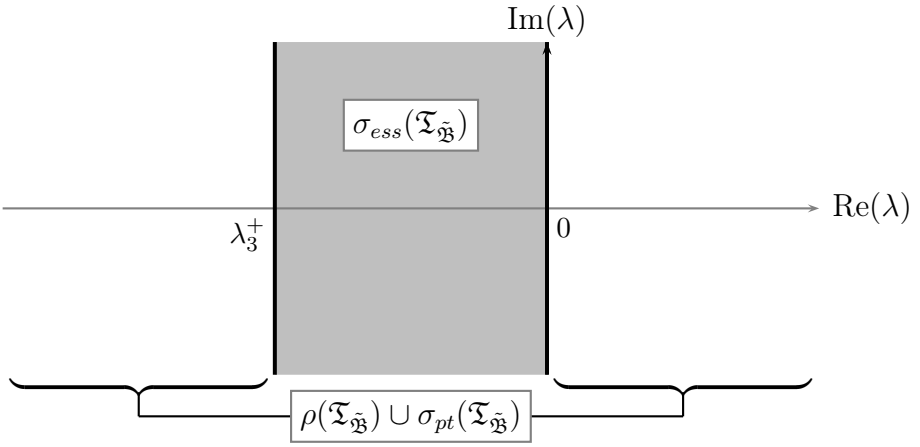

Figure 4.12: Classification of λ for $\mathfrak{T}_{\tilde{\mathfrak{B}}}$ on $\tilde{L}^2_w(\mathbb{R}, \mathbb{C}^3)$ satisfying (4.35) ($s < 0$)

To sum up, for weight functions that ensure the existence of asymptotic matrices we can distinct two cases: If the weight functions contradict the necessary stability condition (4.34), the traveling waves are unstable in the associated weighted norm. If they on the other hand meet condition (4.34), the traveling waves might be stable in the related norm, but for a final stability or instability result further analyses are needed. Although the theoretical approach presented in this thesis is not sufficient to detect a "stable function space", the numerical results in the next section indicate that there exist those spaces.

4.4 Numerical results

The theoretical analyses presented in the previous sections shall be supplemented with numerical simulations. To this end we consider a concrete example for each bioremediation model, (3.1) and (3.8), and interpret the numerical results, which are produced by Java applets, with respect to the developed theory.

In order to study the stability of certain traveling waves in the bioremediation models (3.1) and (3.8), we proceed as follows[8]:

(i) *Solution of the ordinary differential equation → wave profile:* We choose a certain set of parameters satisfying the requirements of propositions 1 and 7, respectively. For these parameters the ODE with appropriate initial conditions is solved by the *classical Runge-Kutta method*.

(ii) *Solution of the partial differential equation → traveling wave:* In order to picture the solution of the PDE for a sufficiently large time interval, we solve this equation in a coordinate system that moves with speed s (in this coordinate system a wave traveling with speed s is a stationary solution). The adjusted[9] PDE with appropriate boundary conditions is solved by means of the *explicit first-order upwind scheme*, where the initial condition is given by one of the following functions:
   (a) *No perturbation of the initial profile:* The initial condition is represented by the profile resulting from (i).
   (b) *Perturbation of the initial profile:* The initial condition is given by the profile resulting from (i) plus a perturbation function.

In order to specify the procedure outlined above and to visualize the results, we revert to the examples 8 and 9 on pages 37 and 49 in the past chapter:

Example 12 ($m=1$)**.** For the parameters

$$\begin{aligned} u &= \ \ 7.81, \qquad \nu = 1.12, \qquad C(-26) = 0.76, \\ s &= -0.13, \qquad R = 0.34, \qquad N(-26) = 3.34 \cdot 10^{-18} \end{aligned}$$

we solve the ordinary differential equation (3.2) with step size $\Delta z = 0.02$. The solution in the Interval $I_{vis} = [0, 25]$ is visualized in the first graph in figure 4.13. The additionally given characteristic value $N_{tot} = 12.65$ is computed by the *composite Simpson's rule* in the interval $I = [-26, 25]$. It differs slightly from the theoretical value $N_{tot} = 12.60$, which results from proposition 1 on page 36, and it depends on the step sizes as stated in remark 15.

[8] In order to discuss both models at the same time, we denote by ODE the models (3.2) and (3.24)/(3.25) and by PDE the models (3.1) and (3.8).

[9] The change from the space variable x to the "moving" one $z = x - st$ results in replacing the speed matrix $\tilde{D}$ in the PDE by $\tilde{D} - sI$ (see equation (4.2) in section 4.1).

Using this profile (undisturbed or disturbed) as initial condition we solve the partial differential equation (3.1) with step sizes $\Delta t = 0.002$ and $\Delta z = 0.02$ in a coordinate system that moves with speed $\tilde{s} = s - 0.00145$ (for more details about the additional constant see remark 15). The boundary conditions are given by $(c, n)(-26, t) = (C + u_c, N + u_n)(-26)$, where $u(z) = (u_c, u_n)(z)$ denotes the initial perturbation. The evolution of the undisturbed initial profile, as well as the effects of three specific perturbations, are the following:

- If the initial profile is not perturbed, a specific profile, close to the initial one, is reached quickly and remains unchanged (see first row in figure 4.13).
- In a bounded interval on the left of the biomass maximum we add a parabola to $C(z)$. This perturbation moves to the right while the maximum value of the biomass, as well as the total biomass, increase and decrease again. The limit profile in the interval I_{vis} equals the limit profile in the undisturbed case (see second row in figure 4.13). This result is consistent with the theory since any compact perturbation is zero for $|z|$ large enough, and hence an element of each "stable weighted space" $\tilde{L}^2_w$, i.e. $\tilde{L}^2_w$ satisfying (4.30). One particular property of exponentially weighted spaces shall be emphasized in this context: Even if the perturbation that travels to the right does not decay, it is reduced by the weight function such that it does not cause instability in the weighted L^2 norm. In this sense, an instability in the L^2 norm that is caused by certain traveling perturbations can be considered as stability in an appropriate weighted L^2 norm.
- In the entire interval I we add a Gaussian function to $N(z)$. The maximum value of the biomass first decreases, then increases significantly, combined with a change in the slope of $C(z)$. Finally, the profile tends to the limit one in the undisturbed case (see third row in figure 4.13). With respect to the theoretical analysis, this result is the expected one: Since Gaussian functions decay faster than exponential functions for large values of $|z|$, they are elements of all weighted spaces $\tilde{L}^2_w$ that satisfy the stability condition (4.30). In particular, they are elements of all function spaces L^2_w that meet the condition (4.25).
- In the interval I we perturb the wave profile $N(z)$ by a function that decays exponentially on either side of the maximum of $N(z)$. At this we choose the growth rates such that the perturbation decays slower than $N(z)$ as z tends to $-\infty$. The maximum value of the biomass decreases, and the wave form tends to another profile, which is characterized by slower decays in both components. This profile travels with a speed different from the initial one to the left (see fourth row in figure 4.13). This result is consistent with the theory since due to the particular growth rate the perturbation does not belong to any of the "stable weighted spaces" defined in the previous section. Moreover, as expected, the limit profile is the unique one having the asymptotic decay rate of the initial perturbation as z tends to $-\infty$.

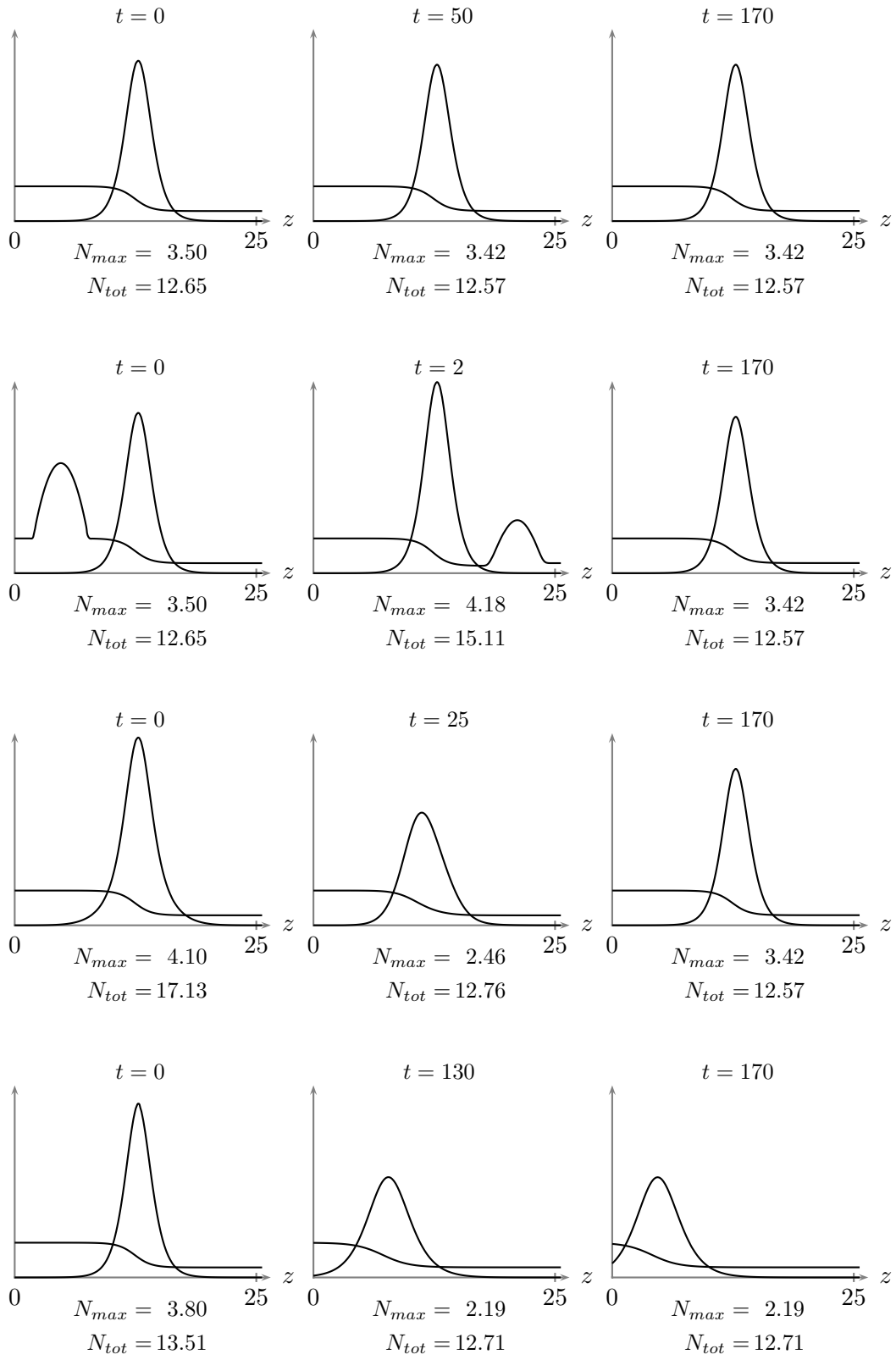

Figure 4.13: Numerical results (for more details see the text in example 12)

Remark 15. The numerically computed maximum biomass N_{max}, the total biomass N_{tot}, as well as the additional constant in the wave speed $\tilde{s}$, are related to the step sizes: For a fixed Δt, a decreasing step size Δz results in decreasing values N_{max} and N_{tot} at $t = 0$, and increasing values N_{max} and N_{tot} at $t = 170$, so that the differences between the limit values and initial values decrease. Furthermore, a decreasing step size Δz yields a decreasing difference between the parameter s that was used to create the initial condition and the numerical wave speed $\tilde{s}$.

Example 13 ($m=2$)**.** With the parameters

$$\begin{aligned} u &= 4.000, & \nu_o &= 1.170, & N^*_{tot} &= 15.000, & C_o(0) &= 2.240, \\ v &= -9.780, & \nu_s &= 1.550, & & & C_s(130) &= 0.432, \\ s &= 0.351, & R &= 0.360, & & & N(0) &= 1 \cdot 10^{-5} \end{aligned}$$

we first compute, according to equation (3.23), the missing initial condition

$$C_s(0) = C_s(130) - \frac{\nu_s}{\nu_o + \nu_s} \frac{R N^*_{tot}}{s - v} = 0.128.$$

With these parameters and initial conditions we solve the ordinary differential equation (3.24)/(3.25) with step size $\Delta z = 0.03$ and visualize the solution in the interval $I_{vis} = [0, 65]$ (see first graph in figure 4.14).

With this profile (undisturbed and disturbed) as initial condition we solve the partial differential equation (3.8) with step sizes $\Delta t = 0.002$ and $\Delta z = 0.03$ in a coordinate system moving with speed $\tilde{s} = s + 0.00195$ (for more details about the additive constant see remark 15). To this end we fix the boundary conditions $c_o(0, t) = (C_o + u_o)(0)$ and $(c_s, n)(130, t) = (C_s + u_s, N + u_n)(130)$, where $u(z) = (u_o, u_s, u_n)(z)$ is the initial perturbation.

As can be verified in figure 4.14, the evolution of the undisturbed profile, as well as the initial profile which is perturbed by parabolas, a Gaussian function or an exponential decaying function, is the following:

- The undisturbed wave profile tends quickly to a very close one, which remains unchanged (see first row in figure 4.14).

- Parabolas, added to $C_o(z)$ and $C_s(z)$ in bounded intervals, move in the direction of flow, i.e. the perturbation of $C_o(z)$ travels to the right, while the perturbation of $C_s(z)$ moves to the left. The limit profile in the visible interval I_{vis} equals the one in the undisturbed case (see second row in figure 4.14). This compact perturbation is an element of any weighted space $\tilde{L}^2_w$ defined by (4.31) and satisfying the necessary stability condition (4.34). Consequently, if there exists a "stable weighted space" $\tilde{L}^2_w$, then this perturbation belongs to it.

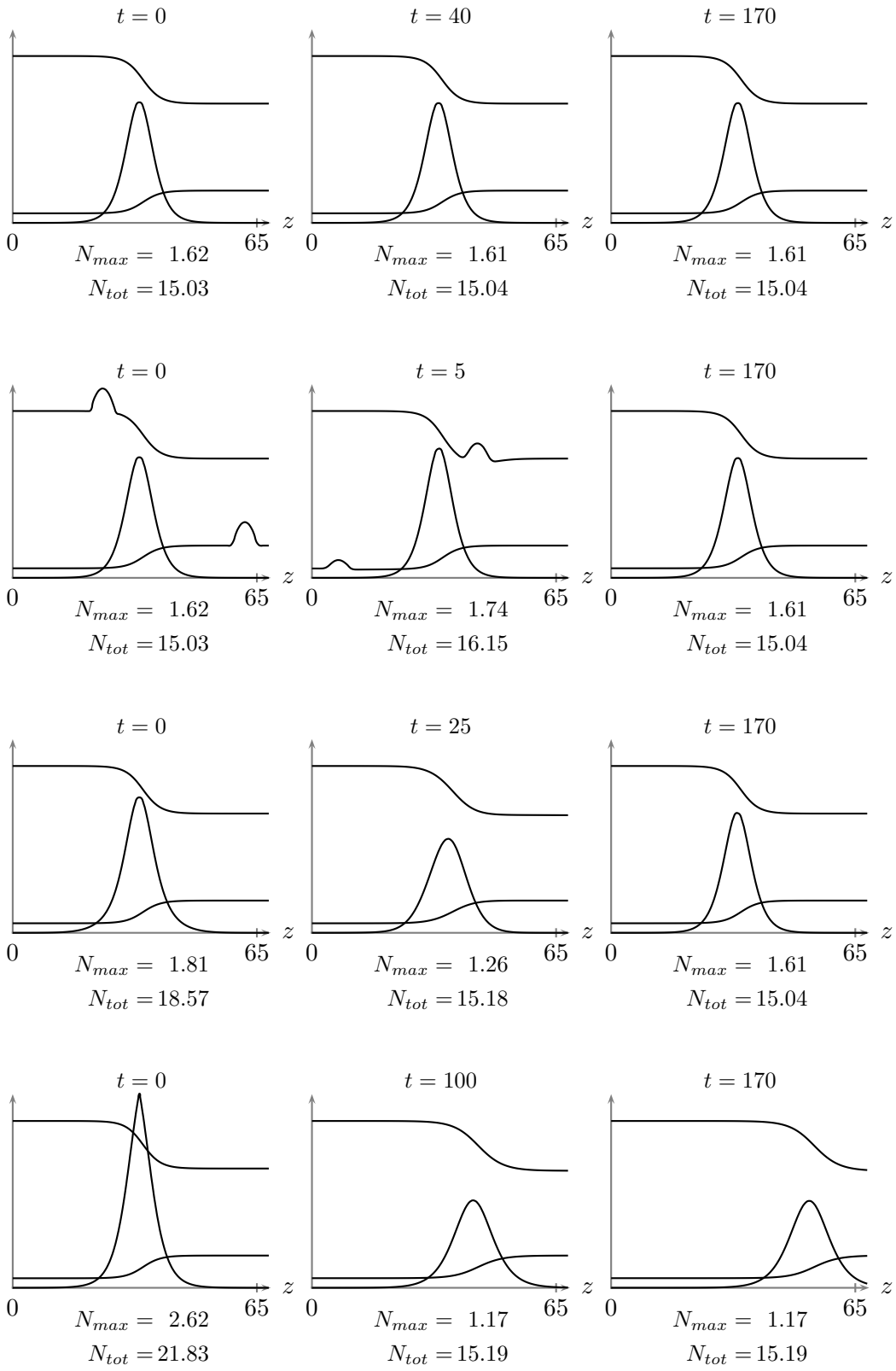

Figure 4.14: Numerical results (for more details see the text in example 13)

- If we perturb the wave profile $N(z)$ by a Gaussian function, the maximum of the biomass decreases and increases again, and finally the solution tends to the limit profile in the undisturbed case (see third row in figure 4.14). Due to the specific decay of Gaussian functions, this perturbation belongs to any weighted space $\tilde{L}^2_w$ satisfying (4.31) and the necessary stability condition (4.34). The numerical results are therefore consistent with the theory.

- We add a function to the wave profile $N(z)$ that decays exponentially on either side of the biomass maximum. The growth rate chosen for the right-hand side of the maximum is greater than the asymptotic growth rate of the biomass, i.e. the perturbation decays slower than $N(z)$ as z tends to infinity. The solution tends to a profile that is different to the limit one in the undisturbed case. This profile shows slower decays in all three components and travels to the right (see fourth row in figure 4.14). This result is in line with the theory: Due to its particular growth rate the initial perturbation does not belong to any of the weighted spaces $\tilde{L}^2_w$ satisfying (4.31) and the necessary stability condition (4.34).

To sum up, the theoretical results concerning the single-substrate model, as well as the double-substrate model, are consistent with the numerical ones. But in addition to the theoretical results regarding the double-substrate case, the numerical data indicate the existence of a certain norm that ensures stability of the traveling waves.

4.5 Conclusions

The traveling wave front solutions of the single-substrate bioremediation model are linearly unstable in the L^2 norm since the essential spectrum, and in particular the set of eigenvalues of the linearization about the traveling wave, crosses the imaginary axis. But the waves are linearly stable in the L^2_w norm defined by a scalar exponential weight function whose growth rates meet a specific condition. This condition ensures that the perturbations in the associated weighted spaces decay in both components faster than the biomass profile $N(z)$ as z tends to $-\infty$.

More generally, the traveling wave solutions of the above model are linearly stable in certain weighted spaces $\tilde{L}^2_w$, which allow different exponential weight functions for each component of the perturbation vector. A sufficient stability condition on the growth rates of these weight functions is given by (4.30), which restricts the asymptotic behavior of admissible perturbations. In particular, the substrate perturbations are less restricted than in the conventional weighted spaces L^2_w, while the constraints on the biomass perturbations could not be relaxed by considering the more general function spaces $\tilde{L}^2_w$.

The traveling wave fronts in the double-substrate bioremediation model are linearly unstable under perturbations in L^2, as well as in L^2_w, which is defined by a scalar exponential weight function. Independent of its growth rates, the essential spectrum of the associated differential operator crosses the imaginary axis. The analysis of the more general weighted spaces $\tilde{L}^2_w$, defined by different exponential weight functions for each component, did not yield a stability result either: Weight functions that satisfy (4.31), but not (4.34), yield instability caused by the essential spectrum, which crosses the imaginary axis. Weight functions that meet both conditions might yield stability of the traveling waves in the related norm, but due to the fact that the essential spectrum includes the imaginary axis, and that the point spectrum cannot be localized by means of theorem 3, this case cannot conclusively be studied by the procedure presented in this thesis. Thus, further analyses are required to detect function spaces that the traveling waves are stable for, which the numerical results indicate do exist.

	description[10]
$q(x,t)$	concentration vector
$Q(z)$	concentration vector (traveling wave)
$F(q)$	function that contains the non-linear growth terms
$J_F(q)$	Jacobian matrix of $F(q)$
$f(C)$	modified growth rate of the biomass for $m=1$: $f(C)=\nu\mu_1(C)$
$f(C_o,C_s)$	growth rate of the biomass for $m=2$: $f(C_o,C_s)=\mu_2(C_o,C_s)$
$\tilde{D}$	diagonal matrix containing the speeds of the substrates
D	diagonal matrix containing the speeds of the substrates and biomass in a moving coordinate system, $D=\tilde{D}-sI=\operatorname{diag}(d_1,\ldots,d_m)$
d_i	speeds of substrates and biomass in a moving coordinate system
$p(z,t)$	perturbation vector
$u(z)$	initial perturbation: $p(z,0)=u(z)$
$u_w(z)$	initial perturbation in weighted L^2 spaces
$\mathfrak{L}$, $\mathfrak{B}$, $\tilde{\mathfrak{B}}$	differential operators
$\mathfrak{T}$, $\mathfrak{T}_{\mathfrak{B}}$, $\mathfrak{T}_{\tilde{\mathfrak{B}}}$	differential operators with the same spectrum as $\mathfrak{L}$, $\mathfrak{B}$, $\tilde{\mathfrak{B}}$
$A(z,\lambda)$	matrix occurring in $\mathfrak{T}$: $\mathfrak{T}(\lambda)=\frac{d}{dz}-A(z,\lambda)$
$A^{\pm}(\lambda)$	asymptotic matrices of $A(z,\lambda)$: $\lim_{z\to\pm\infty}A(z,\lambda)=A^{\pm}(\lambda)$
$R^{\pm}(z)$	difference between $A(z,\lambda)$ and $A^{\pm}(\lambda)$: $A(z,\lambda)=A^{\pm}(\lambda)+R^{\pm}(z)$
$(\cdot)_w$	matrices above related to $\mathfrak{T}_{\mathfrak{B}}$
$\tilde{(\cdot)}_w$	matrices above related to $\mathfrak{T}_{\tilde{\mathfrak{B}}}$
$\mu_i^{\pm}(\lambda)$	eigenvalues of $A^{\pm}(\lambda)$
$g_i^{\pm}(\lambda)$	eigenvectors of $A^{\pm}(\lambda)$
$\lambda_i^{\pm}$	value λ such that $\operatorname{Re}(\mu_i^{\pm}(\lambda))=0$
$(\cdot)_w$	values above related to $A_w^{\pm}(\lambda)$
$\tilde{(\cdot)}_w$	values above related to $\tilde{A}_w^{\pm}(\lambda)$
$w(z), w_i(z)$	weight functions
$W(z)$	weight matrix: $W(z)=\operatorname{diag}\big(w_1(z),\ldots,w_m(z)\big)$
$k(z), k^i(z)$	exponential growth rates of $w(z), w_i(z)$ depending on z
$k_{\pm}, k_{\pm}^i$	exponential growth rates of $w(z), w_i(z)$ for $z\geq 0$ and $z<0$
$\operatorname{ind}(\cdot)$	Fredholm index of an operator
$i_{\pm}(\lambda)$	instability indices of $A^{\pm}(\lambda)$
x	space
z	space along the characteristics: $z=x-st$
t	time

Table 4.1: Notation[11] used in chapter 4

[10] Note that according to subsection 2.4.2 the models under consideration are dimensionless. The descriptions thus correspond to the related dimensional values.

[11] For notations that are directly related to the mathematical models we refer to table 3.1 on page 38 and table 3.2 on page 54.

Chapter 5

Summary

Due to its effectiveness and cost-efficiency, bioremediation is a promising technology for restoring contaminated groundwater and soil. In order to predict the merits of this method, and to adjust influencing factors such as the concentrations of additionally injected substrates, mathematical models are of special interest. One particular bioremediation model has been derived and analyzed in this thesis.

Bioremediation is based on the utilization of contaminants by specific microorganisms. Great importance is therefore attached to the metabolism of the organisms involved, which is again closely linked to enzymatic reactions inside their cells. The first step in deriving a bioremediation model is therefore the analysis of enzymatic reactions and microbial growth.

At first, we analyzed specific enzymatic reactions that involve an arbitrary number of substrates. Based on these results we derived a bacterial growth model and in particular a formula for the bacterial growth rate that includes an optional number of substrates and contaminants.

This bacterial growth rate was compared to a similar one that is commonly used in several articles without a detailed declaration of underlying model assumptions. For bacterial growth depending on one or two substrates, both growth rates can be equalized, which lends, according to other authors, support to existing single- and double-substrate bacterial growth models. For more than two involved substrates, however, no biologically reasonable assumptions result in equal growth rates. Hence, either the growth rates suggested by various authors for different numbers of substrates are based on assumptions that differ from the ones made in this work, or they include an additional simplification which cannot be justified from a chemical or biological point of view.

Finally, by taking into account spatial changes and environmental properties, we extended the derived bacterial growth model to a bioremediation model consisting of advection-reaction equations for the substrates and a rate equation for the bacteria.

Subsequently, the above bioremediation model for one and two substrates was analyzed with respect to traveling waves, which form an important class of solutions in natural scientific applications. By deriving planar autonomous systems of ordinary differential equations from the original model, phase plane analysis yielded results concerning the existence of traveling wave solutions, their shape and propagation speed.

It could be shown that under certain requirements on parameters the single-substrate model has wave front solutions that travel with any negative propagation speed. All those solutions are qualitatively of the same shape, but they differ in particular in their characteristic value of total biomass, as well as in the asymptotic behavior of the biomass concentration.

For the double-substrate model we could also establish a sufficient condition for the existence of wave fronts. All fronts resulting from this condition travel in the same direction with speeds in a certain bounded interval. Furthermore, their profiles have the same qualitative properties, while in particular each value of total biomass is taken at most twice.

In the final step, the traveling wave solutions that were specified above were tested for their stability. To this end we derived a mathematical model that describes the evolution of small perturbations about the wave profile. Linear stability results could be deduced from the spectral analysis of the occurring differential operator, where its Fredholm properties and specific asymptotic properties were of particular importance.

All traveling wave fronts in the single-substrate bioremediation model turned out to be linearly unstable under perturbations in L^2, but linearly stable in the L^2_w norm which is defined by an exponential weight function whose growth rates meet certain conditions. Roughly speaking, these conditions ensure that the initial perturbations decay faster than the biomass wave front on the upstream side. We could widen this result by introducing the class of more general weighted spaces $\tilde{L}^2_w$, defined by different exponential weight functions for each component of the perturbation vector. With certain constraints on their growth rates, which restrict the asymptotic behavior of the perturbations, we could prove stability of the traveling waves in the associated weighted norms.

In contrast, the traveling wave fronts in the double-substrate bioremediation model are linearly unstable in L^2, as well as in any weighted space L^2_w, defined by a scalar exponential weight function. The generalization to the weighted spaces $\tilde{L}^2_w$, which allows different exponential weight functions in each component, did not yield a stability result either: For certain spaces $\tilde{L}^2_w$ we could prove instability of the traveling waves, while for the remaining cases further analyses are needed to deduce final stability or instability results. Although numerical runs indicate the existence of a function space that yields stability of the traveling waves in the associated norm, this remains to be proven theoretically.

Appendix

A Modeling: Asymptotic analysis of enzymatic reactions

Many mathematical problems are not solvable explicitly. However, if one of those problems contains a small parameter ε, one can try to describe its solution by an asymptotic series that approximates the solution in a certain order.

In the following we will give an overview about this procedure and refer to related literature for more details.

Scaling:
An important step in finding a reliable approximation of the solution of the original model by asymptotic expansion and perturbation methods is to choose an appropriate scaling, i.e. proper reference parameters. Using an adequate scaling often enables us to reduce the number of model parameters and to detect small parameters.

According to [Seg72] and [Seg89], some of the essential points in scaling are the following:

(i) The *scale of a dependent variable* is a combination of parameters with the appropriate dimension that provides an estimate of the variable's maximum order of magnitude.

(ii) The *scale of an independent variable* is a combination of parameters with the appropriate dimension that estimates the range of the independent variable over which there is a significant change in the dependent variables.

Although the above conditions impose some restrictions on the choice of reference parameters, there does not exist a unique scaling.

Asymptotic expansion:
Given the case that the scaled model $P(f(t,\varepsilon),\varepsilon) = 0$ contains a small parameter ε, we try to describe the solution in the asymptotic expansion

$$f(t,\varepsilon) = \sum_{k=0}^{\infty} f_k(t)\varepsilon^k$$

that approximates the solution satisfactorily in a certain order. For computing the coefficients $f_k(t)$ of the asymptotic series, we plug the asymptotic series into the scaled problem. Comparing the coefficients of powers of ε yields problems whose solutions are exactly the coefficients $f_k(t)$. The remaining issue is to find out whether the asymptotic expansion in a certain order approximates the solution satisfactorily. This will be explained in the next step.

For more details concerning asymptotic expansions see [Hin91, Mei01].

Perturbation theory:
We define the *reduced problem*

$$P(f^0(t), 0) = 0$$

as the limit of the *full problem*

$$P(f(t, \varepsilon), \varepsilon) = 0$$

for $\varepsilon \to 0$. If $f^0(t)$ is a good approximation of $f(t, \varepsilon)$ in the sense that $f(t, \varepsilon)$ converges uniformly to $f^0(t)$, we call the full problem *regularly perturbed*, otherwise *singularly perturbed*.

In the former case of a regularly perturbed problem we can approximate

$$f(t, \varepsilon) \approx f^0(t),$$

where $f^0(t)$ equals the main term $f_0(t)$ of the asymptotic expansion. The qualitative dynamics are already captured by this approximation, which can be improved by higher order terms of the asymptotic expansion.

In the case of a singularly perturbed problem we have to correct the approximation $f^0(t)$ in those intervals where uniform convergence is not achieved. With respect to our application we concentrate on problems with *initial layers* where very fast dynamics occur that are not captured by $f^0(t)$. In order to describe these dynamics that happen on a very short time scale, we introduce a local time variable

$$\tau = t\varepsilon^{-\alpha}, \quad \alpha > 0$$

that, roughly speaking, blows up the initial layer so that we can regard the solution under a magnifying glass. We approximate the solution of this initial layer problem

$$P(\hat{f}(\tau, \varepsilon), \varepsilon) = 0$$

by solving the reduced problem

$$P(\hat{f}^0(\tau), 0) = 0,$$

where the function $\hat{f}(\tau, \varepsilon) = f(t(\tau, \varepsilon), \varepsilon)$ converges uniformly to $\hat{f}^0(\tau)$. An approximation of the solution $f(t, \varepsilon)$ is therefore given by

$$f(t, \varepsilon) \approx f^0(t) + \hat{f}^0(t\varepsilon^{-\alpha}) - f^0(0).$$

For further information about perturbation theory see [Hin91, O'M91, Gas03].

In the following we will apply the above procedure of scaling, asymptotic expansion and perturbation analysis to the enzymatic reactions presented in chapter 2. While various approaches concerning the quasi-steady-state assumption of Briggs and Haldane for single-substrate reactions exist in the literature (see for example [Seg88, Seg89, Din08]), neither the equilibrium assumption by Michaelis and Menten for single-substrate reactions, nor the quasi-steady-state assumption for multi-substrate reactions have been mentioned to the best of our knowledge.

The notation used throughout this appendix is listed in table A.1 on page 112.

A.1 Single-substrate reactions

The general scaling

$$s_1 = s_r \bar{s}_1, \qquad c_1 = c_r \bar{c}_1, \qquad t = t_r \bar{t}$$

of model (2.10)-(2.12) yields

$$\frac{s_r}{t_r}\frac{d\bar{s}_1}{d\bar{t}} = -k_1 s_r \bar{s}_1 (e_0 - c_r \bar{c}_1) + k_{-1} c_r \bar{c}_1 \tag{A.1}$$

$$\frac{c_r}{t_r}\frac{d\bar{c}_1}{d\bar{t}} = \quad k_1 s_r \bar{s}_1 (e_0 - c_r \bar{c}_1) - (k_{-1} + k_f) c_r \bar{c}_1 \tag{A.2}$$

with initial conditions

$$\bar{s}_1(0) = \frac{s_0}{s_r}, \qquad \bar{c}_1(0) = 0,$$

where the dimensionless variables are denoted by bars, and the reference parameters by index r. This problem is not explicitly solvable, but we can derive approximations of the solution that hold well under certain assumptions.

Common assumption of Michaelis/Menten and Briggs/Haldane

Both Michaelis/Menten and Briggs/Haldane assumed that c_1 is always negligibly small compared with s_1, hence the reference parameters should satisfy $c_r << s_r$. Taking this into account we rewrite the general scaled model to

$$\frac{d\bar{s}_1}{d\bar{t}} = -k_1 t_r \bar{s}_1 (e_0 - c_r \bar{c}_1) + k_{-1} t_r \frac{c_r}{s_r} \bar{c}_1$$

$$\frac{c_r}{s_r}\frac{d\bar{c}_1}{d\bar{t}} = \quad k_1 t_r \bar{s}_1 (e_0 - c_r \bar{c}_1) - (k_{-1} + k_f) t_r \frac{c_r}{s_r} \bar{c}_1$$

with a small parameter $\varepsilon := \frac{c_r}{s_r}$.

With respect to (i) on page 99, and because of $s_1(t) \leq s_0$ and $s_1(0) = s_0$, the reference parameter s_r should be of the order of magnitude of s_0. Due to $c_1(t) \leq e_0$, the parameter c_r should be of the order of at most e_0. Furthermore, we choose t_r such that we concentrate on the decay of the substrate and consumption of the complex for the benefit of the product.

As already mentioned on page 99, there does not exist a unique scaling. For demonstrating reasons we choose a rather simple one in this context and refer to [Seg89] and [Din08] for a detailed discussion of various other scalings.

A particular scaling that satisfies the above conditions[1] is

$$s_r = s_0, \qquad c_r = e_0, \qquad t_r = \frac{s_0}{k_f e_0}.$$

[1]The slow time scale that captures the decay of the substrate is chosen in orientation on [Seg89, page 450], where also $t_r = (k_f \varepsilon)^{-1}$ is chosen with a slightly different ε.

This yields the scaled model

$$\frac{d\bar{s}_1}{d\bar{t}} = -\frac{k_1}{k_f} s_0 \bar{s}_1 (1 - \bar{c}_1) + \frac{k_{-1}}{k_f} \bar{c}_1 \tag{A.3}$$

$$\varepsilon \frac{d\bar{c}_1}{d\bar{t}} = \frac{k_1}{k_f} s_0 \bar{s}_1 (1 - \bar{c}_1) - \frac{k_{-1} + k_f}{k_f} \bar{c}_1 \tag{A.4}$$

with initial conditions

$$\bar{s}_1(0) = 1, \qquad \bar{c}_1(0) = 0 \tag{A.5}$$

and the small parameter $\varepsilon := \frac{c_r}{s_r} = \frac{e_0}{s_0}$.

Michaelis/Menten assumption

Besides the assumption that the concentration of the complex is always negligibly small compared to the concentration of the substrate (particularly that the initial conditions satisfy $e_0 << s_0$), Michaelis and Menten stated the assumption that the substrate and enzyme are in equilibrium with their complex, which means that $k_f << k_{-1}$. This results in the existence of a second small parameter in the model that we assume to be of the same order of magnitude as ε. With the notation

$$\frac{k_f}{k_{-1}} =: \beta\varepsilon = \beta \frac{e_0}{s_0},$$

the model (A.3)/(A.4) becomes

$$\beta\varepsilon \frac{d\bar{s}_1}{d\bar{t}} = -\frac{k_1}{k_{-1}} s_0 \bar{s}_1 (1 - \bar{c}_1) + \bar{c}_1$$

$$\beta\varepsilon^2 \frac{d\bar{c}_1}{d\bar{t}} = \frac{k_1}{k_{-1}} s_0 \bar{s}_1 (1 - \bar{c}_1) - (1 + \beta\varepsilon)\bar{c}_1,$$

where the term $\frac{k_1}{k_{-1}} s_0$ is supposed to be of $O(1)$.

The main term of the asymptotic expansion and the solution of the reduced model[2], respectively, satisfies

$$\frac{d\bar{s}_1^0}{d\bar{t}} = -\bar{c}_1^0 \tag{A.6}$$

$$\bar{c}_1^0(\bar{t}) = \frac{s_0 \bar{s}_1^0}{s_0 \bar{s}_1^0 + K} \tag{A.7}$$

with $K = \frac{k_{-1}}{k_1}$. After rescaling, these equations equal (2.14)/(2.15) and explain in particular equation (2.13), the basis of the Michaelis-Menten theory.

[2]Before building the reduced model as the limit of the full model, we replace the differential equation for $\bar{s}_1$ by the sum of both equations so that we can cancel one ε. Otherwise, the reduced model would only consist of one equation, and the differential equation for $\bar{s}_1$ would be lost.

Since the solution of this reduced model cannot satisfy the initial conditions (A.5), we expect the existence of fast dynamics in an initial layer. We therefore rescale[3] the time by $\tau = \bar{t}\varepsilon^{-2}$ and find the model

$$\begin{aligned}\frac{d\hat{s}_1}{d\tau} &= \frac{\varepsilon}{\beta}\left(-\frac{k_1}{k_{-1}}s_0\hat{s}_1(1-\hat{c}_1)+\hat{c}_1\right)\\ \frac{d\hat{c}_1}{d\tau} &= \frac{1}{\beta}\left(\frac{k_1}{k_{-1}}s_0\hat{s}_1(1-\hat{c}_1)-(1+\beta\varepsilon)\hat{c}_1\right).\end{aligned}$$

The solution of the reduced model with respect to the initial data is

$$\begin{aligned}\hat{s}_1^0(\tau) &= 1\\ \hat{c}_1^0(\tau) &= \frac{s_0}{s_0+K}\left(1-e^{-\frac{s_0+K}{\beta K}\tau}\right)\\ &= \frac{s_0}{s_0+K}\left(1-e^{-\frac{k_1}{k_f}(s_0+K)\varepsilon\tau}\right).\end{aligned}$$

An approximation of the solution of (A.3)-(A.5) is therefore given by

$$\bar{s}_1(\bar{t}) \approx \bar{s}_1^0(\bar{t}) \tag{A.8}$$

$$\begin{aligned}\bar{c}_1(\bar{t}) &\approx \frac{s_0\bar{s}_1^0(\bar{t})}{s_0\bar{s}_1^0(\bar{t})+K}-\frac{s_0}{s_0+K}e^{-\frac{s_0+K}{\beta K}\bar{t}\varepsilon^{-2}}\\ &= \frac{s_0\bar{s}_1^0(\bar{t})}{s_0\bar{s}_1^0(\bar{t})+K}-\frac{s_0}{s_0+K}e^{-\frac{k_1}{k_f}(s_0+K)\bar{t}\varepsilon^{-1}}\end{aligned} \tag{A.9}$$

with $K = \frac{k_{-1}}{k_1}$. These functions are visualized in figure A.1, where the dynamics in the initial layer are illustrated enlarged.

The approximation derived above holds well if the assumptions $e_0 << s_0$ and $k_f << k_{-1}$ with $\frac{k_f}{k_{-1}} = O(\frac{e_0}{s_0}) = O(\varepsilon)$ and $\frac{k_1}{k_{-1}}s_0 = O(1)$ are satisfied, and as long as the concentration of the substrate is much greater than of the complex. In particular, since equation (2.13), presented by Michaelis and Menten for the derivation of the rate equation, equals equation (A.7), this approximation holds well following the dynamics in the initial layer.

[3]Rescaling by $\tau = \bar{t}\varepsilon^{-1}$ yields a time scale on which the assumed equilibrium of the first reaction step can be seen, which means that both the concentration of the substrate and the complex stay constant. Since these dynamics are captured by the other time scales (the solution on this scale is canceled in the approximation by adding the constant and subtracting the limit), we do not look at this time scale (compare also (ii) on page 99).

Briggs/Haldane assumption

Since Briggs and Haldane did not make any further assumption, we directly analyze the model (A.3)-(A.5), where $\frac{k_1}{k_f}s_0$ and $\frac{k_{-1}}{k_f}$ are supposed to be $O(1)$.

The reduced model, whose solution equals the main term of the asymptotic expansion, is

$$\frac{d\bar{s}_1^0}{d\bar{t}} = -\bar{c}_1^0 \tag{A.10}$$

$$\bar{c}_1^0(\bar{t}) = \frac{s_0\bar{s}_1^0}{s_0\bar{s}_1^0 + K} \tag{A.11}$$

with $K = \frac{k_{-1}+k_f}{k_1}$. In the rescaled variables, the above model equals (2.17)/(2.18), and hence explains the equation (2.16), proposed by Briggs and Haldane.

Since the initial conditions (A.5) cannot be satisfied by this solution, we expect again fast dynamics in an initial layer. Rescaling the time by $\tau = \bar{t}\varepsilon^{-1}$ yields the full model

$$\begin{aligned}\frac{d\hat{s}_1}{d\tau} &= \varepsilon\left(-\frac{k_1}{k_f}s_0\hat{s}_1(1-\hat{c}_1) + \frac{k_{-1}}{k_f}\hat{c}_1\right)\\ \frac{d\hat{c}_1}{d\tau} &= \frac{k_1}{k_f}s_0\hat{s}_1(1-\hat{c}_1) - (1+\frac{k_{-1}}{k_f})\hat{c}_1\end{aligned}$$

and the following solution of the reduced one:

$$\begin{aligned}\hat{s}_1^0(\tau) &= 1\\ \hat{c}_1^0(\tau) &= \frac{s_0}{s_0+K}\left(1 - e^{-\frac{k_1}{k_f}(s_0+K)\tau}\right).\end{aligned}$$

With this correction of the main term of the asymptotic expansion we can approximate the solution of (A.3)-(A.5) by

$$\bar{s}_1(\bar{t}) \approx \bar{s}_1^0(\bar{t}) \tag{A.12}$$

$$\bar{c}_1(\bar{t}) \approx \frac{s_0\bar{s}_1^0(\bar{t})}{s_0\bar{s}_1^0(\bar{t}) + K} - \frac{s_0}{s_0+K}e^{-\frac{k_1}{k_f}(s_0+K)\bar{t}\varepsilon^{-1}} \tag{A.13}$$

with $K = \frac{k_{-1}+k_f}{k_1}$ (see figure A.1).

This approximation holds if the assumption $e_0 << s_0$, as well as $\frac{k_{-1}}{k_f} = O(1)$ and $\frac{k_1}{k_f}s_0 = O(1)$, are satisfied, and as long as c_1 is negligibly small compared with s_1.

Particularly, since the equation (2.16) of Briggs and Haldane equals equation (A.11), this approximation holds after a short transient, in which the concentration of the substrate stays almost constant and the concentration of the complex grows.

Comparison of Michaelis/Menten and Briggs/Haldane approximations

As can be easily seen, the approximations (A.8)/(A.9) and (A.12)/(A.13), which result from the Michaelis/Menten and Briggs/Haldane assumption, respectively, show qualitatively the same dynamics. According to figure A.1, the approximations only differ slightly[4] in the scaled variables. But this should not mislead us over the fact that the differences between both approximations, namely the differences in the constants K, as well as in the order of magnitude of k_f, are of fundamental character: Since the time scaling involves the crucial parameter k_f, the impact of its different orders of magnitude is masked in the scaled variables, but it is revealed in the rescaled approximations

$$\begin{aligned} s_1(t) &\approx s_1^0(t) \\ c_1(t) &\approx e_0 \frac{s_1^0(t)}{s_1^0(t)+K} - e_0 \frac{s_0}{s_0+K} e^{-k_1(s_0+K)t}, \end{aligned}$$

where $s_1^0(t)$ denotes the solution behind the initial layer, which satisfies

$$\frac{ds_1^0}{dt} = -k_f e_0 \frac{s_1^0(t)}{s_1^0(t)+K}.$$

As shown in figure A.2, after the complex concentration in the Michaelis/Menten approximation increased quickly up to a value which is greater than in the Briggs/Haldane case, the substrate and complex concentrations decay much slower than in the solution that results from the Briggs/Haldane assumption.

Closing this section, we will compare and summarize the results concerning the Michaelis/Menten and Briggs/Haldane assumptions that are presented in the present chapter, as well as in chapter 2:

Both Michaelis/Menten and Briggs/Haldane stated the same assumptions about the concentrations of the compounds that are involved in the enzymatic reaction, while Michaelis/Menten made an additional assumption concerning the rate constant of the product yielding reaction step.

Despite the above mentioned discrepancy and different argumentations, their assumptions result in similar conclusions, namely in rate equations for the enzymatic reaction that qualitatively just differ in the constants K.

But neither Michaelis/Menten nor Briggs/Haldane analyzed the overall dynamics of the enzymatic reaction that result from their assumptions. It is easily seen that the equations resulting from their assumptions cannot hold at all times. This can be specified, and intervals in which these equations hold can be identified by means of asymptotic methods: By taking into account the different

[4]For the visual comparison we choose the same set of parameters except k_f, which is negligibly small compared to k_{-1} in the Michaelis/Menten case but of the same order of magnitude as k_{-1} in the Briggs/Haldane case.

assumptions we can derive approximations of the overall dynamics, which hold as long as the assumptions are met, namely as long as the substrate concentration is large enough. In particular, the equations derived by Michaelis/Menten and Briggs/Haldane are both valid after a short initial layer, which shows different dynamics, and as long as the substrate concentration is large enough.

As well as in the derivation of the rate equation, the different assumptions in the asymptotic analysis yield identical qualitative dynamics, i.e. the resulting models just differ in the constants K. But the negligibly small constant k_f, assumed by Michaelis/Menten, is related to a much slower decay of substrate and complex concentrations after the initial layer. Therefore, having the common assumption concerning the concentrations in mind, the approximation of enzymatic reactions that satisfy the additional assumption of Michaelis/Menten holds at much longer times than the approximation of enzymatic reactions that satisfy the Briggs/Haldane assumption.

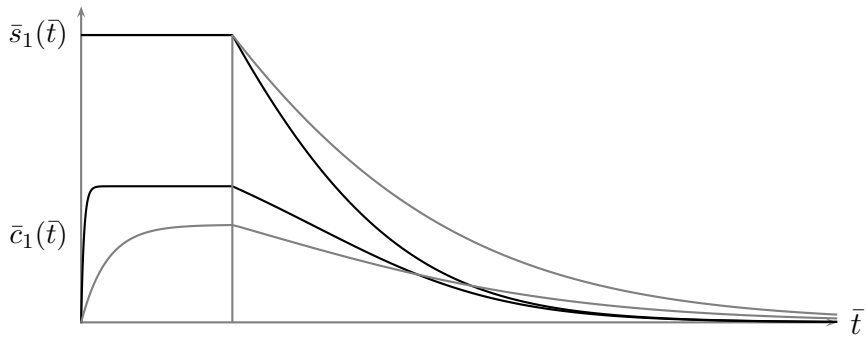

Figure A.1: Comparison of the Michaelis/Menten approximation (black) and the Briggs/Haldane approximation (gray) in scaled variables (for a better comparison the same initial interval is pictured enlarged, although the scaled times τ differ)

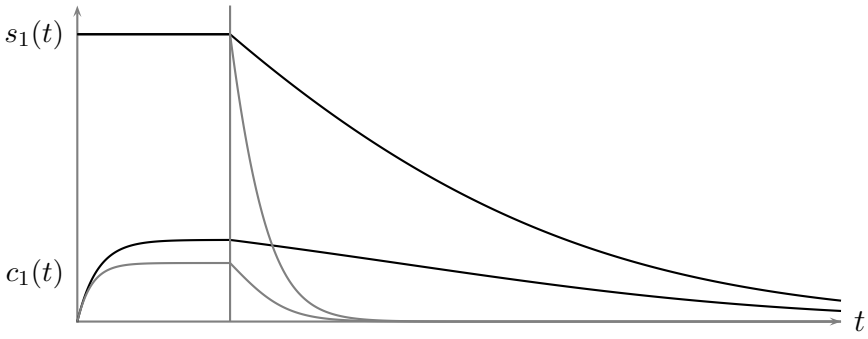

Figure A.2: Comparison of the Michaelis/Menten approximation (black) and the Briggs/Haldane approximation (gray) in rescaled variables (for a better comparison both functions $c_1(t)$ are pictured enlarged)

A.2 Multi-substrate reactions

For multi-substrate reactions that follow the reaction mechanism (2.28), we assume that all substrates on the one hand and all complexes on the other hand occur in the same order of magnitude. Due to this assumption it suffices to employ one reference parameter, s_r, to scale all substrates and one parameter, c_r, to scale all complex concentrations. If we transfer the single-substrate assumption of Briggs and Haldane, namely that the concentration of the complex is always much smaller than of the substrate, to the multi-substrate case, we have $c_r << s_r$. With the general scaling

$$s_i^* = s_r \bar{s}_i^*, \qquad c_i = c_r \bar{c}_i, \qquad t = t_r \bar{t}$$

we thus have the model

$$\begin{aligned}
\frac{d\bar{s}_1^*}{d\bar{t}} &= -k_1 t_r \left(e_0 - \sum_{j=1}^{m} c_r \bar{c}_j \right) \bar{s}_1^* + k_{-1} t_r \frac{c_r}{s_r} \bar{c}_1 \\
\frac{d\bar{s}_i^*}{d\bar{t}} &= -k_i t_r c_r \bar{c}_{i-1} \bar{s}_i^* + k_{-i} t_r \frac{c_r}{s_r} \bar{c}_i, && i = 2,...,m \\
\frac{c_r}{s_r} \frac{d\bar{c}_1}{d\bar{t}} &= k_1 t_r \left(e_0 - \sum_{i=1}^{m} c_r \bar{c}_i \right) \bar{s}_1^* - k_{-1} t_r \frac{c_r}{s_r} \bar{c}_1 - k_2 t_r c_r \bar{c}_1 \bar{s}_2^* + k_{-2} t_r \frac{c_r}{s_r} \bar{c}_2 \\
\frac{c_r}{s_r} \frac{d\bar{c}_i}{d\bar{t}} &= k_i t_r c_r \bar{c}_{i-1} \bar{s}_i^* - k_{-i} t_r \frac{c_r}{s_r} \bar{c}_i - k_{i+1} t_r c_r \bar{c}_i \bar{s}_{i+1}^* + k_{-(i+1)} t_r \frac{c_r}{s_r} \bar{c}_{i+1}, && i = 2,...,m-1 \\
\frac{c_r}{s_r} \frac{d\bar{c}_m}{d\bar{t}} &= k_m t_r c_r \bar{c}_{m-1} \bar{s}_m^* - (k_{-m} + k_f) t_r \frac{c_r}{s_r} \bar{c}_m
\end{aligned}$$

with initial conditions

$$\bar{s}_i^*(0) = \frac{s_{i0}^*}{s_r}, \qquad \bar{c}_i(0) = 0$$

and a small parameter $\varepsilon := \frac{c_r}{s_r}$.

With the same argumentation as stated on page 101 for the single-substrate case, we choose for demonstrating reasons the simple scaling

$$s_r = s_{10}^*, \qquad c_r = e_0, \qquad t_r = \frac{s_{10}^*}{k_f e_0}, \tag{A.14}$$

which yields the model

$$
\begin{aligned}
\frac{d\bar{s}_1^*}{d\bar{t}} &= -\frac{k_1}{k_f}s_{10}^*\left(1-\sum_{j=1}^{m}\bar{c}_j\right)\bar{s}_1^* + \frac{k_{-1}}{k_f}\bar{c}_1 \\
\frac{d\bar{s}_i^*}{d\bar{t}} &= -\frac{k_i}{k_f}s_{10}^*\bar{c}_{i-1}\bar{s}_i^* + \frac{k_{-i}}{k_f}\bar{c}_i, && i=2,\dots,m \\
\varepsilon\,\frac{d\bar{c}_1}{d\bar{t}} &= \frac{k_1}{k_f}s_{10}^*\left(1-\sum_{i=1}^{m}\bar{c}_i\right)\bar{s}_1^* - \frac{k_{-1}}{k_f}\bar{c}_1 - \frac{k_2}{k_f}s_{10}^*\bar{c}_1\bar{s}_2^* + \frac{k_{-2}}{k_f}\bar{c}_2 \\
\varepsilon\,\frac{d\bar{c}_i}{d\bar{t}} &= \frac{k_i}{k_f}s_{10}^*\bar{c}_{i-1}\bar{s}_i^* - \frac{k_{-i}}{k_f}\bar{c}_i - \frac{k_{i+1}}{k_f}s_{10}^*\bar{c}_i\bar{s}_{i+1}^* + \frac{k_{-(i+1)}}{k_f}\bar{c}_{i+1}, && i=2,\dots,m-1 \\
\varepsilon\frac{d\bar{c}_m}{d\bar{t}} &= \frac{k_m}{k_f}s_{10}^*\bar{c}_{m-1}\bar{s}_m^* - \frac{k_{-m}+k_f}{k_f}\bar{c}_m
\end{aligned}
$$

with initial conditions

$$\bar{s}_i^*(0) = \frac{s_{i0}^*}{s_{10}^*}, \qquad \bar{c}_i(0) = 0.$$

Here, the dimensionless parameters $\frac{k_i}{k_f}s_{10}^*$ and $\frac{k_{-i}}{k_f}$ are supposed to be $O(1)$.

If we take into account the properties

$$
\begin{aligned}
\varepsilon\frac{d\bar{c}_i}{d\bar{t}} &= -\frac{d\bar{s}_i^*}{d\bar{t}} + \frac{d\bar{s}_{i+1}^*}{d\bar{t}}, && i=1,\dots,m-1 \\
\varepsilon\frac{d\bar{c}_m}{d\bar{t}} &= -\frac{d\bar{s}_m^*}{d\bar{t}} - \bar{c}_m,
\end{aligned}
$$

we can write the reduced model in the form

$$
\begin{aligned}
\frac{d\bar{s}_i^{*0}}{d\bar{t}} &= -\bar{c}_m^0, && i=1,\dots,m \\
0 &= k_1 s_{10}^*\left(1-\sum_{j=1}^{m}\bar{c}_j^0\right)\bar{s}_1^{*0} - k_{-1}\bar{c}_1^0 - k_2 s_{10}^*\bar{c}_1^0\bar{s}_2^{*0} + k_{-2}\bar{c}_2^0 \\
0 &= k_i s_{10}^*\bar{c}_{i-1}^0\bar{s}_i^{*0} - k_{-i}\bar{c}_i^0 - k_{i+1}s_{10}^*\bar{c}_i^0\bar{s}_{i+1}^{*0} + k_{-(i+1)}\bar{c}_{i+1}^0, && i=2,\dots,m-1 \\
0 &= k_m s_{10}^*\bar{c}_{m-1}^0\bar{s}_m^{*0} - (k_{-m}+k_f)\bar{c}_m^0.
\end{aligned}
$$

In the rescaled variables, the above model equals model (2.29)-(2.31).

The latter m equations can be solved for $\bar{c}_i$ $(i=1,\dots,m)$ analogously to the algorithm stated on page 19. In this case we take advantage of the equation $\bar{c}_0^0 = \bar{e}^0 = 1 - \sum_{j=1}^{m}\bar{c}_j^0$, and compute the complexes for $i \neq m$ by substituting the result of (iii) into the results of (ii).

Since not all initial conditions can be satisfied, we expect again fast dynamics in an initial layer. Rescaling by $\tau = \bar{t}\varepsilon^{-1}$ yields

$$\begin{aligned}
\frac{d\hat{s}_1^*}{d\tau} &= \varepsilon\left(-\frac{k_1}{k_f}s_{10}^*\left(1-\sum_{j=1}^{m}\hat{c}_j\right)\hat{s}_1^* + \frac{k_{-1}}{k_f}\hat{c}_1\right)\\
\frac{d\hat{s}_i^*}{d\tau} &= \varepsilon\left(-\frac{k_i}{k_f}s_{10}^*\hat{c}_{i-1}\hat{s}_i^* + \frac{k_{-i}}{k_f}\hat{c}_i\right), && i=2,\dots,m\\
\frac{d\hat{c}_1}{d\tau} &= \frac{k_1}{k_f}s_{10}^*\left(1-\sum_{i=1}^{m}\hat{c}_i\right)\hat{s}_1^* - \frac{k_{-1}}{k_f}\hat{c}_1 - \frac{k_2}{k_f}s_{10}^*\hat{c}_1\hat{s}_2^* + \frac{k_{-2}}{k_f}\hat{c}_2\\
\frac{d\hat{c}_i}{d\tau} &= \frac{k_i}{k_f}s_{10}^*\hat{c}_{i-1}\hat{s}_i^* - \frac{k_{-i}}{k_f}\hat{c}_i - \frac{k_{i+1}}{k_f}s_{10}^*\hat{c}_i\hat{s}_{i+1}^* + \frac{k_{-(i+1)}}{k_f}\hat{c}_{i+1}, && i=2,\dots,m-1\\
\frac{d\hat{c}_m}{d\tau} &= \frac{k_m}{k_f}s_{10}^*\hat{c}_{m-1}\hat{s}_m^* - \frac{k_{-m}+k_f}{k_f}\hat{c}_m,
\end{aligned}$$

with the reduced model

$$\begin{aligned}
\frac{d\hat{s}_i^{*0}}{d\tau} &= 0, && i=1,\dots,m\\
\frac{d\hat{c}_1^0}{d\tau} &= \frac{k_1}{k_f}s_{10}^*\left(1-\sum_{j=1}^{m}\hat{c}_j^0\right)\hat{s}_1^{*0} - \frac{k_{-1}}{k_f}\hat{c}_1^0 - \frac{k_2}{k_f}s_{10}^*\hat{c}_1^0\hat{s}_2^{*0} + \frac{k_{-2}}{k_f}\hat{c}_2^0\\
\frac{d\hat{c}_i^0}{d\tau} &= \frac{k_i}{k_f}s_{10}^*\hat{c}_{i-1}^0\hat{s}_i^{*0} - \frac{k_{-i}}{k_f}\hat{c}_i^0 - \frac{k_{i+1}}{k_f}s_{10}^*\hat{c}_i^0\hat{s}_{i+1}^{*0} + \frac{k_{-(i+1)}}{k_f}\hat{c}_{i+1}^0, && i=2,\dots,m-1\\
\frac{d\hat{c}_m^0}{d\tau} &= \frac{k_m}{k_f}s_{10}^*\hat{c}_{m-1}^0\hat{s}_m^{*0} - \frac{k_{-m}+k_f}{k_f}\hat{c}_m^0.
\end{aligned}$$

Taking into account the initial conditions $\hat{s}_i^{*0}(0) = \frac{s_{i0}^*}{s_{10}^*}$ and using the notation

$$a_i := \frac{k_i}{k_f}s_{i0}^*, \qquad a_{-i} := \frac{k_{-i}}{k_f} \tag{A.15}$$

gives the reduced model

$$\begin{aligned}
\hat{s}_i^{*0}(\tau) &= \frac{s_{i0}^*}{s_{10}^*}, && i=1,\dots,m\\
\frac{d\hat{c}_1^0}{d\tau} &= a_1 - (a_1+a_{-1}+a_2)\hat{c}_1^0 + (a_{-2}-a_1)\hat{c}_2^0 - a_1\sum_{j=3}^{m}\hat{c}_j^0\\
\frac{d\hat{c}_i^0}{d\tau} &= a_i\hat{c}_{i-1}^0 - (a_{-i}+a_{i+1})\hat{c}_i^0 + a_{-(i+1)}\hat{c}_{i+1}^0, && i=2,\dots,m-1\\
\frac{d\hat{c}_m^0}{d\tau} &= a_m\hat{c}_{m-1}^0 - (a_{-m}+1)\hat{c}_m^0.
\end{aligned}$$

This model includes a linear inhomogeneous system of first order differential equations with constant coefficients for the complexes $\hat{c}_i^0$. This problem has a unique solution with respect to the initial conditions $\hat{c}_i^0(0) = 0$.

An approximation of the solution is therefore given by

$$\begin{aligned} \bar{s}_i^*(\bar{t}) &\approx \bar{s}_i^{*0}(\bar{t}) + \hat{s}_i^{*0}(\bar{t}\varepsilon^{-1}) - \hat{s}_i^{*0}(\infty), \quad i = 1, \ldots, m \\ \bar{c}_i(\bar{t}) &\approx \bar{c}_i^0(\bar{t}) \ + \hat{c}_i^0(\bar{t}\varepsilon^{-1}) \ - \hat{c}_i^0(\infty), \quad i = 1, \ldots, m. \end{aligned}$$

This approximation holds if the assumption $e_0 << s_{10}^*$, as well as $\frac{k_i}{k_f} s_{10}^* = O(1)$ and $\frac{k_{-i}}{k_f} = O(1)$, are satisfied, and as long as all substrate and complex concentrations are of the same order of magnitude, where the complex concentrations are much smaller than the substrate concentrations.

Example 1 ($m = 2$)**.** We consider an enzymatic reaction that involves two substrates and follows the mechanism

$$S_1^* + E \underset{k_{-1}}{\overset{k_1}{\rightleftharpoons}} S_1^* E + S_2^* \underset{k_{-2}}{\overset{k_2}{\rightleftharpoons}} S_1^* S_2^* E \overset{k_f}{\to} P + E.$$

We assume that the order of magnitude of the substrate concentrations on the one hand and of the complex concentrations on the other hand are of the same order of magnitude. Furthermore, we assume that the latter concentrations are always negligibly small compared to the former ones. Then the dynamics (of the scaled model using the scaling (A.14)) can be approximated by

$$\bar{s}_i^*(\bar{t}) \approx \bar{s}_i^{*0}(\bar{t}) + \hat{s}_i^{*0}\left(\bar{t}\frac{s_{10}^*}{e_0}\right) - \hat{s}_i^{*0}(\infty), \quad i = 1, 2 \tag{A.16}$$

$$\bar{c}_i(\bar{t}) \approx \bar{c}_i^0(\bar{t}) \ + \hat{c}_i^0\left(\bar{t}\frac{s_{10}^*}{e_0}\right) \ - \hat{c}_i^0(\infty), \quad i = 1, 2 \tag{A.17}$$

where the occurring functions are the solutions of the following models:

The long-time behavior is given by

$$\begin{aligned} \frac{d\bar{s}_1^{*0}}{d\bar{t}} &= -\bar{c}_2^0 \\ \frac{d\bar{s}_2^{*0}}{d\bar{t}} &= -\bar{c}_2^0 \\ \bar{c}_1^0(\bar{t}) &= K_2 \frac{s_{10}^* \bar{s}_1^{*0}}{(s_{10}^* \bar{s}_1^{*0} + K_1)(s_{10}^* \bar{s}_2^{*0} + K_2) + L} \\ \bar{c}_2^0(\bar{t}) &= \frac{(s_{10}^*)^2 \bar{s}_1^{*0} \bar{s}_2^{*0}}{(s_{10}^* \bar{s}_1^{*0} + K_1)(s_{10}^* \bar{s}_2^{*0} + K_2) + L} \end{aligned}$$

with

$$\bar{s}_1^{*0}(0) = 1, \quad \bar{s}_2^{*0}(0) = \frac{s_{20}^*}{s_{10}^*}$$

and notation

$$\begin{aligned} K_1 &= \frac{k_f}{k_1} \\ K_2 &= \frac{k_{-2} + k_f}{k_2} \\ L &= \frac{(k_{-2} + k_f)(k_{-1} - k_f)}{k_1 k_2}. \end{aligned}$$

The dynamics in the initial layer are approximated by

$$\begin{aligned} \hat{s}_1^{*0}(\tau) &= 1 \\ \hat{s}_2^{*0}(\tau) &= \frac{s_{20}^*}{s_{10}^*} \\ \frac{d\hat{c}_1^0}{d\tau} &= a_1 - (a_1 + a_{-1} + a_2)\hat{c}_1^0 + (a_{-2} - a_1)\hat{c}_2^0 \\ \frac{d\hat{c}_2^0}{d\tau} &= a_2\hat{c}_1^0 - (a_{-2} + 1)\hat{c}_2^0 \end{aligned}$$

with

$$\hat{c}_1^0(0) = 0, \quad \bar{c}_2^0(0) = 0$$

and the notation introduced in (A.15).

The approximation (A.16)/(A.17) is visualized in figure A.3 for two different sets of parameters, where the dynamics in the initial layer are represented magnified. This figure shows the general dynamics in the sense that the complex concentrations grow initially, while the substrate concentrations stay constant. After these fast dynamics all concentrations decrease.

For the set of parameters that was chosen for the upper visualization, the concentration of the substrate S_1^* tends to zero. After a certain time, the complex S_1^*E can therefore not be built, and hence the substrate S_2^* not be consumed anymore, for which reason the concentration of S_2^* tends to a constant value greater than zero.

For the second set of parameters, the substrate S_2^* is entirely consumed first. The complex $S_1^*S_2^*E$ can therefore not be built anymore, and the first reaction step tends to its equilibrium so that the concentrations of S_1^* and S_1^*E tend to positive constant values.

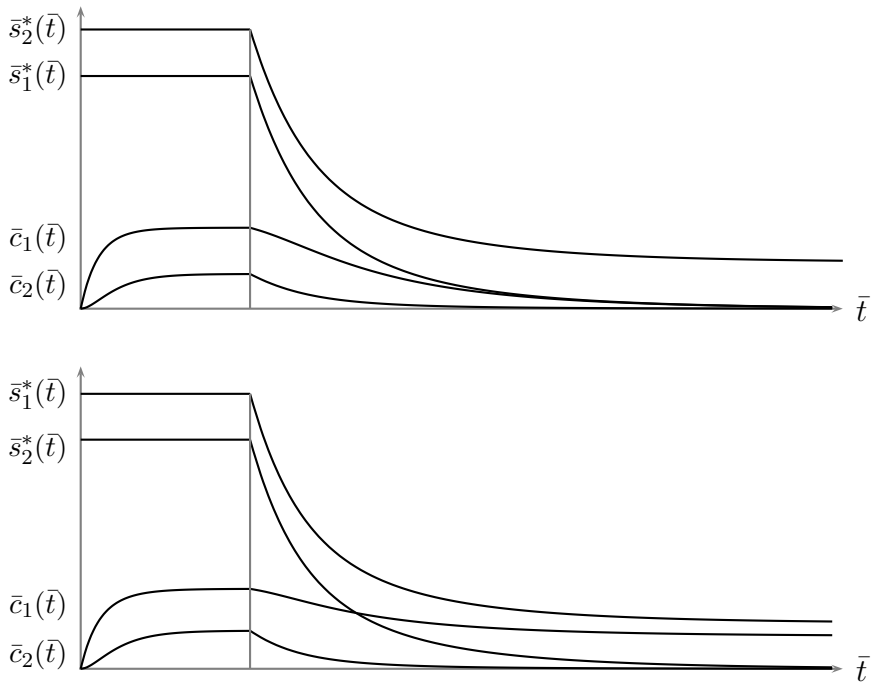

Figure A.3: Approximated dynamics of an enzymatic reaction that involves two substrates (for more details see the text in example 1)

	description
$\bar{f}$	solution of the full problem
$\bar{f}^0$	solution of the reduced problem ($\varepsilon \to 0$)
$\bar{t}$	time variable
$\hat{f}$	solution of the full initial layer problem
$\hat{f}^0$	solution of the reduced initial layer problem ($\varepsilon \to 0$)
τ	time variable in the initial layer

Table A.1: Notation used in appendix A (f replaces s_i, s_i^* and c_i)

B Existence

B.1 Proof related to chapter 3

Below we will prove certain specifications of the wave form $N(z)$ in the single-substrate bioremediation model (3.1) with respect to (A1)-(A3).

Proposition 1. *$N(z)$ is bounded from above by exponentially increasing and decreasing functions. Furthermore, $N(z)$ asymptotically approaches the least of these upper bounds as $z \to \pm\infty$. More precisely, there exist positive constants $K_\pm$ such that*

$$N(z) < K_\pm e^{-\alpha_\pm z}$$

for all $z \in \mathbb{R}$ and

$$N(z) \sim K_\pm e^{-\alpha_\pm z}$$

as z tends to $\pm\infty$ with

$$\alpha_\pm = \frac{1}{s}\big(\nu\mu_1(c_\pm) - R\big),$$

where $\alpha_+ > 0$ and $\alpha_- < 0$.

Proof. With $d_2 := -s > 0$ and $f(C) := \nu\mu_1(C)$, the traveling wave $N(z)$ holds

$$N_z = \frac{f(C) - R}{d_2} N,$$

which is equivalent to

$$\frac{d}{dz}\left(e^{-\int_0^z \frac{f(C(\bar z))-R}{d_2}\,d\bar z} N(z)\right) = 0 \qquad \text{and} \qquad N(z) = N(0) e^{\int_0^z \frac{f(C(\bar z))-R}{d_2}\,d\bar z}.$$

Using the notation $N_{tot} = \int_{-\infty}^{\infty} N(z)\,dz$ we get

$$N(z) = N_{tot} \frac{e^{\int_0^z \frac{f(C(\bar z))-R}{d_2}\,d\bar z}}{\int_{-\infty}^{\infty} e^{\int_0^{\tilde z} \frac{f(C(\bar z))-R}{d_2}\,d\bar z}\,d\tilde z}.$$

Expanding this fraction with $e^{-\int_0^{z_0} \frac{f(C(\bar z))-R}{d_2}\,d\bar z}$ with an arbitrary $z_0 \in \mathbb{R}$, and using the notation

$$G(z) := -\int_{z_0}^{z} \frac{f(C(\bar z)) - R}{d_2}\,d\bar z$$

yields

$$N(z) = N_{tot} \frac{e^{-G(z)}}{\int_{-\infty}^{\infty} e^{-G(\tilde z)}\,d\tilde z}. \tag{B.1}$$

It remains to show that the numerator of (B.1) is bounded from above by exponentially increasing and decreasing functions, and that the denominator is greater than zero.

For characterizing the function $G(z)$, we choose z_0 such that $f(C(z_0)) = R$. Since $f(C)$ is strictly increasing and $C(z)$ strictly decreasing, we have

$$f(C(z)) - R \begin{cases} < 0, & z > z_0 \\ > 0, & z < z_0. \end{cases}$$

These facts, as well as the consequential characteristics of $G(z)$, are shown in figure B.1. In particular, it can easily be verified that the first derivative of the convex function satisfies

$$G'(z) \xrightarrow{z \to \pm\infty} -\frac{f(c_\pm) - R}{d_2} =: \alpha_\pm$$

with $\alpha_+ > 0$ and $\alpha_- < 0$.

In order to prove that the numerator of (B.1) is bounded from above by exponentially increasing and decreasing functions, we notice that there exist constants $b_\pm$ such that $G(z)$ is bounded below by the linear functions

$$G(z) > \alpha_\pm z + b_\pm$$

for all $z \in \mathbb{R}$. We thus get

$$e^{-G(z)} < e^{-(\alpha_\pm z + b_\pm)} =: \beta_\pm e^{-\alpha_\pm z}.$$

The numerator of (B.1) is therefore less than certain functions that decrease and increase exponentially.

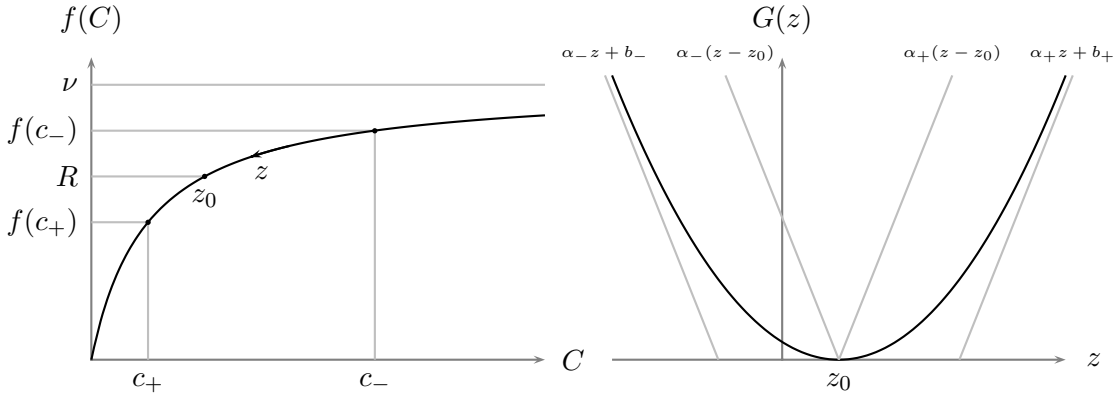

Figure B.1: Functions $f(C)$ and $G(z)$

In order to show that the denominator is greater than zero we distinguish two cases: For $z < z_0$, the function G meets $G(z) < \alpha_-(z - z_0)$, which is equivalent to

$$\int_{-\infty}^{z_0} e^{-G(z)}\,dz > \int_{-\infty}^{z_0} e^{-\alpha_-(z-z_0)}\,dz = -\frac{1}{\alpha_-} > 0.$$

For $z > z_0$, we have $G(z) < \alpha_+(z - z_0)$, which is equivalent to

$$\int_{z_0}^{\infty} e^{-G(z)}\,dz > \int_{z_0}^{\infty} e^{-\alpha_+(z-z_0)}\,dz = \frac{1}{\alpha_+} > 0.$$

Hence, the denominator of (B.1) is positive as well:

$$D := \int_{-\infty}^{\infty} e^{-G(z)}\,dz = \int_{-\infty}^{z_0} e^{-G(z)}\,dz + \int_{z_0}^{\infty} e^{-G(z)}\,dz > \frac{1}{\alpha_+} - \frac{1}{\alpha_-} > 0.$$

We thus have

$$N(z) = \frac{N_{tot}}{D} e^{-G(z)} < \frac{N_{tot}\beta_\pm}{D} e^{-\alpha_\pm z} =: K_\pm^\beta e^{-\alpha_\pm z} \tag{B.2}$$

for all $z \in \mathbb{R}$, which means that $N(z)$ is less than certain functions that decrease and increase exponentially (see figure B.2).

Furthermore, the wave form $N(z)$ asymptotically approaches exponential functions with growth rates $-\alpha_\pm$ as z tends to $\pm\infty$: If we choose $b_\pm =: \bar{b}_\pm$ such that $G(z)$ asymptotically approaches the linear functions $\alpha_\pm z + \bar{b}_\pm$ as z tends to $\pm\infty$, we have

$$N(z) = \frac{N_{tot}}{D} e^{-G(z)} \sim \frac{N_{tot}}{D} e^{-(\alpha_\pm z + \bar{b}_\pm)} = \frac{N_{tot}\bar{\beta}_\pm}{D} e^{-\alpha_\pm z} =: K_\pm e^{-\alpha_\pm z}.$$

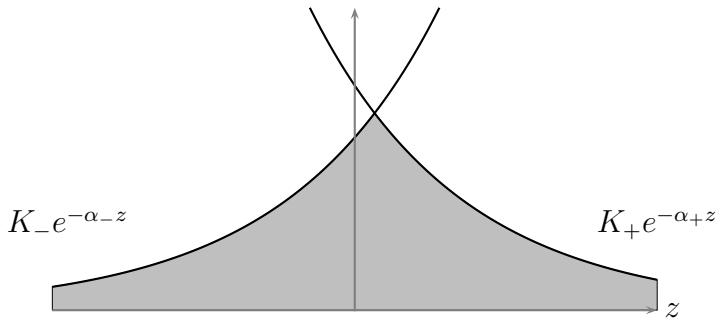

Figure B.2: Upper bounds of $N(z)$

□

B.2 Functions and parameters occurring in chapter 3

The functions occurring in proposition 8 on page 50 are listed below:

$$
\begin{aligned}
s_{v_1}(N_{tot}) &:= v + \frac{\nu_s}{\nu_o + \nu_s} \frac{R}{\bar{c}_{s+}} N_{tot} \\
s_{u_1}(N_{tot}) &:= u - \frac{\nu_o}{\nu_o + \nu_s} \frac{R}{\bar{c}_{o-}} N_{tot} \\
s_{v_2}(N_{tot}) &:= v + \frac{\nu_s}{\nu_o + \nu_s} \frac{R\, d_s}{\bar{c}_{s+}} N_{tot} \\
s_{u_2}(N_{tot}) &:= u - \frac{\nu_o}{\nu_o + \nu_s} \frac{R\, d_o}{\bar{c}_{o-}} N_{tot}.
\end{aligned}
$$

Their intersections among each other, as well as their intersections with the N_{tot} axis, determine the point sets $D_\pm$ defined in the second condition of proposition 8. The argument values of these intersections are stated below, where $N_{tot}^{v_i,u_j}$ denotes the value N_{tot} that meets $s_{v_i}(N_{tot}) = s_{u_j}(N_{tot})$:

$$
\begin{aligned}
N_{tot}^{v_1,u_1} &:= \frac{\nu_o + \nu_s}{R} \frac{\bar{c}_{o-}\bar{c}_{s+}}{\bar{c}_{o-}\nu_s + \bar{c}_{s+}\nu_o} (u - v) \\
N_{tot}^{v_2,u_2} &:= \frac{\nu_o + \nu_s}{R} \frac{\bar{c}_{o-}\bar{c}_{s+}}{\bar{c}_{o-}\nu_s\, d_s + \bar{c}_{s+}\nu_o\, d_o} (u - v) \\
N_{tot}^{0,u_2} &:= \frac{\nu_o + \nu_s}{\nu_o} \frac{\bar{c}_{o-}}{R\, d_o} u \\
N_{tot}^{v_2,0} &:= \frac{\nu_o + \nu_s}{\nu_s} \frac{\bar{c}_{s+}}{R\, d_s} (-v) \\
N_{tot}^{v_1,u_2} &:= \frac{\nu_o + \nu_s}{R} \frac{\bar{c}_{o-}\bar{c}_{s+}}{\bar{c}_{o-}\nu_s + \bar{c}_{s+}\nu_o\, d_o} (u - v) \\
N_{tot}^{v_2,u_1} &:= \frac{\nu_o + \nu_s}{R} \frac{\bar{c}_{o-}\bar{c}_{s+}}{\bar{c}_{o-}\nu_s\, d_s + \bar{c}_{s+}\nu_o} (u - v) \\
N_{tot}^{v_1,0} &:= \frac{\nu_o + \nu_s}{\nu_s} \frac{\bar{c}_{s+}}{R} (-v) \\
N_{tot}^{0,u_1} &:= \frac{\nu_o + \nu_s}{\nu_0} \frac{\bar{c}_{o-}}{R} u.
\end{aligned}
$$

C Stability

C.1 Operators occurring in chapter 4

The differential operators $\mathfrak{L}$ and $\mathfrak{T}$ acting on L^2, as well as the operators $\mathfrak{B}$ and $\mathfrak{T}_{\mathfrak{B}}$ on L^2_w, and $\tilde{B}$ and $\mathfrak{T}_{\tilde{B}}$ on $\tilde{L}^2_w$, are given by

$$\begin{aligned}
\mathfrak{L} &= (J_F(Q) - D\partial_z) & \mathfrak{T}(\lambda) &= \frac{d}{dz} - A(z,\lambda) \\
& & &= \frac{d}{dz} - \big(A^{\pm}(\lambda) + R^{\pm}(z)\big) \\
\mathfrak{B} &= \mathfrak{L} + k(z)D & \mathfrak{T}_{\mathfrak{B}}(\lambda) &= \frac{d}{dz} - A_w(z,\lambda) \\
& & &= \frac{d}{dz} - \big(A^{\pm}_w(\lambda) + R^{\pm}_w(z)\big) \\
\tilde{\mathfrak{B}} &= W\mathfrak{L}W^{-1} & \mathfrak{T}_{\tilde{\mathfrak{B}}}(\lambda) &= \frac{d}{dz} - \tilde{A}_w(z,\lambda) \\
&= WJ_F(Q)W^{-1} - DW(W^{-1})' - D\partial_z & &= \frac{d}{dz} - \big(\tilde{A}^{\pm}_w(\lambda) + \tilde{R}^{\pm}_w(z)\big).
\end{aligned}$$

The included functions are listed below[5], separately for the single-substrate and double-substrate bioremediation model, while in both cases the weight functions are defined as follows:

$$w(z) = \begin{cases} e^{k_+ z}, & z \geq 0 \\ e^{k_- z}, & z < 0 \end{cases}, \qquad k(z) = \begin{cases} k_+, & z \geq 0 \\ k_-, & z < 0 \end{cases}$$

$$w_i(z) = \begin{cases} e^{k^i_+ z}, & z \geq 0 \\ e^{k^i_- z}, & z < 0 \end{cases}, \qquad k^i(z) = \begin{cases} k^i_+, & z \geq 0 \\ k^i_-, & z < 0. \end{cases}$$

Single-substrate bioremediation model

$$\begin{aligned}
f(C) &= \nu \frac{C}{C+1} \\
f'(C) &= \nu \frac{1}{(C+1)^2} \\
D &= \begin{pmatrix} d_1 & 0 \\ 0 & d_2 \end{pmatrix} = \begin{pmatrix} u-s & 0 \\ 0 & -s \end{pmatrix} \\
W(z) &= \begin{pmatrix} w_1(z) & 0 \\ 0 & w_2(z) \end{pmatrix}
\end{aligned}$$

[5]Since the matrices $\tilde{A}^{\pm}_w(\lambda)$ and $\tilde{R}^{\pm}_w(z)$ are not uniquely defined but depend on the choice of the weight functions, we refer to pages 81 and 84 for more details.

$$
\begin{aligned}
J_F(Q) &= J_F(C,N) \\
&= \begin{pmatrix} -f'(C)N & -f(C) \\ f'(C)N & f(C)-R \end{pmatrix} \\
A(z,\lambda) &= D^{-1}\big(J_F(C,N)-\lambda I\big) \\
&= \begin{pmatrix} -\frac{1}{d_1}\big(f'(C)N+\lambda\big) & -\frac{1}{d_1}f(C) \\ \frac{1}{d_2}f'(C)N & \frac{1}{d_2}\big(f(C)-R-\lambda\big) \end{pmatrix} \\
A^{\pm}(\lambda) &= D^{-1}\big(J_F(c_\pm,0)-\lambda I\big) \\
&= \begin{pmatrix} -\frac{\lambda}{d_1} & -\frac{1}{d_1}f(c_\pm) \\ 0 & \frac{1}{d_2}\big(f(c_\pm)-R-\lambda\big) \end{pmatrix} \\
R^{\pm}(z) &= D^{-1}\big(J_F(C,N)-J_F(c_\pm,0)\big) \\
&= \begin{pmatrix} -\frac{1}{d_1}f'(C)N & -\frac{1}{d_1}\big(f(C)-f(c_\pm)\big) \\ \frac{1}{d_2}f'(C)N & \frac{1}{d_2}\big(f(C)-f(c_\pm)\big) \end{pmatrix} \\
A_w(z,\lambda) &= A(z,\lambda)+k(z)I \\
&= \begin{pmatrix} -\frac{1}{d_1}\big(f'(C)N+\lambda\big)+k & -\frac{1}{d_1}f(C) \\ \frac{1}{d_2}f'(C)N & \frac{1}{d_2}\big(f(C)-R-\lambda\big)+k \end{pmatrix} \\
A_w^{\pm}(\lambda) &= A^{\pm}(\lambda)+k_\pm I \\
&= \begin{pmatrix} -\frac{\lambda}{d_1}+k_\pm & -\frac{1}{d_1}f(c_\pm) \\ 0 & \frac{1}{d_2}\big(f(c_\pm)-R-\lambda\big)+k_\pm \end{pmatrix} \\
R_w^{\pm}(z) &= R^{\pm}(z)+\big(k(z)-k_\pm\big)I \\
&= \begin{pmatrix} -\frac{1}{d_1}f'(C)N+(k-k_\pm) & -\frac{1}{d_1}\big(f(C)-f(c_\pm)\big) \\ \frac{1}{d_2}f'(C)N & \frac{1}{d_2}\big(f(C)-f(c_\pm)\big)+(k-k_\pm) \end{pmatrix} \\
\tilde{A}_w(z,\lambda) &= D^{-1}WJ_F(Q)W^{-1}-W(W^{-1})'-\lambda D^{-1} \\
&= \begin{pmatrix} -\frac{1}{d_1}\big(f'(C)N+\lambda\big)+k^1 & -\frac{1}{d_1}\frac{w_1}{w_2}f(C) \\ \frac{1}{d_2}\frac{w_2}{w_1}f'(C)N & \frac{1}{d_2}\big(f(C)-R-\lambda\big)+k^2 \end{pmatrix}
\end{aligned}
$$

Double-substrate bioremediation model

$$
f=f(C_o,C_s)=\frac{C_o}{C_o+1}\frac{C_s}{C_s+1}, \qquad f^{\pm}=f(c_{o\pm},c_{s\pm})
$$

$$
f_{c_o}=f_{c_o}(C_o,C_s)=\frac{1}{(C_o+1)^2}\frac{C_s}{C_s+1}, \qquad f_{c_s}=f_{c_s}(C_o,C_s)=\frac{C_o}{C_o+1}\frac{1}{(C_s+1)^2}
$$

$$
D=\begin{pmatrix} d_1 & 0 & 0 \\ 0 & d_2 & 0 \\ 0 & 0 & d_3 \end{pmatrix}=\begin{pmatrix} u-s & 0 & 0 \\ 0 & v-s & 0 \\ 0 & 0 & -s \end{pmatrix}, \quad W(z)=\begin{pmatrix} w_1(z) & 0 & 0 \\ 0 & w_2(z) & 0 \\ 0 & 0 & w_3(z) \end{pmatrix}
$$

$$
\begin{aligned}
J_F(Q) &= J_F(C_o, C_s, N) \\
&= \begin{pmatrix} -\nu_o f_{c_o} N & -\nu_o f_{c_s} N & -\nu_o f \\ -\nu_s f_{c_o} N & -\nu_s f_{c_s} N & -\nu_s f \\ (\nu_o+\nu_s) f_{c_o} N & (\nu_o+\nu_s) f_{c_s} N & (\nu_o+\nu_s) f - R \end{pmatrix}
\end{aligned}
$$

$$
\begin{aligned}
A(z,\lambda) &= D^{-1}\big(J_F(C_o, C_s, N) - \lambda I\big) \\
&= \begin{pmatrix} -\frac{1}{d_1}(\nu_o f_{c_o} N + \lambda) & -\frac{1}{d_1}\nu_o f_{c_s} N & -\frac{1}{d_1}\nu_o f \\ -\frac{1}{d_2}\nu_s f_{c_o} N & -\frac{1}{d_2}(\nu_s f_{c_s} N + \lambda) & -\frac{1}{d_2}\nu_s f \\ \frac{1}{d_3}(\nu_o+\nu_s) f_{c_o} N & \frac{1}{d_3}(\nu_o+\nu_s) f_{c_s} N & \frac{1}{d_3}\big((\nu_o+\nu_s) f - R - \lambda\big) \end{pmatrix}
\end{aligned}
$$

$$
\begin{aligned}
A^{\pm}(\lambda) &= D^{-1}\big(J_F(c_{o\pm}, c_{s\pm}, 0) - \lambda I\big) \\
&= \begin{pmatrix} -\frac{\lambda}{d_1} & 0 & -\frac{1}{d_1}\nu_o f^{\pm} \\ 0 & -\frac{\lambda}{d_2} & -\frac{1}{d_2}\nu_s f^{\pm} \\ 0 & 0 & \frac{1}{d_3}\big((\nu_o+\nu_s) f^{\pm} - R - \lambda\big) \end{pmatrix}
\end{aligned}
$$

$$
\begin{aligned}
R^{\pm}(z) &= D^{-1}\big(J_F(C_o, C_s, N) - J_F(c_{o\pm}, c_{s\pm}, 0)\big) \\
&= \begin{pmatrix} -\frac{\nu_o}{d_1} f_{c_o} N & -\frac{\nu_o}{d_1} f_{c_s} N & -\frac{\nu_o}{d_1}(f - f^{\pm}) \\ -\frac{\nu_s}{d_2} f_{c_o} N & -\frac{\nu_s}{d_2} f_{c_s} N & -\frac{\nu_s}{d_2}(f - f^{\pm}) \\ \frac{\nu_o+\nu_s}{d_3} f_{c_o} N & \frac{\nu_o+\nu_s}{d_3} f_{c_s} N & \frac{\nu_o+\nu_s}{d_3}(f - f^{\pm}) \end{pmatrix}
\end{aligned}
$$

$$
\begin{aligned}
A_w(z,\lambda) &= A(z,\lambda) + k(z) I \\
&= \begin{pmatrix} -\frac{1}{d_1}(\nu_o f_{c_o} N + \lambda) + k & -\frac{1}{d_1}\nu_o f_{c_s} N & -\frac{1}{d_1}\nu_o f \\ -\frac{1}{d_2}\nu_s f_{c_o} N & -\frac{1}{d_2}(\nu_s f_{c_s} N + \lambda) + k & -\frac{1}{d_2}\nu_s f \\ \frac{1}{d_3}(\nu_o+\nu_s) f_{c_o} N & \frac{1}{d_3}(\nu_o+\nu_s) f_{c_s} N & \frac{1}{d_3}\big((\nu_o+\nu_s) f - R - \lambda\big) + k \end{pmatrix}
\end{aligned}
$$

$$
\begin{aligned}
A_w^{\pm}(\lambda) &= A^{\pm}(\lambda) + k_{\pm} I \\
&= \begin{pmatrix} -\frac{\lambda}{d_1} + k_{\pm} & 0 & -\frac{1}{d_1}\nu_o f^{\pm} \\ 0 & -\frac{\lambda}{d_2} + k_{\pm} & -\frac{1}{d_2}\nu_s f^{\pm} \\ 0 & 0 & \frac{1}{d_3}\big((\nu_o+\nu_s) f^{\pm} - R - \lambda\big) + k_{\pm} \end{pmatrix}
\end{aligned}
$$

$$
\begin{aligned}
R_w^{\pm}(z) &= R^{\pm}(z) + \big(k(z) - k_{\pm}\big) I \\
&= \begin{pmatrix} -\frac{\nu_o}{d_1} f_{c_o} N + (k - k_{\pm}) & -\frac{\nu_o}{d_1} f_{c_s} N & -\frac{\nu_o}{d_1}(f - f^{\pm}) \\ -\frac{\nu_s}{d_2} f_{c_o} N & -\frac{\nu_s}{d_2} f_{c_s} N + (k - k_{\pm}) & -\frac{\nu_s}{d_2}(f - f^{\pm}) \\ \frac{\nu_o+\nu_s}{d_3} f_{c_o} N & \frac{\nu_o+\nu_s}{d_3} f_{c_s} N & \frac{\nu_o+\nu_s}{d_3}(f - f^{\pm}) + (k - k_{\pm}) \end{pmatrix}
\end{aligned}
$$

$$
\begin{aligned}
\tilde{A}_w(z,\lambda) &= D^{-1} W J_F(Q) W^{-1} - W (W^{-1})' - \lambda D^{-1} \\
&= \begin{pmatrix} -\frac{1}{d_1}(\nu_o f_{c_o} N + \lambda) + k^1 & -\frac{1}{d_1}\frac{w_1}{w_2}\nu_o f_{c_s} N & -\frac{1}{d_1}\frac{w_1}{w_3}\nu_o f \\ -\frac{1}{d_2}\frac{w_2}{w_1}\nu_s f_{c_o} N & -\frac{1}{d_2}(\nu_s f_{c_s} N + \lambda) + k^2 & -\frac{1}{d_2}\frac{w_2}{w_3}\nu_s f \\ \frac{1}{d_3}\frac{w_3}{w_1}(\nu_o+\nu_s) f_{c_o} N & \frac{1}{d_3}\frac{w_3}{w_2}(\nu_o+\nu_s) f_{c_s} N & \frac{1}{d_3}\big((\nu_o+\nu_s) f - R - \lambda\big) + k^3 \end{pmatrix}
\end{aligned}
$$

C.2 Proofs related to chapter 4

Proposition 1. *Consider the linear operator*

$$\begin{aligned} \mathfrak{L} : \mathfrak{D}(\mathfrak{L}) \subset L^2(\mathbb{R}, \mathbb{C}^n) &\longrightarrow L^2(\mathbb{R}, \mathbb{C}^n) \\ p &\longmapsto \big(J_F(Q(z)) - D\partial_z\big)p \end{aligned}$$

with $\mathfrak{D}(\mathfrak{L}) := \{p \in L^2(\mathbb{R}, \mathbb{C}^n) : p \text{ absolutely continuous, } p' \in L^2(\mathbb{R}, \mathbb{C}^n)\}$ *and assume that the matrix* D *is invertible,* $Q \in C^1(\mathbb{R}, \mathbb{R}^n)$ *and* $J_F(Q(z))$ *is bounded. Then* $\mathfrak{L}$ *is closed and densely defined in* $L^2(\mathbb{R}, \mathbb{C}^n)$ *with domain* $\mathfrak{D}(\mathfrak{L})$*.*

Proof. The second property follows directly from the fact that $\mathfrak{D}(\mathfrak{L})$ is dense in $L^2(\mathbb{R}, \mathbb{C}^n)$. It thus remains to show that $\mathfrak{L}$ is closed, i.e. if $p_n \in \mathfrak{D}(\mathfrak{L})$, $p_n \to p$ in $L^2(\mathbb{R}, \mathbb{C}^n)$ and $\mathfrak{L}p_n \to g$ in $L^2(\mathbb{R}, \mathbb{C}^n)$, then $p \in \mathfrak{D}(\mathfrak{L})$ and $g = \mathfrak{L}p$.

Consider a sequence $\{p_n\} \in \mathfrak{D}(\mathfrak{L})$ satisfying

$$\begin{aligned} p_n &\longrightarrow p \in L^2(\mathbb{R}, \mathbb{C}^n) \\ \mathfrak{L}p_n = J_F(Q(z))p_n - D\partial_z p_n &\longrightarrow g \in L^2(\mathbb{R}, \mathbb{C}^n), \end{aligned}$$

and note that for all $[a, b] \subset \mathbb{R}$ the functions p_n satisfy

$$p_n(b) = p_n(a) + \int_a^b \partial_z p_n(z)\, dz. \tag{C.1}$$

Since $Q(z)$ is continuously differentiable and $J_F(Q(z))$ is bounded, we have

$$J_F(Q(z))p_n \longrightarrow J_F(Q(z))p \in L^2(\mathbb{R}, \mathbb{C}^n),$$

and hence

$$-D\partial_z p_n \longrightarrow g - J_F(Q(z))p \in L^2(\mathbb{R}, \mathbb{C}^n).$$

Due to the invertibility of D, this is equivalent to

$$\partial_z p_n \longrightarrow -D^{-1}g + D^{-1}J_F(Q(z))p \in L^2(\mathbb{R}, \mathbb{C}^n).$$

With respect to the above results, the limit of (C.1) is

$$p(b) = p(a) + \int_a^b -D^{-1}g(z) + D^{-1}J_F(Q(z))p(z)\, dz,$$

i.e. p is absolutely continuous and

$$\partial_z p = -D^{-1}g + D^{-1}J_F(Q(z))p \in L^2(\mathbb{R}, \mathbb{C}^n),$$

and hence $p \in \mathfrak{D}(\mathfrak{L})$. Moreover, the latter equation is equivalent to

$$g = J_F(Q(z))p - D\partial_z p = \mathfrak{L}p,$$

which completes the proof. □

The remainder of this subsection is devoted to theorem 3 on page 74. We consider the differential equations

$$u'(z) = \big(A_w^+(\lambda) + R_w^+(z)\big)u(z) \quad \text{and} \quad \hat{u}'(z) = \big(\hat{A}_w^-(\lambda) + \hat{R}_w^-(z)\big)\hat{u}(z)$$

with $\hat{u}(z) = u(-z)$, $\hat{A}_w^-(\lambda) = -A_w^-(\lambda)$ and $\hat{R}_w^-(z) = -R_w^-(-z)$ related to the eigenvalue problem (4.20) of the bioremediation model (3.1).

Below it is proven that for every fixed $\lambda \in \mathbb{C}$ each pair of matrices $A_w^+(\lambda)/R_w^+(z)$ and $\hat{A}_w^-(\lambda)/\hat{R}_w^-(z)$ either satisfies the assumptions of theorem 3 (i) or (ii).

Proposition 2. *Consider the matrices*

$$A_w^\pm(\lambda) = \begin{pmatrix} \mu_{1w}^\pm(\lambda) & -\frac{1}{d_1} f(c_\pm) \\ 0 & \mu_{2w}^\pm(\lambda) \end{pmatrix}$$

and $\hat{A}_w^-(\lambda) = -A_w^-(\lambda)$.

(i) For $\lambda \neq \frac{d_1}{d_1 - d_2}(f(c_+) - R)$, *and hence* $\mu_{1w}^+(\lambda) \neq \mu_{2w}^+(\lambda)$, *there exists a matrix* P *such that* $J = P^{-1}A_w^+(\lambda)P$ *is diagonal.*

For $\lambda = \frac{d_1}{d_1 - d_2}(f(c_+) - R)$, *and hence* $\mu_{1w}^+(\lambda) = \mu_{2w}^+(\lambda)$, *there exists a matrix* P *such that* $J = P^{-1}A_w^+(\lambda)P$ *is a non-diagonal Jordan block.*

(ii) For $\lambda \neq \frac{d_1}{d_1 - d_2}(f(c_-) - R)$, *and hence* $\mu_{1w}^-(\lambda) \neq \mu_{2w}^-(\lambda)$, *there exists a matrix* P *such that* $J = P^{-1}\hat{A}_w^-(\lambda)P$ *is diagonal.*

For $\lambda = \frac{d_1}{d_1 - d_2}(f(c_-) - R)$, *and hence* $\mu_{1w}^-(\lambda) = \mu_{2w}^-(\lambda)$, *there exists a matrix* P *such that* $J = P^{-1}\hat{A}_w^-(\lambda)P$ *is a non-diagonal Jordan block.*

Proof. In the mentioned order, the matrices

$$P = \begin{pmatrix} a & b \\ 0 & (\mu_{2w}^+(\lambda) - \mu_{1w}^+(\lambda))\frac{b}{r_+} \end{pmatrix} \quad \text{and} \quad P = \begin{pmatrix} a & b \\ 0 & \frac{a}{r_+} \end{pmatrix}$$

satisfy the requirements of (i), while

$$P = \begin{pmatrix} a & b \\ 0 & (\mu_{2w}^-(\lambda) - \mu_{1w}^-(\lambda))\frac{b}{r_-} \end{pmatrix} \quad \text{and} \quad P = \begin{pmatrix} a & b \\ 0 & -\frac{a}{r_-} \end{pmatrix}$$

satisfy (ii) for arbitrary values $a, b \in \mathbb{R} \setminus \{0\}$ and with notation $r_\pm := -\frac{1}{d_1} f(c_\pm)$. □

Due to the fact that the equalities $R_w^+(z) = R^+(z)$ and $\hat{R}_w^-(z) = \hat{R}^-(z)$ are true for $z > 0$, the requests on $R_w^+(z)$ and $\hat{R}_w^-(z)$ claimed in theorem 3 can be verified by considering the matrices $R^+(z)$ and $\hat{R}^-(z)$ in the subsequent proposition.

Proposition 3. *Consider the matrices*

$$R^{\pm}(z) = \begin{pmatrix} -\frac{1}{d_1} f'(C)N & -\frac{1}{d_1}\big(f(C) - f(c_{\pm})\big) \\ \frac{1}{d_2} f'(C)N & \frac{1}{d_2}\big(f(C) - f(c_{\pm})\big) \end{pmatrix}$$

and $\hat{R}^-(z) = -R^-(-z)$. *Both matrices* $R(z) = R^+(z)$ *and* $R(z) = \hat{R}^-(z)$ *satisfy*

$$\int_1^\infty |R(z)|\, dz < \infty \qquad \textit{and} \qquad \int_1^\infty z|R(z)|\, dz < \infty.$$

Remark 1. Taking into account

$$\int_1^\infty |\hat{R}^-(z)|\, dz = \int_{-\infty}^{-1} |R^-(z)|\, dz \quad \text{and} \quad \int_1^\infty z|\hat{R}^-(z)|\, dz = \int_{-\infty}^{-1} -z|R^-(z)|\, dz$$

we can trace the statements about $\hat{R}^-(z)$ back to statements about $R^-(z)$.

Proof. Since all four statements are shown analogously, we restrict the proof to the first one.

Since $d_1 = u - s$, $d_2 = -s$, N, $f'(C)$ and $f(C) - f(c_+)$ are positive, it is

$$|R^+(z)| = \left(\frac{1}{d_1} + \frac{1}{d_2}\right)\Big(f(C) - f(c_+) + f'(C)N\Big).$$

It thus remains to show that

$$\int_1^\infty f(C) - f(c_+)\, dz < \infty \qquad \text{and} \qquad \int_1^\infty f'(C)N\, dz < \infty.$$

Due to the mean value theorem there exists a constant K_1 with

$$f(C) - f(c_+) \le K_1(C - c_+).$$

Integration of the first differential equation of (3.2) yields

$$C - c_+ = \frac{1}{d_1}\int_z^\infty f(C)N\, d\bar{z}.$$

Using $f(C) < f(c_-)$ and the result (B.2) gives

$$C - c_+ < K_2 \int_z^\infty e^{-\alpha_+ \bar{z}}\, d\bar{z} = K_3 e^{-\alpha_+ z},$$

and therefore

$$\int_1^\infty f(C) - f(c_+)\, dz \le K_1 \int_1^\infty C - c_+\, dz < K_4 \int_1^\infty e^{-\alpha_+ z}\, dz =: K < \infty$$

with positive constants K_i $(i = 1, \ldots, 4)$ and K.

Using $f'(C) < L_1$ and (B.2) again yields

$$\int_1^\infty f'(C)N\, dz < L_1 \int_1^\infty N\, dz < L_2 \int_1^\infty e^{-\alpha_+ z}\, dz =: L < \infty$$

with positive constants L_1, L_2 and L. □

C.3 Eigenvalues of certain operators

Consider the differential equation

$$u' = A(z, \lambda)u$$

with

$$A(z, \lambda) = A^{\pm}(\lambda) + R^{\pm}(z) \xrightarrow{z \to \pm\infty} A^{\pm}(\lambda),$$

and suppose that the pairs (λ, u) solving this equation with $u \in L^2(\mathbb{R}, \mathbb{C}^n)$ are eigenvalues and eigenvectors of a related differential operator $\mathfrak{L}$ on $L^2(\mathbb{R}, \mathbb{C}^n)$.

If $A^+(\lambda)/R^+(z)$ and $-A^-(\lambda)/-R^-(-z)$ satisfy the assumptions of theorem 3 (i) or (ii), the asymptotic behavior of the solutions is dominated by the eigenvalues $\mu_i^{\pm}(\lambda)$ of $A^{\pm}(\lambda)$. Since the signs of $\mathrm{Re}(\mu_i^{\pm}(\lambda))$ determine the signs of the gradient of the solutions at large $|z|$, the instability indices $i_{\pm}(\lambda)$ of $A^{\pm}(\lambda)$ are a measure for the number of linearly independent decreasing/increasing solutions at $\pm\infty$. We can therefore express necessary and sufficient conditions for the existence and non-existence of solutions that decay at both ends, and hence for λ being an eigenvalue or no eigenvalue of $\mathfrak{L}$, in terms of instability indices.

These conditions, combined with results of theorem 2, are visualized in table C.1. In certain cases, namely $i_-(\lambda) = 0$ and $i_+(\lambda) = n$, they enable us to distinguish $\rho(\mathfrak{L})$ from $\sigma_{pt}(\mathfrak{L})$, and to differentiate between eigenvalues and non-eigenvalues in $\sigma_{ess}(\mathfrak{L})$ without computing $\dim(N(\mathfrak{L} - \lambda I))$.

$i_-(\lambda)$ \ $i_+(\lambda)$		0	1	2	$\cdots$	n
0	ind $=$	0	-1	-2		$-n$
	λ is	no eigenvalue	no eigenvalue	no eigenvalue		no eigenvalue
	$\lambda \in$	$\rho(\mathfrak{L})$	$\sigma_{ess}(\mathfrak{L})$	$\sigma_{ess}(\mathfrak{L})$		$\sigma_{ess}(\mathfrak{L})$
1	ind $=$	1	0	-1		$-(n-1)$
	λ is	eigenvalue				no eigenvalue
	$\lambda \in$	$\sigma_{ess}(\mathfrak{L})$	$\rho(\mathfrak{L}) \cup \sigma_{pt}(\mathfrak{L})$	$\sigma_{ess}(\mathfrak{L})$		$\sigma_{ess}(\mathfrak{L})$
2	ind $=$	2	1	0		$-(n-2)$
	λ is	eigenvalue	eigenvalue			no eigenvalue
	$\lambda \in$	$\sigma_{ess}(\mathfrak{L})$	$\sigma_{ess}(\mathfrak{L})$	$\rho(\mathfrak{L}) \cup \sigma_{pt}(\mathfrak{L})$		$\sigma_{ess}(\mathfrak{L})$
$\vdots$						
n	ind $=$	n	$n-1$	$n-2$		0
	λ is	eigenvalue	eigenvalue	eigenvalue		no eigenvalue
	$\lambda \in$	$\sigma_{ess}(\mathfrak{L})$	$\sigma_{ess}(\mathfrak{L})$	$\sigma_{ess}(\mathfrak{L})$		$\rho(\mathfrak{L})$

Table C.1: Classification of λ with respect to the instability indices according to theorem 2 and the conditions following from theorem 3

Remark 2. Note that the instability index is only defined for hyperbolic matrices. The results visualized in table C.1 are therefore not applicable to values λ that are related to either a non-hyperbolic matrix $A^-(\lambda)$ or a non-hyperbolic matrix $A^+(\lambda)$. Nevertheless, counting negative and positive eigenvalues of $A^{\pm}(\lambda)$ in these cases also yields necessary and sufficient conditions concerning the eigenvalues of the differential operator $\mathfrak{L}$ with the same arguments as before.

Remark 3. Consider the single-substrate bioremediation model (3.1) and the related differential operator $\mathfrak{L}$ on $L^2(\mathbb{R}, \mathbb{C}^2)$. Since the matrices $A^+(\lambda)/R^+(z)$ and $-A^-(\lambda)/-R^-(-z)$ satisfy the assumptions of theorem 3, the results visualized in table C.1 are applicable to this problem. It is thus easily deduced from figure 4.3 that the point spectrum $\sigma_{pt}(\mathfrak{L})$ is empty, as already mentioned on page 65.

Bibliography

[Bad78] Bader, F.G.: *Analysis of double-substrate limited growth.* Biotechnol. Bioeng., 20:183–202, 1978.

[Ben84] Benefield, L. / Molz, F.: *A model for the activated sludge process which considers wastewater characteristics, floc behavior, and microbial population.* Biotechnol. Bioeng., 26:352–361, 1984.

[Ben92] Ben-Artzi, A. / Gohberg, I.: *Dichotomy of systems and invertibility of linear ordinary differential operators.* In Gohberg, I. (editor): *Time-variant Systems and Interpolation*, volume 56 of *Oper. Theory Adv. Appl.*, pages 90–119. Birkhäuser, Basel - Boston - Berlin, 1992.

[Bis08] Bisswanger, H.: *Enzyme Kinetics: Principles and Methods.* Wiley-VCH, Weinheim, 2nd edition, 2008.

[Bla05] Blackman, F.F.: *Optima and limiting factors.* Ann. Bot., 19(2):281–295, 1905.

[Bol01] Boll, M. et al.: *Redox centers of 4-hydroxybenzoyl-CoA reductase, a member of the xanthine oxidase family of molybdenum-containing enzymes.* J. Biol. Chem., 276(51):47853–47862, 2001.

[Bol05a] Boll, M.: *Dearomatizing benzene ring reductases.* J. Mol. Microbiol. Biotechnol., 10:132–142, 2005.

[Bol05b] Boll, M.: *Key enzymes in the anaerobic aromatic metabolism catalysing Birch-like reductions.* Biochim. Biophys. Acta, 1707:34–50, 2005.

[Bol05c] Boll, M. / Fuchs, G.: *Unusual reactions involved in anaerobic metabolism of phenolic compounds.* Biol. Chem., 386:989–997, 2005.

[Bor86] Borden, R.C. / Bedient, P.B.: *Transport of dissolved hydrocarbons influenced by oxygen-limited biodegradation – 1. Theoretical development.* Water Resour. Res., 22(13):1973–1982, 1986.

[Bri25] Briggs, G.E. / Haldane, J.B.S.: *A note on the kinetics of enzyme action.* Biochem. J., 19(2):338–339, 1925.

[Che06] Chen, C. / Chadam, J.: *Bioremediation of waste in a porous medium.* In Nagata, W. / Namachchivaya, N. (editor): *Bifurcation Theory and Spatio-Temporal Pattern Formation*, volume 49 of *Fields Institute Communications*, pages 65–78. American Mathematical Society, Providence, Rhode Island, 2006.

[Cir99] Cirpka, O.A. / Frind, E.O. / Helmig, R.: *Numerical simulation of biodegradation controlled by transverse mixing.* J. Contam. Hydrol., 40:159–182, 1999.

[Cod55] Coddington, E.A. / Levinson, N.: *Theory of Ordinary Differential Equations.* McGraw-Hill Book Company, New York - Toronto - London, 1955.

[Coo07] Cook, P.F. / Cleland, W.W.: *Enzyme Kinetics and Mechanism.* Garland Science Publishing, London, 2007.

[Cop78] Coppel, W.A.: *Dichotomies in Stability Theory*, volume 629 of *Lecture Notes in Mathematics.* Springer, Berlin, 1978.

[Din08] Dingee, J.W. / Anton, A.B.: *A new perturbation solution to the Michaelis-Menten problem.* AIChE J, 54:1344–1357, 2008.

[Gas03] Gasser, I.: *Mathematische Modellierung in der Angewandten Mathematik.* lecture notes University of Hamburg, 2002/2003.

[Got86] Gottschalk, G.: *Bacterial Metabolism.* Springer, New York, 2nd edition, 1986.

[Gri91] Grindrod, P.: *Patterns and Waves – The Theory and Applications of Reaction-Diffusion Equations.* Oxford Applied Mathematics and Computing Science Series. Clarendon Press, Oxford, 1991.

[Gru08] Gruhn, A. / Kummer, E.: *Sanierung durch Stimulierung des natürlichen In-situ-CKW-Abbaus.* Terra Tech, 3:18–20, 2008.

[Hem07] Hempel, D.C.: *Bioverfahrenstechnik.* In Grote, K.-H. / Feldhusen, J. (editor): *Dubbel – Taschenbuch für den Maschinenbau*, pages N 34–N 52. Springer, Berlin - Heidelberg, 22nd edition, 2007.

[Hen81] Henry, D.: *Geometric Theory of Semilinear Parabolic Equations.* Number 840 in *Lecture Notes in Mathematics.* Springer, Berlin - Heidelberg - New York, 1981.

[Hin91] Hinch, E.J.: *Perturbation Methods.* Cambridge University Press, Cambridge, 1991.

[Klö02] Klöfkorn, R. / Kröner, D. / Ohlberger, M.: *Local adaptive methods for convection dominated problems.* Int. J. Numer. Meth. Fluids, 40:79–91, 2002.

[Las87] Lasch, J.: *Enzymkinetik: Eine Einführung für Biochemiker, Mediziner, Biologen, Chemiker und Pharmazeuten.* Springer, Berlin - Heidelberg - New York, 1987.

[Log01] Logan, J.D.: *Transport Modeling in Hydrogeochemical Systems.* Springer, New York, 2001.

[May01] Mayer, K.U. / Benner, S.G. / Frind, E.O. / Thornton, S.F. / Lerner, D.N.: *Reactive transport modeling of processes controlling the distribution and natural attenuation of phenolic compounds in a deep sandstone aquifer.* J. Contam. Hydrol., 53:341–368, 2001.

[Meg72] Megee III, R.D.: *Studies in intermicrobial symbiosis.* Saccharomyces cerevisiae *and* Lactobacillus casei. Can. J. Microbiol., 18:1733–1742, 1972.

[Mei01] Meister, A.: *Asymptotic Expansions and Numerical Methods in Computational Fluid Dynamics.* Technical report, University of Hamburg, 2001. Hamburger Beiträge zur Angewandten Mathematik, Reihe F, Computational Fluid Dynamics and Data Analysis 17.

[Mic13] Michaelis, L. / Menten, M.L.: *Die Kinetik der Invertinwirkung.* Biochemische Zeitschrift, 49:333–369, 1913.

[Möb04] Möbitz, H. / Friedrich, T. / Boll, M.: *Substrate binding and reduction of benzoyl-CoA reductase: Evidence for nucleotide-dependent conformational changes.* Biochemistry, 43:1376–1385, 2004.

[Mon42] Monod, J.: *Recherches sur la croissance des cultures bactériennes.* Hermann & C^{ie}, Paris, 1942.

[Mon49] Monod, J.: *The growth of bacterial cultures.* Annu. Rev. Microbiol., 3:371–394, 1949.

[Mur98] Murray, R. / Xin, J.X.: *Existence of traveling waves in a biodegradation model for organic contaminants.* SIAM J. Math. Anal., 30(1):72–94, 1998.

[Ode93] Odencrantz, J.E. / Valocci, A.J. / Rittmann, B.E: *Modeling the interaction of sorption and biodegradation on transport in ground water* in situ *remediation systems.* In Poeter, E. /Ashlock, S. / Proud J. (editor): *Proceedings 1993 Ground Water Modeling Conference*, Golden, Colorado, 1993.

[O'M91] O'Malley, R.E., Jr.: *Singular Perturbation Methods for Ordinary Differential Equations.* Springer, New York, 1991.

[Pal84] Palmer, K.J.: *Exponential dichotomies and transversal homoclinic points.* J. Diff. Eqns., 55:225–256, 1984.

[Pal88] Palmer, K.J.: *Exponential dichotomies and Fredholm operators.* Proc. Amer. Math. Soc., 104(1):149–156, 1988.

[Pan95] Panikov, N.S.: *Microbial Growth Kinetics.* Chapman&Hall, London, 1995.

[Pir90] Pirt, S.J.: *The dynamics of microbial processes: a personal view.* In Poole, R. K. / Bazin, M. J. / Keevil, C. W. (editor): *Microbial Growth Dynamics.* Oxford University Press, New York, 1990.

[San93] Sandstede, B.: *Verzweigungstheorie homokliner Verdopplungen.* PhD thesis, University of Stuttgart, 1993.

[San00] Sandstede, B. / Scheel, A.: *Absolute and convective instabilities of waves on unbounded and large bounded domains.* Phys. Nonlinear Phenom., 145:233–277, 2000.

[San01] Sandstede, B. / Scheel, A.: *Essential instability of fronts: bifurcation, and bifurcation failure.* Dyn. Syst. Int. J., 16(1):1–28, 2001.

[San02] Sandstede, B.: *Stability of travelling waves.* In Hasselblatt, B. / Katok, A. (editor): *Handbook of Dynamical Systems*, volume 2, pages 983–1055. Elsevier/North-Holland, Amsterdam, 2002.

[Sch98] Schäfer, D. / Schäfer, W. / Kinzelbach, W.: *Simulation of reactive processes related to biodegradation in aquifers. 1. Structure of the three-dimensional reactive transport model.* J. Contam. Hydrol., 31:167–186, 1998.

[Sch02] Schechter, M.: *Principles of Functional Analysis*, volume 36 of *Graduate Studies in Mathematics.* American Mathematical Society, Providence, Rhode Island, 2nd edition, 2002.

[Sch04] Schäfer, D.: *Numerische Modellierung reaktiver Prozesse organischer Kontaminanten in Grundwasserleitern.* Habilitationsschrift, Institut für Geowissenschaften, Christian-Albrechts-Universität zu Kiel, October 2004.

[Seg72] Segel, L.A.: *Simplification and scaling.* SIAM Review, 14(4):547–571, 1972.

[Seg88] Segel, L.A.: *On the validity of the steady state assumption of enzyme kinetics.* Bull. Math. Biol., 50(6):579–593, 1988.

[Seg89] Segel, L.A. / Slemrod, M.: *The quasi-steady-state assumption: A case study in perturbation.* SIAM Review, 31(3):446–477, 1989.

[Voe02] Voet, D. / Voet, J.G. / Pratt C.W.: *Lehrbuch der Biochemie.* WILEY VCH, Weinheim, 2002.

[Wid88] Widdowson, M.A. / Molz, F.J. / Benefield, L.D.: *A numerical transport model for oxygen- and nitrate-based respiration linked to substrate and nutrient availability in porous media.* Water Resour. Res., 24(9):1553–1565, 1988.

[Xin98] Xin, J. / Zhang, D.: *Stochastic analysis of biodegradation fronts in one-dimensional heterogeneous porous media.* Adv. Water Resour., 22(2):103–116, 1998.

[Xin00] Xin, J.X. / Hyman, J.M.: *Stability, relaxation, and oscillation of biodegradation fronts.* SIAM J. Appl. Math., 61(2):472–505, 2000.